Optimization of Drilling Fluid Rheological Properties for Improved Cuttings Transport and Dynamic Filtration Loss Control Performance: A Comparative Study of the Fluid Viscoelasticity versus the Shear Viscosity Effects

By

Hongbo Chen

A thesis submitted in partial fulfillment of the requirements for the degree of

Master of Science

In

Petroleum Engineering

Department of Civil and Environmental Engineering

University of Alberta

Abstract

Recent studies highlighted the significant role of drilling fluid viscoelasticity in the assessment of frictional pressure loss, particle settling velocity, hole cleaning efficiency, and dynamic filtration loss control. Although the impact of drilling fluid viscoelasticity on the various functions of drilling fluids has been well recognized, the field implementation of these research findings have been hampered mainly because there has not been any standard field technique available for measuring the fluid viscoelastic properties.

A comprehensive experimental investigation has, therefore, been conducted to develop a generalized model to determine the viscoelasticity of drilling fluids using standard field-testing equipment. The new field measurement-based methodology has then been used for developing new models and strategies that can be used for formulating optimum drilling fluid rheological properties for improving drilling fluid performance in two key applications areas; i-) Enhancing solids suspension ability, ii-) Reducing dynamic filtration loss.

Ninety-three fluid formulations used in this study included field samples of oil-based drilling fluids as well as laboratory samples of water-based, invert emulsion and other oil-based fluids. Basic rheological characterizations of these fluids were done by using a funnel viscometer and a rotational viscometer. Elastic properties of the drilling fluids (quantified in terms of the energy required to cause an irreversible deformation in the fluid's structure called "energy dissipation") were obtained from oscillatory tests conducted by using a research grade rheometer with double gap concentric cylinder geometry. Using an empirical approach, a non-iterative model for quantifying drilling fluid elasticity was developed by correlating test results from a funnel

viscometer and a rotational viscometer to energy required to cause an irreversible deformation of the fluid's elastic structure.

Using the field measurement-based methodology for assessing the drilling fluid viscoelasticity , further experimental studies have been conducted to develop a generalized model for the field assessment of particle settling velocity in shear-thinning viscoelastic fluids by using the energy dissipation concept as an indicator of the fluid viscoelasticity.

Ten different fluids were prepared in two groups based on their shear viscosity values. In each group, five fluids were having similar shear viscosity and variable elasticity values. Nineteen different spherical particles were used to conduct particle settling experiments with a density range from 2700 kg/m^3 to 6000kg/m^3 and a diameter range from 1mm to 4mm. Rheological characterizations of the fluids have been conducted by using funnel viscometer, API Rotational viscometer, controlled shear rate, and amplitude sweep test measurements.

Fluid shear viscosity and elasticity have been identified as the most influential factors controlling filtration loss. However, past studies were mostly inconclusive regarding the individual effects of fluid shear viscosity vs elasticity, as it was very difficult to measure their effect independently.

24 water-based drilling fluids were prepared using various blends of three different molecular weight PHPA polymers. Two groups of fluids; one group having the same shear viscosity and variable elasticity and the other group having the same elasticity and variable shear viscosities, were developed. Additionally, 3 Xanthan Gum fluids were used as an example of

visco-inelastic drill-in fluids commonly used for drilling long horizontal wellbore sections in the reservoir.

Static filtration tests and core flooding experiments were conducted to measure the static filtration rate, pressure drop across the core at different flow rates, and formation damage induced by each fluid. By investigating the independent effects of viscoelasticity and shear viscosity on the fluid filtration loss characteristics, it was observed that: 1-) The static filtration rate can be more effectively controlled by altering fluid viscoelasticity as compared to the fluid shear viscosity. 2-) Both shear viscosity and viscoelasticity have a proportional relationship to the pressure drop associated with the core flow. However, the effect of viscoelasticity on the pressure drop is more pronounced. 3-) Increasing fluid viscoelasticity does not cause the formation damage as much as the shear viscosity. 4-)The viscoelasticity has been found to be the predominant rheological property that controls the solid-free drill-in fluids' filtration loss characteristics.

The results have suggested that viscoelasticity can help develop non-invasive fluids by reducing static filtration rate, increasing pressure drop (effectively building internal cake), and minimizing formation damage.

Preface

This thesis is an original work by Hongbo(Rob) Chen. The research work was conducted under the supervision of Prof. Ergun Kuru at the University of Alberta. The data acquisition, data analysis, and manuscript organization were completed by Hongbo(Rob) Chen, the revision of the manuscript was primarily carried out by Prof. Ergun Kuru with the help of Temi Okesanya, Garett Heath, and Dylan Hadley. Two sections of this thesis have been accepted for conference presentations.

Chapter 4 was presented at the Annual Technical Conference Exhibition 2021 as "Chen, H., Okesanya, T., Kuru, E., Garett, H., & Dylan, H. (2021) A Generalized Model for the Field Assessment of Drilling Fluid Viscoelasticity." with a paper number SPE-205953-MS. The extended version of the chapter has also been submitted to the SPE Drilling Journal for review and possible publication.

Chapter 5 was accepted for conference presentation at the 41st International Conference on Ocean, Offshore & Arctic Engineering, Hamburg, Germany, June 5 – June 10, 2022, as "Chen, H., & Kuru, E.(2022) A Generalized Model for Field Assessment of Particle Settling Velocity in Viscoelastic Fluids." with paper number OMAE2022-78264.

Acknowledgments

First and foremost, I would like to express my deepest gratitude toward Prof. Ergun Kuru, who has been providing earnest guidance during my graduate career. His patience, inspiration, and motivation have endowed me with tremendous faith in conquering various obstacles encountered during research. His commitment toward research is heuristic and there is always something new that I can learn during each discussion. It wouldn't be exaggerating to say that it's my pleasure to have him as my supervisor.

Special thanks to John Czuroski, Rinbo Lin, Sussi Sun, and Zhaopeng Zhu for providing support and knowledge for me to build the experimental systems. Also, I'm grateful for the committee members serving in my MSc final exam: Dr. Tayfun Babadagli, Dr. Andy Li and Dr. Nobuo Maeda.

I sincerely thank Mr. Temi Okesanya, Mr. Garett Heath, and Mr. Dylan Hadley for providing technical support and valuable industrial experience to make the work more practical and comprehensive.

I would also express my gratitude toward my parents for their unconditional support. They are always there to comfort me during the hard times. Their love and encouragement are indispensable for my success in the past twenty-four years.

This work is financially supported through the funds available from the Natural Sciences and Engineering Research Council of Canada (NSERC-Kuru-242248 and NSERC RGPIN-2016-04647 Kuru) and New Park Resource Ltd.

Table of Contents

List of Tables

Table of Figures

Nomenclature

Symbol		Full Name (Unit)
AV	=	apparent viscosity (cp)
A	=	cross-sectional area of flow (cm^2)
C_D	=	drag coefficient (-)
$C_{D\text{-}exp}$	=	experimental drag coefficient (-)
$C_{D\text{-}uni}$	=	universal drag coefficient (-)
D	=	characteristic linear dimension (m)
d	=	particle diameter (mm)
E_{DF}	=	field energy dissipation (J/m^3)
E_{DT}	=	true energy dissipation (J/m^3)
g	=	gravity constant (m/s^2)
G'	=	elastic modulus (Pa)
G''	=	viscous modulus (Pa)
$G'\text{-}LVE$	=	elastic modulus in LVE region (Pa)

I	=	polydispersity index (-)
K	=	power-law consistency index ($Pa.s^n$)
k	=	permeability (Darcy)
L	=	length of the core (cm)
LVE	=	linear viscoelastic region (-)
M_w	=	molecular weight (g/g mol)
$MAPE$	=	mean average percentage error (%)
MFV	=	measured funnel viscosity (s)
n	=	power-law flow behavior index (-)
PFV	=	predicted funnel viscosity (s)
Q	=	volumetric flow rate (cm^3/s)
Re_p	=	particle Reynolds number (-)
$RMSE$	=	root mean square error (m/s)
V	=	flow velocity (m/s)

V_m	=	measured terminal velocity (m/s)
V_p	=	predicted terminal velocity (m/s)
V_t	=	terminal velocity (m/s)
V_{ti}	=	visco-inelastic terminal velocity (m/s)
V_{te}	=	viscoelastic terminal velocity (m/s)
γ	=	oscillation/ shear strain (%)
$\dot{\gamma}$	=	shear rate (1/s)
Ω	=	weight fraction (-)
μ	=	shear viscosity (Pa.s)
ρ_f	=	fluid density (kg/m^3)
ρ_s	=	particle density (kg/m^3)
τ	=	oscillation shear stress (Pa)
$\bar{\tau}$	=	mean surficial stress (Pa)
τ_f	=	flow point stress (Pa)
τ_y	=	yield stress (Pa)
$\Theta 600$	=	600 RPM reading (lbs./100ft^2)

CHAPTER 1 Introduction

1.1 Overview

Viscoelastic properties of drilling fluids have drawn much attention in the drilling industry because of the critical role they play in the evaluation of frictional pressure loss, particle settling velocity, and cuttings transport efficiency (Powell et al., 1991; Zamora et al., 1993; Saasen et al., 2002; Bui et al., 2012 and Savindla et al., 2017). Particle settling velocity is one of the key variables required for optimum hydraulic design of fluid-solid transport systems that has been used in various oil field operations such as proppant transport in hydraulic fracturing (Shah et al., 2007) and cuttings transport in drilling (Baldino et al., 2015 and Altindal et al., 2017). Arnipally and Kuru, (2018) reported that models not taking the fluid elasticity effect into account could over predict the settling velocity of particles in a viscoelastic fluid by as much as 14 to 50 times. Researchers investigating the proppant transport efficiency of fracturing fluids recommended that both shear viscosity and viscoelasticity of the fracturing fluid need to be considered to determine optimum fracturing fluid rheological properties for effective proppant transportation (Malhotra et al., 2012 and Biheri et al., 2021).

Recent laboratory investigations (Bizhani and Kuru, 2018; Hirpa and Kuru, 2020) have shown that much higher critical flow rates were required for the initiation of bed erosion/hole cleaning when using viscoelastic drilling fluids. Bizhani and Kuru, (2018) concluded that additional elastic normal forces arising from the variable normal stress differences of viscoelastic fluids could be responsible for delaying the onset of the bed erosion.

Fluid loss prevention is a key performance attribute of drilling fluids; for water-based drilling fluids, significant loss of water or fluid into the formation can cause irreversible change in the borehole (Fink, 2021). Based on the research conducted by Lomba et al., (2002), it is concluded that evaluating fluid loss and invasion characteristics of drilling fluids into porous media is crucial to guarantee a successful operation and ensure high oil and gas zones. In some cases, especially at ultra-deep water drilling, the availability of non-invasive fluid formulations may even be demanding to make an oil field development possible. Cobianco et al., (2001) suggested that a strict control of drilling fluid filtration characteristics is required to limit borehole instability, excessive torque and drag, differential pipe stuck and formation damage; the problem becomes more critical when drilling/completing horizontal wells with water-based fluids where the fluid remain in contact with the pay zone for an extended period. All these previous studies have emphasized the importance of fluid loss prevention; it is within reason to consider controlling filtration loss characteristics as one of the most critical tasks in versatile oil and gas operations, including completion, drilling, and preserving formation integrity. Fluid rheological properties (e.g., shear viscosity, viscoelasticity) have been identified as the most influential factors controlling filtration loss. However, past studies were mostly inconclusive regarding the individual effects of fluid shear viscosity vs elasticity, as it was very difficult to measure their effect independently.

All these previous field experience and lab data strongly suggest that fluid elastic properties significantly influences various drilling fluid functions and should be given due consideration when designing optimum drilling fluid formulation together with the viscous properties to effectively meet the drilling fluid requirements for successfully performing critical functions (e.g., effective hole cleaning and cuttings transport, mitigating Barite sag, minimizing fluid loss, etc.)

1.2 Problem Statement

Despite the impact of fluid viscoelasticity on the drilling hydraulics design has been well recognized, currently there is no standard field technique available for measuring the fluid viscoelastic properties. The viscoelastic properties can only be measured in the lab by using advanced rheometers, which are not suitable for field applications. There is a need for development of a methodology that can be used in the field to determine the viscoelastic properties of drilling fluids using standard field-testing equipment.

The settling behavior of particles in Newtonian (Clift et al., 1978; Chhabra, 2007 and Shahi et al., 2016) and non-Newtonian fluids (Shah et al., 2007; Okesanya et al., 2020 and Wilson et al., 2003) have been extensively investigated in the past. However, in addition to showing non-Newtonian rheological behavior, most fluids used in the oil field also have elastic characteristics (Agwu et al., 2018 and Bui et al., 2012). Results of the previous lab investigations and field observations strongly suggest that fluid elastic properties need to be considered together with the viscous properties for a more accurate prediction of solids' transport ability of drilling fluids. Investigating the effect of fluid elasticity on the particle settling velocity independent from shear viscosity has been a real challenge in theoretical developments as well as in experimental studies, which complicates the accurate assessment of the particle settling velocity in viscoelastic fluids (Arnipally and Kuru, 2018; Malhotra and Mukul, 2012 and Okesenya et al., 2020).

Although the significance of fluid loss prevention has been well recognized and appreciable research effort has been contributed toward the plight, the current strategy of dealing with the problem has some underlying deficiencies. The traditional solution to minimize the fluid loss into the reservoir generally includes two techniques, enhancing the mud cake functionalities

with innovative fluid loss additives(Salehi et al., 2015; Zamir and Siddiqui, 2017; Ikram et al., 2021) and increasing the shear viscosity of drilling fluid(Sassen et al., 1990; Zamora et al., 2000 and Khan et al., 2007). The presence of mud cake can lead to a severe outcome of the borehole, such as reducing the borehole diameter and causing differential pipe stuck; also, this strategy usually requires the implementation of additional processes to clean the wellbore post drilling activities. Dehghanpour and Kuru, (2011) propounded that increasing the drilling fluid's shear viscosity to improve filtration loss characteristics may not be desirable all the time due to the fact that additional shear viscosity can induce high annular pressure losses when drilling long horizontal and extended reach wells. To address these problems, the solid-free drill-in fluid will be analyzed in this study to develop a more comprehensive solution for better preventing fluid loss into the formation zone. The solid-free feature will avert the problem induced by mud cake; it also mitigates the chip-hold down effect during drilling operation since it will make drilling fluid penetrate beneath the chip painlessly with less interference of the solid content from drilling fluid.

1.3 Objectives and Scope of Study

The thesis is comprised of three main studies as presented in the Chapters 4,5 and 6. Followings are the specific objectives in each study area:

A Generalized Model for the Field Assessment of Drilling Fluid Viscoelasticity

1. Investigate the factors affecting the viscoelastic properties of a drilling fluid.

2. Develop a generalized model for determining viscoelasticity of a drilling fluid using measurements from standard field-testing equipment.

A Generalized Model for Field Assessment of Particle Settling Velocity in Viscoelastic Fluids

1. Develop a generalized model for the field assessment of particle settling velocity in shear-thinning viscoelastic fluids by using the energy dissipation concept as an indicator of the fluid viscoelasticity.

2. Investigate the significant factors that influence the particle settling velocity to help provide a solution to the potential problem encountered in field drilling operations.

Dynamic Filtration Loss Control Through Optimization of Drilling Fluid Rheological Properties: A Comparative Study of the Fluid Viscoelasticity versus Shear Viscosity Effects

1.Determine the sole contribution of shear viscosity and viscoelasticity to solid-free drill-in fluid's filtration loss characteristics, including static filtration rate, pressure drop, and formation damage.

2.Investigate the dominant fluid properties that controls filtration loss characteristics between shear viscosity and viscoelasticity.

1.4 Contributions of the Current Study

Followings are the contributions of the thesis as presented in their respective areas of the study as follows:

A Generalized Model for the Field Assessment of Drilling Fluid Viscoelasticity:

A new generalized model for estimating drilling fluid elasticity using standard drilling fluid field-testing equipment is presented; it proposes a prudent approach for quantifying the viscoelastic property of a drilling fluid by measuring the amount of energy required to irreversibly

deform a unit volume of viscoelastic fluid. The new methodology, combined with the recommended use of energy dissipation concept, provides a practical tool that can be used for developing optimum drilling fluid formulations and hydraulic programs for effective hole cleaning operations, improved ECD management, and mitigating barite sag problems.

A Generalized Model for Field Assessment of Particle Settling Velocity in Viscoelastic Fluids:

A generalized model for determining particle terminal settling velocity in shear-thinning viscoelastic fluids has been developed. The model uses the concept of energy dissipation to quantify fluid elasticity, which can be conveniently determined by using standard field measurements of AV and funnel viscosity. The new methodology provides a practical tool for determining particle terminal velocity in shear-thinning viscoelastic drilling fluids based on the standard field measurements of drilling fluid properties. Therefore, it can be conveniently used in the field to develop optimum hydraulic programs for effective cuttings transport.

Dynamic Filtration Loss Control Through Optimization of Drilling Fluid Rheological Properties: A Comparative Study of the Fluid Viscoelasticity versus Shear Viscosity Effects

By conducting static filtration rate tests and core flooding experiments to measure, pressure drop, and permeability of the rock samples, we have investigated the individual effect of varying fluid shear viscosity and elasticity on these variables. Understanding the influence of these parameters on filtration loss characteristics, the viscoelasticity of fluid can be adjusted to optimize the filtration loss characteristics. Alternatively, additional viscoelasticity can be utilized to compensate the functionality of shear viscosity, lower concentration of viscosifier will be needed, therefore reducing the cost of drilling fluid. With this in mind, the industry professionals can

ultimately solve the complication to the greatest extend, by designing drilling fluid formulation with a versatile level of viscoelasticity.

1.5 Structure of Thesis

This thesis is comprised of seven chapters. The functionality of each section is explained below:

Chapter 1 Introduction:

The section provides the necessary background information for the current study, including problem statement, objectives, and the contribution of the current study, it also includes the explanation of the thesis structure.

Chapter 2 Literature Review:

The section provides the fundamental rheology knowledge for the better understanding of the current study, including basic rheological principles, different type of non-Newtonian fluids and viscoelasticity phenomena.

Chapter 3 Experimental Program:

This chapter provides a detailed explanation of the experimental set up used in each paper presented in this study, including the methodology for preparing viscoelastic fluids, explanation of various field-testing equipment, design of particle settling system and core-flooding system assembling.

Chapter 4 A Generalized Model for the Field Assessment of Drilling Fluid Viscoelasticity:

This chapter mainly presents the content of the first paper, including assessment of fluid viscoelasticity, field measurements of rheological properties, laboratory characterization of fluid viscoelastic fluid properties, factors affecting the viscoelasticity of drilling fluids model development and statistical evaluation of the model accuracy.

Chapter 5 A Generalized Model for Field Assessment of Particle Settling Velocity in Viscoelastic Fluids:

This chapter mainly presents the content of the second paper, including characterization of fluid viscoelastic behavior, field evaluation of energy dissipation, assessment of true energy dissipation, model development and statistical evaluation of the accuracy of the model prediction.

Chapter 6 Dynamic Filtration Loss Control Through Optimization of Drilling Fluid Rheological Properties: A Comparative Study of the Fluid Viscoelasticity versus Shear Viscosity Effects:

This chapter mainly presents the content of the third paper, including characterization of fluid viscoelasticity, concept of polydispersity and weighted average molecular weight, assessment of formation damage and investigation of sole effects of shear viscosity and fluid viscoelasticity on filtration loss characteristics.

Chapter 7 Conclusions and Recommendations:

The section provides the major conclusions obtained through the experimental study conducted in this thesis, furthermore recommendations are listed out based on the understanding of current study.

1.6 References

Altindal, M C, E Ozbayoglu, S Miska, M Yu, and N Takach. (2017). Impact of Viscoelastic Characteristics of Oil-Based Muds / Synthetic Based Muds on Cuttings Settling Velocities. OMAE2017-62129. ASME 2017 36th International Conference on Ocean, Offshore and Arctic Engineering. June 25–30, 2017. Trondheim, Norway. https://doi.org/10.1115/OMAE2017-62129

Agwu, O. E., Akpabio, J.U, Alabi, S. B et al. 2018. Settling Velocity of Drill Cuttings in Drilling Fluids: A Review of Experimental, Numerical Simulations, and Artificial Intelligence Studies. Powder Tech.339: 728–46. https://doi.org/10.1016/j.powtec.2018.08.064.

Arnipally, S. K., Kuru, E. (2018). Settling Velocity of Particles in Viscoelastic Fluids: A Comparison of the Shear Viscosity vs Elasticity Effect. SPE J. 23 (05):1689–1705.https://doi.org/10.2118/187255-PA

Baldino, S., R. E. Osgouei, E. Ozbayoglu, S. Miska, N. Takach, R. May, and D. Clapper. 2015. "Cuttings Settling and Slip Velocity Evaluation in Synthetic Drilling Fluids." In Offshore Mediterranean Conference and Exhibition, OMC 2015.

Biheri, G., & Imqam, A. (2021). Settling of Spherical Particles in High Viscosity Friction Reducer Fracture Fluids. Energies 2021, Vol. 14, Page 2462, 14(9), 2462. https://doi.org/10.3390/EN14092462

Bizhani, M. and Kuru, E. (2018). Particle Removal From Sandbed Deposits in Horizontal Annuli Using Viscoelastic Fluids. SPE J. 23 (2018): 256–273. Doi: https://doi.org/10.2118/189443-PA

Bui, B., Saasen, A., Maxey, J., Ozbayoglu, E., Miska, S., Yu, M. (2012). Viscoelastic properties of oil-based drilling fluids. Annual Trans Nordic Rheol Soc. 20. 33-47.

Chhabra, R. P. (2007). Bubbles, Drops, and Particles in Non-Newtonian Fluids. Bubbles, Drops, and Particles in Non-Newtonian Fluids. CRC Press. Boca Raton, FL. https://doi.org/10.1201/9781420015386

Clift, R, J R Grace, and M E Weber. 1978. Bubbles, Drops, and Particles., 2005. Dover Publications Inc. Mineola, New York. ISBN:0-486-44580-1.

Cobianco, S., Bartosek, M., Lezzi, A., & Guarneri, A. (2001). How To Manage Drill-In Fluid Composition To Minimize Fluid Losses During Drilling Operations. *SPE Drilling & Completion*, *16*(03), 154–158. https://doi.org/10.2118/73567-PA

Dehghanpour, H., & Kuru, E. (2011). Effect of viscoelasticity on the filtration loss characteristics of aqueous polymer solutions. *Journal of Petroleum Science and Engineering*, *76*(1–2), 12–20. https://doi.org/10.1016/J.PETROL.2010.12.005

Fink, J. (2021). Fluid loss additives. In *Petroleum Engineer's Guide to Oil Field Chemicals and Fluids*. Elsevier. https://doi.org/10.1016/B978-0-323-85438-2.00002-5

Hirpa, M.M. and Kuru, E. (2020). Hole Cleaning in Horizontal Wells Using Viscoelastic Fluids: An Experimental Study of Drilling-Fluid Properties on the Bed-Erosion Dynamics. SPE J. 25 (2020): 2178–2193. Doi: https://doi.org/10.2118/199636-PA

Ikram, R., Jan, B. M., Sidek, A., Kenanakis, G., Jan, M., Sidek, B. ;, Kulinich, S., Svetlichnyi, V. A., Kuchmizhak, A., & Honda, M. (2021). Utilization of Eco-Friendly Waste Generated

Nanomaterials in Water-Based Drilling Fluids; State of the Art Review. *Materials 2021, Vol. 14, Page 4171*, *14*(15), 4171. https://doi.org/10.3390/MA14154171

Khan, R., Kuru, E., Tremblay, B., & Saasen, A. (2007). Extensional Viscosity of Polymer Based Fluids as a Possible Cause of Internal Cake Formation. *Http://Dx.Doi.Org/10.1080/00908310600626630*, *29*(16), 1521–1528. https://doi.org/10.1080/00908310600626630

Lomba, R. F. T., Martins, A. L., Soares, C. M., Brandao, E. M., Magalhaes, J. V. M., & Ferreira, M. V.D. (2002). Drill-In Fluids: Identifying Invasion Mechanisms. *Proceedings - SPE International Symposium on Formation Damage Control*, 131–142. https://doi.org/10.2118/73714-MS

Malhotra, Sahil, and Mukul M. Sharma. 2012. "Settling of Spherical Particles in Unbounded and Confined Surfactant-Based Shear Thinning Viscoelastic Fluids: An Experimental Study." Chemical Eng. Sci. 84 (1:646–55). https://doi.org/10.1016/j.ces.2012.09.010.

Okesanya, T., Kuru, E., & Sun, Y. (2020). A New Generalized Model for Predicting the Drag Coefficient and the Settling Velocity of Rigid Spheres in Viscoplastic Fluids. SPE Journal, 25(06), 3217–3235. https://doi.org/10.2118/196104-PA.

Powell, J. W., Parks, C. F., and Seheult, J. M. (1991). Xanthan and Welan: The Effects of Critical Polymer Concentration on Rheology and Fluid Performance. International Arctic Technology Conference. Society of Petroleum Engineers. https://doi.org/10.2118/22066-MS.

Saasen, A., Tengbreg-Hansen, H., Marken C., and Stavland A.: “Influence of linear Viscoelastic Properties on Invasion of Drilling Fluid Filtrate into a Porous Formation”, Oil Gas European Magazine, Vol.4, 1990.

Saasen, A. and Løklingholm, G. (2002). The Effect of Drilling Fluid Rheological Properties on Hole Cleaning. IADC/SPE Drilling Conference. Dallas, Texas, 26-28 February, SPE-74558-MS, DOI: 10.2118/74558-MS.

Salehi, S. (2015). SPE-174273-MS Study of Filtrate and Mud Cake Characterization in HPHT: Implications for Formation Damage Control. http://onepetro.org/SPEEFDC/proceedings-pdf/15EFDC/All-15EFDC/SPE-174273-MS/1438069/spe-174273-ms.pdf/1

Shah, S. N, El-Fadili, Y.E, and Chhabra, R.P. 2007. New Model for Single Spherical Particle Settling Velocity in Power Law (Visco-Inelastic) Fluids. International Journal of Multiphase Flow. 33: 51–66. https://doi.org/10.1016/j.ijmultiphaseflow.2006.06.006

Shahi, S., & Kuru, E. (2016). Experimental investigation of the settling velocity of spherical particles in Power-law fluids using particle image shadowgraph technique. International Journal of Mineral Processing, 153, 60–65. https://doi.org/10.1016/J.MINPRO.2016.06.002.

Wilson, K. C., Horsley, R. R., Kealy, T., Reizes, J. and Horsley, M. (2003). Direct prediction of fall velocities in non-Newtonian materials. International Journal of Mineral Processing. 71(1–4), pp. 17–30. DOI: 10.1016/S0301-7516(03)00027-9.

Zamora, M., Jefferson, D. T., Powell, J. W. (1993). Hole-Cleaning Study of Polymer-Based Drilling Fluids. Society of Petroleum Engineers. Doi :10.2118/26329-MS.

Zamir, A., & Ahmad Siddiqui, N. (2017). *Investigating and Enhancing Mud Cake Reduction Using Smart Nano Clay Based WBM*. *8*, 1. https://doi.org/10.4172/2157-7463.1000315

CHAPTER 2 Literature Review

The purpose of this chapter is to provide fundamental knowledge and review the previous literature for specific research area presented in the chapter 4, 5, and 6. The fundamental knowledge includes the basic rheological principles, characteristics of different types of non-Newtonian fluids, polydispersity, weighted average molecular weight and viscoelasticity phenomena. The literature review is intended to provide the interpretation of the existing literature and provide background information for better understanding of the research problems investigated in this study.

2.1 Background

Viscoelastic properties of drilling fluids have drawn much attention in the drilling industry because of the critical role they play in various drilling activities, including evaluation of frictional pressure loss, particles suspension ability, hole cleaning efficiency, fluid loss prevention and preserving formation integrity. The functionality of drilling fluids in these critical processes is primarily dependent on their rheological properties, to be more specific the performance of drilling fluid is largely influenced by shear viscosity and viscoelasticity. For example, the particle's settling velocity tend to be hindered with increasing viscoelasticity, such phenomena is induced by the unique characteristic of viscoelasticity, the viscoelastic structure within the fluid tend to regain its original shape when experiencing deformation, the particle tend to bear more resistance during its settling process. Utilizing the idea of viscoelasticity can be beneficial for drilling fluid's suspension ability, and ultimately help field personnel to optimize hydraulic design. Knowing the importance of drilling fluid's rheological properties, in this section, necessary rheological

principles will be explained for a better understanding. Furthermore, previous research will be reviewed here to understand how the rheological properties affect various key process in different drilling activities.

2.2 Basic Rheological Principles

Rheological behavior of drilling fluids is one of the most dominant factors that controls the functionality of drilling fluids. It is indeed necessary to get familiar with basic principles. In this section, a summary of basic rheological properties will be presented to understand how the behavior of non-Newtonian fluid influence specific drilling activities.

2.2.1 Shear Stress, Shear Rate, Shear Strain and Viscosity

Shear stress is induced by the tangential force acting on the fluid, (F) shown in Fig 2.1. The tangential force tend to cause top fluid layers to slide over the bottom layers. The shear stress can be computed with Eq 2.1, it is calculated by dividing the tangential force acting on fluid by the shear area (A), the S.I unit of shear stress is Pa (pascal).

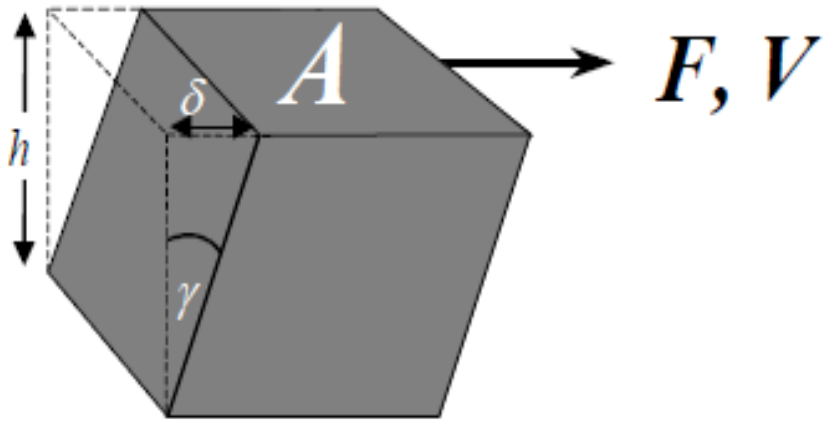

Figure 2.1 Demonstration of Shear Flow (Barnes, 2000)

$$\tau = \frac{F}{A} \qquad 2.1$$

Shear rate is defined as the shear gradient between the neighbouring flowing layers in the perpendicular direction of the flow. Sometimes it is also referred as velocity gradient and rate of deformation. It can be computed by dividing the velocity of the top layer (V) by the distance between the top and bottom layers (h), the shear rate can be mathematically represented with Eq 2.2, the S.I unit of shear rate is 1/s.

$$\dot{\gamma} = \frac{V}{h} \qquad 2.2$$

Shear strain is the ratio of the change induced by deformation to its original length, it is shown as (γ) in Fig 2.1, the unit for shear strain is fraction.

For all flowing fluids, the molecules are showing relative motion between each other, and this process is always combined with internal frictional forces, therefore for all fluids in motion, a certain flow resistance is occurring which may be determined in terms of viscosity. (Mezger, 2006) The viscosity can be computed by dividing the shear stress over shear rate, and the equation is shown as Eq 2.3, the S.I unit of viscosity is Pa.s (pascal seconds).

$$\mu = \frac{\tau}{\dot{\gamma}} \qquad 2.3$$

2.2.2 Shear-Thinning Flow Behavior and Viscoelastic Behavior

Two major types of non-Newtonian fluids were utilized in this study, including shear-thinning fluid and viscoelastic fluid; detailed explanation will be provided to help understand characteristic of these fluids.

2.2.2.1 Shear-Thinning Behavior

Viscosity of a shear-thinning material depends on the degree of the shear load (shear rate or shear stress, respectively). The flow curve shows a decreasing curve slope as shown in Fig 2.2, viscosity decreases with increasing load as shown in Fig 2.3. The trend in these graphs have shown that the apparent viscosity of shear-thinning fluid is inverse proportional to the shear stress and shear rate. The shear-thinning behavior can be characterized mathematically in various ways (Chhabbra, 2006); however, we utilized the most general approach to characterize the shear-thinning behavior, which is shown in Eq 2.4, also referred as the power-law relationship.

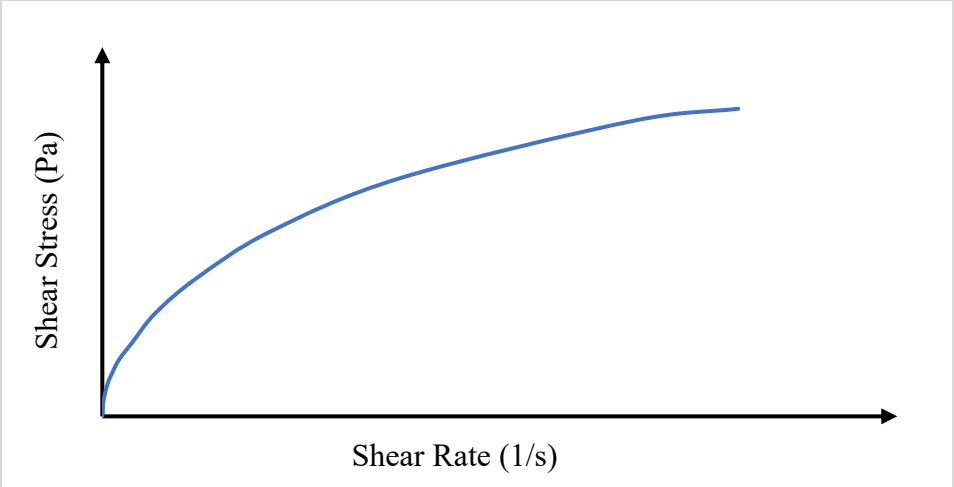

Figure 2.2 Flow Curve of a Shear-Thinning Liquid

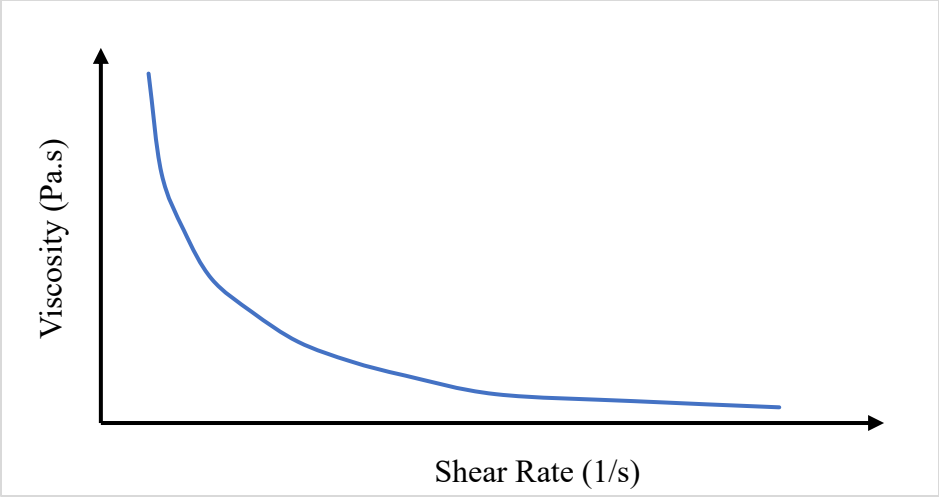

Figure 2.3 Viscosity Curve of a Shear-Thinning Liquid

$$\tau = K\dot{\gamma}^{n} \qquad 2.3$$

The term "K" is called flow consistency index, the S.I unit for it is $Pa.s^n$, the term "n" is called flow behavior index, it has no unit. A typical shear-thinning fluid will have a rheogram like Fig 2.2. One can obtain the power law relationship between shear stress and shear rate by conducting controlled shear rate test.

2.2.2.2 Viscoelastic Behavior

Viscoelasticity is a property of materials that exhibit elastic and viscous properties at the same time when undergoing deformation. Elastic property is the unique characteristic of a material to regain its original shape after being deformed, which is achieved by storing energy. The elastic state follows the Hooke's law which states that shear stress is directly proportional to the strain (Eq 2.4). A representative example for elastic portion of viscoelastic material is a steel spring. The

spring can fully recover after releasing the stress exerted on it, and it will not bear permanent deformation.

$$\tau = G\frac{dx}{dy} \qquad 2.4$$

Where:

G = Shear Modulus, Pa

$\frac{dx}{dy}$ = Strain

The viscous property refers to its ability to dissipate energy after experiencing external stress, causing irreversible deformation. Knowing the attributes of both viscous properties and elastic properties, the viscoelastic behavior can be illustrated with the famous Maxwell model, which consists of a dashpot and a spring (Fig 2.4). When the viscoelastic material experiences external stress, it will only regain partial of its original shape; a portion of energy is dissipated during deformation, which corresponds to the viscous property of the viscoelastic material; the rest of energy is stored within the structure for returning to its original state which corresponds to the elastic property of the viscoelastic material.

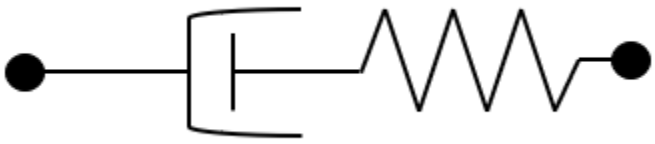

Figure 2.4 Spring Dashpot/Maxwell Model

There are some also common phenomena associated with the viscoelastic properties, including die swell and Weissenberg effect. To show an example, die swell can be utilized to judge if the fluid is viscoelastic; the effect is also referred as post-extrusion swelling effect (Fig 2.5). The viscoelastic fluid tends to be deformed when existing the extrusion die, after leaving the die (removing the load), it will immediately try to regain its original structure, therefore the expansion of fluid can be observed. On the other hand, the purely viscous fluid does not show die swell feature since it does not possess elastic property, the external deformation energy is totally dissipated.

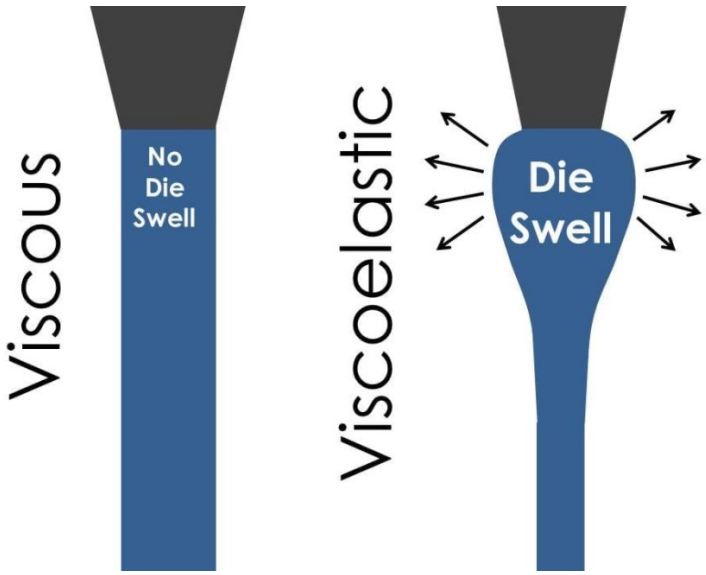

Figure 2.5 Die Swell/Post Extrusion Effect (The Centre for Industrial Rheology, 2022)

There have been numerous approaches to quantify the level of viscoelasticity in the past, including elastic modulus in linear viscoelastic region (G'-LVE), stretchiness (elastic modulus-viscous modulus cross-over strain), longest relaxation time, extensional viscosity, Deborah number, and Weissenberg number (Veerabhadrappa et al., 2013; Trivedi and Kuru, 2010; Poole, 2012 and Ofei et al., 2020). These elasticity indicators have been utilized frequently in engineering

research; however, some demerits need to be cogitated depending on the specific trait of versatile engineering processes. Considering the practicality of field operations, including drilling, completion, and stimulation activities, the characterization of drilling fluid's viscoelasticity needs to be accomplished in a timely-urgent and field-accessible manner to fit into the nature of these operations. In such a case, the longest relaxation time, extensional viscosity, Deborah number, and Weissenberg number would not be the recommended choice since these parameters generally require advanced rheometer measurements and are mainly subject to characterize viscoelasticity of the small-scale deformation process. This study will utilize an innovative approach to assess viscoelastic behavior with energy dissipation to address the plight. The energy dissipation not only can be quantified by using conventional field-testing equipment, including funnel viscometer and Fann viscometer but also can be determined with amplitude sweep test with a comprehensive physical origin (Chen et al., 2021), providing convenience for both industry professionals and researchers. A detailed explanation of the concept of "Energy Dissipation" will be provided in the next section.

2.3 Polydispersity and Weighted Average Molecular Weight

The fluid's shear-thinning characteristics and viscoelasticity are primarily dependent on two properties, including the weighted average molecular weight and the molecular distribution of the polymer additive. The polymer additive with the same weighted average molecular weight can be used to formulate fluids with similar shear viscosity (Santhosh, 2012); therefore, to prepare the fluids with similar shear-thinning characteristics, the polymer blend for viscosifying the fluid should have the same average molecular weight, which can be computed with Eq 2.5.

Furthermore, to have various levels of viscoelasticity, the polymer blend should have a different polydispersity index, which has been proved to be an acceptable criterion for quantifying the molecular weight distribution. Knowing the proportional ship between viscoelasticity and molecular weight distribution, higher the polydispersity index therefore signifies more significant viscoelastic behavior (Santhosh,2012). As the polydispersity index value increases the heterogeneity in cross-linking, network formation, chain length, branching, hyper branching will be more with more random arrangement, which is also believed to increase the fluid elasticity. (Dehghanpour, 2011; Zang, 1987; and Veerabhadrappa, 2013) Therefore, we used the polydispersity index (PI) as a relative measure of the degree of fluid elasticity for initial formulation and screening purposes of the different polymer blends. Generally, polymer blends of the same average molecular weight and different polydispersity index values can be used to formulate fluids with similar shear viscosity and variable elasticity. (Dehghanpour, 2011; Zang, 1987; and Veerabhadrappa, 2013) The polydispersity index can be computed with Eq 2.6. Both average molecular weight and polydispersity index can be controlled by adjusting the polymer blend composition.

$$M_{w,B} = \prod_{i=1}^{n} M_{w,i}^{\omega_i} \tag{2.5}$$

$$I = \frac{M_w}{M_n} = \left(\sum_{i=1}^{n} \omega_i M_{w,i} \right) \times \left(\sum_{i=1}^{n} \frac{\omega_i}{M_{w,i}} \right) \tag{2.6}$$

Where:

M_w = average molecular weight of polymer blend, g/g mol

I = polydispersity index

ω_i = weight fraction, fraction

2.4 Concept of Energy Dissipation

Viscoelastic characteristics of a fluid can be determined by using amplitude sweep test data. Typical amplitude sweep data obtained from oscillatory rheometer tests are shown in Fig 2.6 and Fig 2.7 , where variations of the elastic modulus (G') and loss modulus (G") measurements were plotted as a function of the oscillation strain and oscillation stress, respectively.

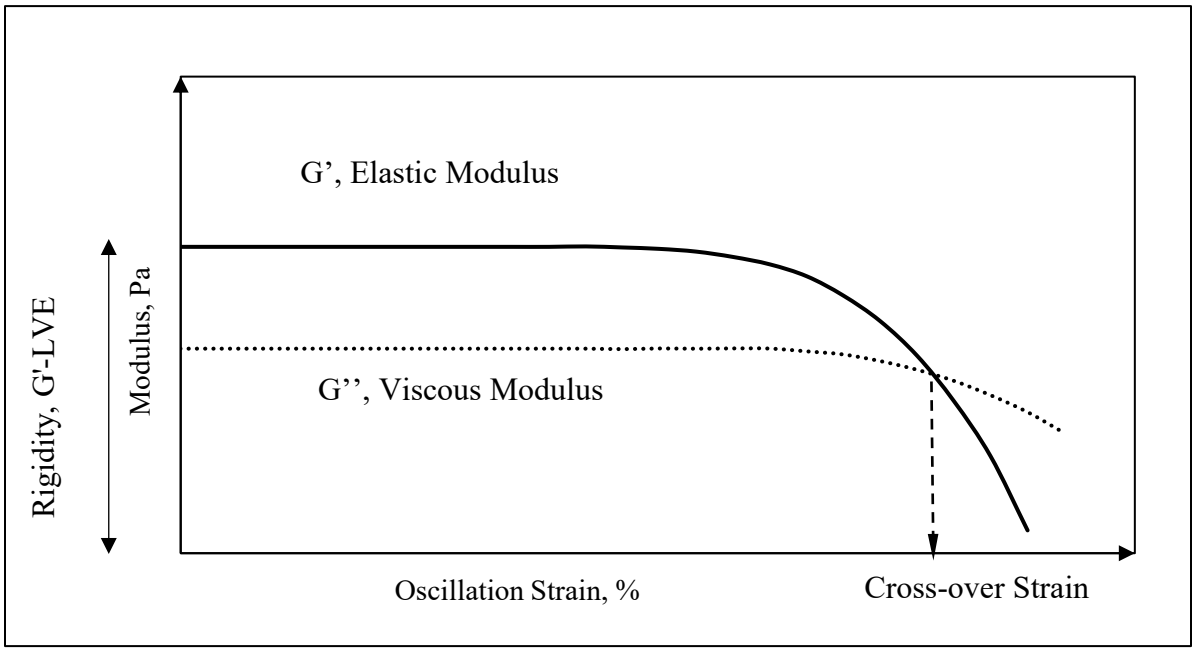

Figure 2.6 Typical Amplitude Sweep Test Result Shown as a Function of Oscillation Strain

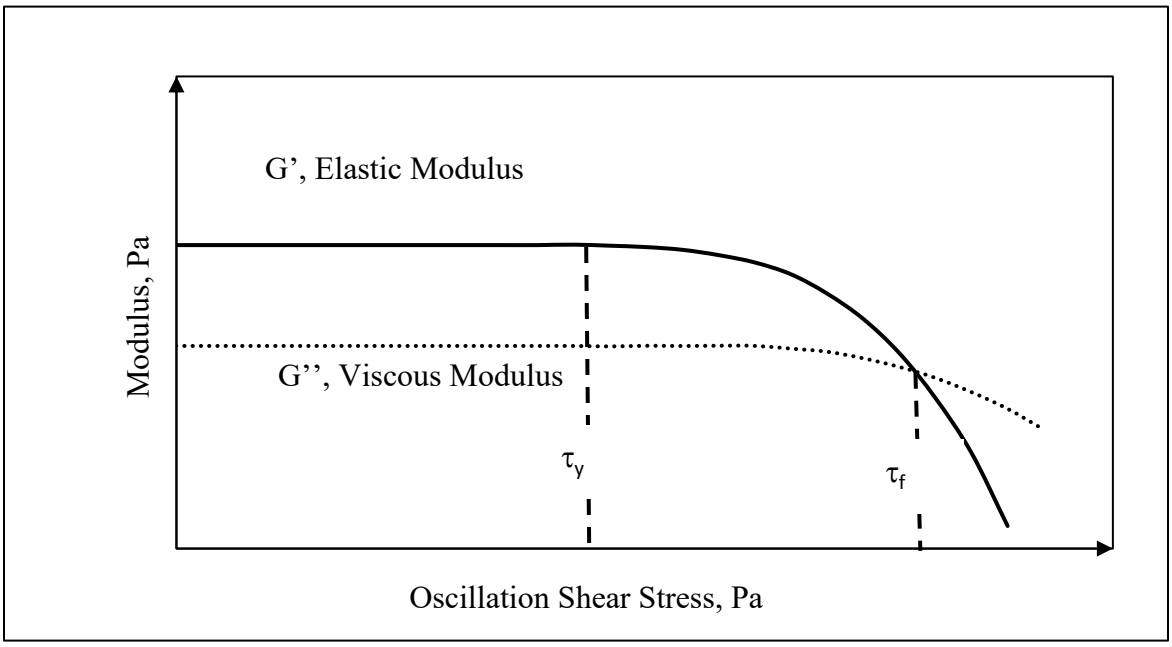

Figure 2.7 Typical Amplitude Sweep Test Result Shown as a Function of Oscillation Stress

The elastic modulus, G', corresponds to the constant plateau value in the linear viscoelastic region (LVE), where the deformation of the fluid-structure under stress is reversible, and the fluid can fully recover from the deformation once the stress is released. The crossover strain defines the maximum strain that can be applied before the viscous modulus (G") surpasses the elastic modulus (G'). After the cross-over point, the viscous behavior dominates over the elastic behavior, and the sample would experience permanent deformation under stress. The fluid viscoelasticity is generally quantified either by using the fluid rigidity (i.e., G' in the LVE region) or stretchiness (i.e., strain value at the crossover of G' and G") values, and both parameters can be obtained from an Amplitude Sweep Test result (Fig 2.6). Both the rigidity and stretchiness parameters can serve as the indicator of the strength of the viscoelasticity to some extent; however, from the practical point of view, neither the rigidity nor the stretchiness can fully demonstrate the level of fluid

elasticity. Two viscoelastic fluids with the same rigidity (G') values but with different stretchiness do not necessarily have identical performance under the same deformation process. Therefore, a more comprehensive approach is needed for the more realistic assessment of the fluid elasticity.

Maxey(2010) claimed that the fluid viscoelasticity could be better described by using the concept of Energy Dissipation (E_D), which entails the minimum energy required for transferring liquid from elastic state to viscous state. In a physical sense, E_D describes the threshold energy needed to break the internal structure of the viscoelastic fluid. Generally, fluids with higher elasticity will require more energy dissipation per unit volume to transfer from elastic to the viscous state of flow. Having obtained the stress versus strain relationship of a fluid from a typical amplitude sweep test data (i.e., the combination of data shown in Figs 2.6 and 2.7), the energy dissipation can be conveniently assessed by simple integration of the oscillation stress as a function of the oscillation strain. (Eq 2.7) The S.I unit for energy dissipation is J/m^3.

$$E_D = \int \tau \, d\gamma \qquad 2.7$$

Where:

E_D = energy dissipation, J/m^3

τ = oscillation stress, pa

γ = oscillation strain

To be more specific, energy dissipation can be computed using a simple two-step method, first plot the oscillation stress versus oscillation strain until gel point using amplitude sweep test

result (Fig. 2.8), then calculate the area under the plotted curve, which is the integral of oscillation stress over oscillation strain, the produced value is the energy dissipation.

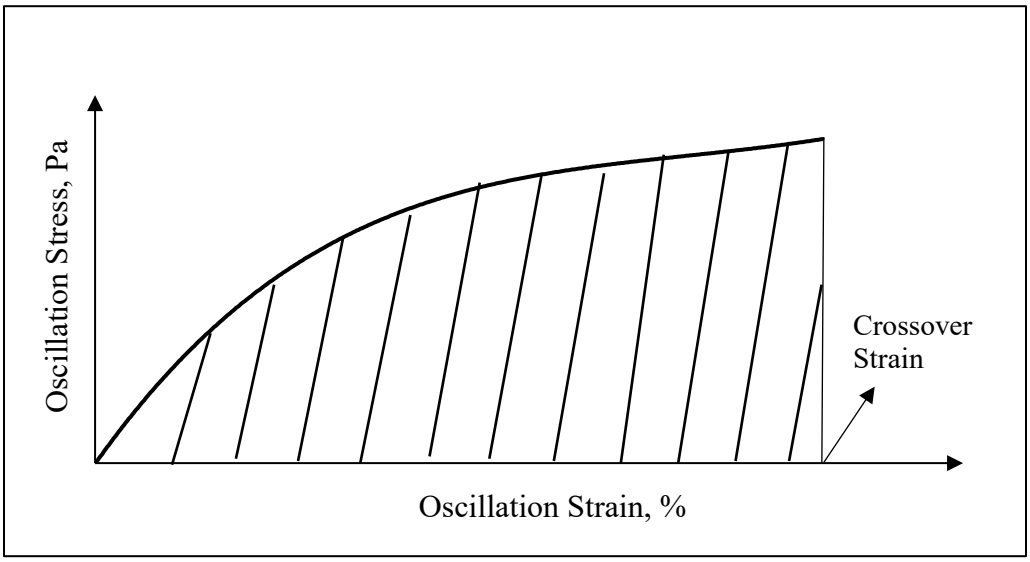

Figure 2.8 Oscillation Shear Stress Versus Oscillation Strain Plot Used for the Assessment of Energy Dissipation

Maxey(2010) also suggested that the energy dissipation can be estimated by using the crossover point (also known as gel point or flow point) in a typical amplitude sweep test data (Figs. 2.6 and 2.7) as a reference point, i.e., cross-over strain (Fig 2.6) is the upper limit of the integral in Eq 2.7. The flow point in an amplitude sweep test indicates the maximum stress-strain values (and hence the total energy) required for a fluid to transfer from an elastic state to a viscous state. Therefore, it is plausible to determine the energy dissipation at this specific point.

2.5 Literature Review

This section will include three separate parts of literature review, corresponding to the three papers presented in Chapter 4, 5 and 6 respectively.

2.5.1 Importance of Having a Practical Tool to Quantify Viscoelasticity in the Field

Viscoelasticity of drilling fluids has drawn significant attention in the drilling industry recently, due to the important role it plays in the assessment of frictional pressure loss, particle settling velocity, and hole cleaning efficiency (Bui et al., 2012).

Powell et al., (1991) related the gel-like behavior of biopolymer fluids to their viscoelasticity and reported that fluid elasticity improved the solid suspension ability of these fluids. Zamora et al., (1993) investigated cuttings transport performance of biopolymer fluids under laminar flow conditions and stated that superior drill cuttings suspension ability and hole-cleaning performance of biopolymer fluids in laminar flow could be attributed to the viscoelastic characteristics of these fluids.

Based on their field experiences from North Sea operations, Saasen and Loklingholm, (2002) concluded that the gel forming as a result of the interaction of cuttings bed and viscoelastic polymer-based drilling fluids would be one of the main factors causing the observed poor hole cleaning performance of these fluids. Similar results were also reported by Rabenjafimanantsoa et al., (2005), where they observed that the polymer-water mixture forms a gel, which resulted particles to be glued together and, as a result, the cuttings bed became more consolidated.

Cuttings transport experiments conducted by Sayindla et al., (2017) and Werner et al., (2017) have shown that oil-based fluids have superior cuttings transport abilities as compared to water-based fluids with similar viscometry properties but different viscoelastic properties. Werner et al., (2017) also reported that the water-based drilling fluids used in their study had no yield stress but a 50 to 100% higher elasticity than the oil-based drilling fluids, indicating the lower

viscoelasticity of the oil-based fluids would be one of the main reasons behind their favorable cuttings transport performance.

Arnipally and Kuru, (2018) reported that models not taking the fluid elasticity effect into account could over predict the settling velocity of particles in a viscoelastic fluid by as much as 14 to 50 times.

Recent laboratory investigations (Bizhani and Kuru, 2018; Hirpa and Kuru, 2020) have shown that much higher critical flow rates were required for the initiation of bed erosion/hole cleaning when using viscoelastic drilling fluids. Bizhani and Kuru, (2018) concluded that additional elastic normal forces arising from the variable normal stress differences of viscoelastic fluids could be responsible for delaying the onset of the bed erosion.

All these previous field experience and lab data strongly suggest that fluid elastic properties are important in hole cleaning and should be given due consideration together with the viscous properties to assess the solids transport ability of a drilling fluid.

Despite the impact of fluid viscoelasticity on the drilling hydraulics design has been well recognized, currently there is no standard field technique available for measuring the fluid viscoelastic properties. The viscoelastic properties can only be measured in the lab by using advanced rheometers, which are not suitable for field applications. There is a need for development of a methodology that can be used in the field to determine the viscoelastic properties of drilling fluids using standard field-testing equipment.

2.5.2 Development of Generalized Model for Determining Particle's Settling Velocity in Viscoelastic Fluid

Viscoelastic properties of drilling fluids have drawn much attention in the drilling industry because of the critical role they play in the evaluation of frictional pressure loss, particle settling velocity, and cuttings transport efficiency (Powell et al., 1991; Zamora et al., 1993; Saasen and Loklingholm, 2002; Bui et al., 2012; Sayindla et al., 2017; Werner et al., 2017; Arnipally and Kuru, 2018; Bizhani and Kuru, 2018; Hirpa and Kuru, 2020).

Powell et al., (1991) observed that fluid elasticity could enhance the solid suspension ability of polymer-based drilling fluids. Zamora et al., (1993) suggested that improved drill cuttings suspension ability and cuttings transport performance of polymer-based fluids could be due to the viscoelastic characteristics of these fluids.

Saasen and Loklingholm, (2002) reported that the gel-forming due to the interaction of cuttings bed and viscoelastic polymer-based drilling fluids would be one of the main factors causing the observed poor hole cleaning performance of these fluids in North Sea operations. Similarly, Rabenjafimanantsoa et al., (2005) claimed that the polymer-based fluids could form a gel, causing to bond the particles together and, as a result, consolidate the cuttings bed.

Sayindla et al., (2017) and Werner et al., (2017) have shown that oil-based fluids have better hole cleaning abilities than water-based fluids having similar shear viscosity but higher elasticity. Recent laboratory studies (Bizhani and Kuru, 2018; Hirpa and Kuru, 2020) have reported that much higher critical flow rates were needed for the onset of bed erosion/hole cleaning when using viscoelastic drilling fluids. Arnipally and Kuru, (2018) reported that models not taking

the fluid elasticity effect into account could overpredict the settling velocity of particles in a viscoelastic fluid by as much as 14 to 50 times.

Researchers investigating the proppant transport efficiency of fracturing fluids recommended that both shear viscosity and viscoelasticity of the fracturing fluid need to be considered to determine optimum fracturing fluid rheological properties for effective proppant transportation (Malhotra and Sharma, 2013; Biheri et al., 2021).

Particle settling velocity is one of the key variables required for optimum hydraulic design of fluid-solid transport systems that have been commonly used in various oil field operations such as proppant transport in hydraulic fracturing (Shah et al., 2007) and cuttings transport in drilling (Baldino et al., 2015 and Altindal et al., 2017).

Settling behavior of particles in Newtonian (Clift et al., 1978; Turton and Levenspiel, 1986; R. Chhabra, 2006; Shahi and Kuru, 2015) and non-Newtonian fluids (Chien, 1994; Miura et al., 2001; Wilson, 2003; Kelessidis, and Mpandelis, 2004; Shah et al., 2007; Arabi et al., 2016; Shahi and Kuru, 2016; Rushd et al., 2018 and Okesanya et al., 2020) have been extensively investigated in the past. However, in addition to showing non-Newtonian rheological behavior, most fluids used in the oil field also have elastic characteristics (Bui et al., 2012 and Agwu et al., 2018).

Traditionally, the hole cleaning/cuttings transport performance in drilling has been managed by controlling low shear rate viscosity (LSRV) and the yield point (YP) of the drilling fluids or using higher flow rates. However, from the field operational point of view, using fluids with high YP or pumping at higher flow rates may not always be feasible; because of the resultant increase in parasitic pressure losses, which potentially has a negative effect on the drilling rate and

pumping costs. Results of the previous lab investigations and field observations strongly suggest that fluid elastic properties need to be considered together with the viscous properties for a more accurate prediction of solids' transportability of drilling fluids. Therefore, it is critical to find a balance between the viscous and elastic properties when adjusting the rheological properties of drilling fluids aiming to fulfill their diverse functions in drilling operations. It is essential to predict the terminal velocity in the shear-thinning viscoelastic drilling fluid considering both viscous and elastic properties synchronously.

Investigating the effect of fluid elasticity on the particle settling velocity independent from shear viscosity has been a real challenge in theoretical developments as well as in experimental studies, which complicates the accurate assessment of the particle settling velocity in viscoelastic fluids (Malhotra and Sharma, 2012; Arnipally and Kuru, 2018 and Okesanya et al., 2020).

Researchers used the concept of polydispersity index to resolve this conundrum; which enables the formulation of viscoelastic fluids that have similar shear thinning characteristics while having different elasticity (Dehghanpour and Kuru, 2011; Arnipally and Kuru, 2018). By doing so, the effect of viscoelasticity could be better monitored and eventually correlated with the extra resistance experienced by the particles settling in shear-thinning viscoelastic fluid during the settling process.

The rheological characterization of drilling fluid is usually accomplished on-site in an urgent, timely manner with field assessment. Although the importance of the fluid viscoelastic properties on the cuttings transport and other drilling hydraulics-related design problems have been well recognized; there has not been any standard procedure available for determining the fluid viscoelastic properties in the field. The viscoelastic fluid properties are usually measured in the lab

using advanced rheometers, which are not suitable for field applications. It is, therefore, crucial to come up with a methodology for the field assessment of the terminal settling velocity of particles in the viscoelastic fluids; which would allow field people to conveniently monitor the performance of drilling fluids in terms of their particle suspension ability and carrying capacity in drilling operations.

2.5.2 The Influence of Shear Viscosity and Viscoelasticity on Filtration Loss Characteristics

Strict control of drilling fluid filtration loss characteristics is required to limit borehole instability, excessive torque, and drag, differential pipe stuck, and formation damage (Cobianco et al., 2001). The problem becomes more critical when drilling/completing horizontal wells with water-based fluids where the fluid remains in contact with the pay zone for an extended period. Controlling filtration loss characteristics is, therefore, considered as one of the most critical tasks when designing optimum drilling fluid formulations for best drilling performance while preserving the original reservoir rock properties (Chesser et al., 1994; Lomba et al., 2002; Anyanwu and Momoh, 2016 and Fink, 2021).

Despite the fact that the significance of fluid loss prevention has been well recognized and appreciable research effort has been contributed toward the plight, the current strategy of dealing with the problem has some underlying deficiencies. The traditional solution to minimize the fluid loss into the reservoir generally includes two techniques, enhancing the mud cake functionalities with innovative fluid loss additives(Salehi et al., 2015; Zamir and Siddiqui, 2017 and Ikram et al., 2021) and increasing the shear viscosity of drilling fluid(Sassen et al., 1990; Zamora et al., 2000 and Khan et al., 2007). The presence of mud cake can lead to a severe outcome of the borehole, such as reducing the borehole diameter and causing differential pipe stuck; also, this strategy

usually requires the implementation of additional processes to clean the wellbore post drilling activities. Increasing the drilling fluid's shear viscosity to improve filtration loss characteristics may not be desirable all the time due to the fact that additional shear viscosity can induce high annular pressure losses when drilling long horizontal and extended reach wells (Dehghanpour and Kuru, 2011).

To address these problems, the solid-free drill-in fluids will be analyzed in this study to develop a more comprehensive solution for better preventing fluid loss into the reservoir. The solid-free feature will avert the problem induced by mud cake; it also mitigates the chip-hold down effect during drilling operation since it will make drilling fluid penetrate beneath the chip painlessly with less interference of the solid content from drilling fluid.

Although solid-free drill-in fluid has many merits compared with traditional drilling fluid, maintaining the flow resistance from the wellbore to formation can be a significant challenge; mainly because higher pressure loss is needed to compensate for the flow resistance induced by mud cake. Purely increasing the shear viscosity for increasing the pressure loss across the wellbore will likely cause undesirable outcomes, as mentioned previously. Instead of exclusively relying on the shear viscosity of drilling fluid to amplify the flow resistance, the viscoelastic fluid is utilized to ameliorate the performance of drill-in fluid in this study. Dehghanpour and Kuru, (2011) have asserted that the viscoelastic fluid has a very practical appeal in many petroleum engineering applications because controlling the damage due to the drilling fluid invasion into the reservoir rock has a significant impact on the oil and gas production rates. Durst et al., (1987) also found evidence that as much as 75% of the pressure losses in the formation may result from extensional viscosity, which is generally considered as the elasticity indicator.

Albeit viscoelasticity has been proven to be beneficial in preventing fluid loss (Gupta and Sridhar, 1985; Saasen et al., 1990; Khan et al., 2004 and Khan et al., 2007), there has not been adequate research conducted toward determining the independent effect of shear viscosity and viscoelasticity on filtration loss characteristics, including static filtration rate, pressure drop, and formation damage; explicitly because of the difficulty of differentiating two properties. In this study, by using the concept of polydispersity (Arnipally and Kuru, 2018 and Okesanya et al., 2020), the fluids are prepared in an ideal condition to demonstrate the sole contribution of two rheological properties toward filtration loss characteristics.

Furthermore, there is still extant confusion about the dominant role in controlling filtration loss properties; such confusion is not a trivial problem; possessing an excess of either rheological property can potentially cause undesired issues that will have a tremendous negative impact on the subsequent operations post drilling activities, leading to enormous economic and time expense. Therefore, determining the prominent role in controlling filtration loss characteristics becomes the primary objective in this study.

2.6 References

Altindal, M C, E Ozbayoglu, S Miska, M Yu, and N Takach. (2017). Impact of Viscoelastic Characteristics of Oil-Based Muds / Synthetic Based Muds on Cuttings Settling Velocities. OMAE2017-62129. ASME 2017 36th International Conference on Ocean, Offshore and Arctic Engineering. June 25–30, 2017. Trondheim, Norway. https://doi.org/10.1115/OMAE2017-62129.

Agwu, Okorie E., Julius U. Akpabio, Sunday B. Alabi, and Adewale Dosunmu. 2018. Settling Velocity of Drill Cuttings in Drilling Fluids: A Review of Experimental, Numerical Simulations,

and Artificial Intelligence Studies. Powder Technology 339: 728–46. https://doi.org/10.1016/j.powtec.2018.08.064.

Anyanwu, C., and Momoh, U. "Experimental Evaluation of Particle Sizing in Drilling Fluid to Minimize Filtrate Losses and Formation Damage." Paper presented at the SPE Nigeria Annual International Conference and Exhibition, Lagos, Nigeria, August 2016. doi: https://doi.org/10.2118/184303-MS

Arabi, Ameneh S., Sean Sanders, R., 2016. Particle terminal settling velocities in non- Newtonian visco-plastic fluids. Can. J. Chem. Eng. 94 (6), 1092–1101. https://doi. org/10.1002/cjce.22496.

Arnipally, S. K., & Kuru, E. (2018). Settling Velocity of Particles in Viscoelastic Fluids: A Comparison of the Shear-Viscosity and Elasticity Effects. *SPE Journal*, *23*(05), 1689–1705. https://doi.org/10.2118/187255-PA

Baldino, S., R. E. Osgouei, E. Ozbayoglu, S. Miska, N. Takach, R. May, and D. Clapper. 2015. "Cuttings Settling and Slip Velocity Evaluation in Synthetic Drilling Fluids." In Offshore Mediterranean Conference and Exhibition, OMC 2015.

Biheri, G., & Imqam, A. (2021). Settling of Spherical Particles in High Viscosity Friction Reducer Fracture Fluids. Energies 2021, Vol. 14, Page 2462, 14(9), 2462. https://doi.org/10.3390/EN14092462

Bizhani, M. and Kuru, E. (2018). Particle Removal from Sand bed Deposits in Horizontal Annuli Using Viscoelastic Fluids. SPE J. 23 (2018): 256–273. Doi: https://doi.org/10.2118/189443-PA

Bui, B., Saasen, A., Maxey, J., Ozbayoglu, E., Miska, S., Yu, M. (2012). Viscoelastic properties of oil-based drilling fluids. Annual Trans Nordic Rheol Soc. 20. 33-47.

Chen, H., Temi, O., Ergun, K., Garett, H., & Dylan, H. (2021). A Generalized Model for the Field Assessment of Drilling Fluid Viscoelasticity. *Proceedings - SPE Annual Technical Conference and Exhibition*, *2021-September*, 205953. https://doi.org/10.2118/205953-MS

Chhabra, R. P. (2006). Bubbles, Drops, and Particles in Non-Newtonian Fluids. Bubbles, Drops, and Particles in Non-Newtonian Fluids. https://doi.org/10.1201/9781420015386.

Chesser, B. G., Clark, D. E., and W. V. Wise. "Dynamic and Static Filtrate-Loss Techniques for Monitoring Filter-Cake Quality Improves Drilling-Fluid Performance." *SPE Drill & Compl* 9 (1994): 189–192. doi: https://doi.org/10.2118/20439-PA

Chien, S. F. (1994). Settling velocity of irregularly shaped particles. Proceedings - SPE Annual Technical Conference and Exhibition, Delta, 9–22. https://doi.org/10.2118/26121-PA

Clift, R, J R Grace, and M E Weber. 1978. Bubbles, Drops, and Particles., 2005. Dover Publications Inc. Mineola, New York. ISBN:0-486-44580-1.

Cobianco, S., Bartosek, M., Lezzi, A., & Guarneri, A. (2001). How To Manage Drill-In Fluid Composition to Minimize Fluid Losses During Drilling Operations. *SPE Drilling & Completion*, *16*(03), 154–158. https://doi.org/10.2118/73567-PA

Dehghanpour, H., & Kuru, E. (2011). Effect of viscoelasticity on the filtration loss characteristics of aqueous polymer solutions. *Journal of Petroleum Science and Engineering*, *76*(1–2), 12–20. https://doi.org/10.1016/J.PETROL.2010.12.005

Fink, J. (2021). Fluid loss additives. In *Petroleum Engineer's Guide to Oil Field Chemicals and Fluids*. Elsevier. https://doi.org/10.1016/B978-0-323-85438-2.00002-5

Foshee, W. C., Jennings, R. R., & West, T. J. (1976). Preparation and Testing of Partially Hydrolyzed Polyacrylamide Solutions. *Proceedings - SPE Annual Technical Conference and Exhibition*, *1976-Octob*. https://doi.org/10.2118/6202-MS

Gupta, R.K., Sridhar, T., 1985. Viscoelastic effects in non-Newtonian flows through porous media. Rheol. Acta 24, 148–151.

Hirpa, M.M. and Kuru, E. (2020). Hole Cleaning in Horizontal Wells Using Viscoelastic Fluids: An Experimental Study of Drilling-Fluid Properties on the Bed-Erosion Dynamics. SPE J. 25 (2020): 2178–2193. doi: https://doi.org/10.2118/199636-PA

Ikram, R., Jan, B. M., Sidek, A., Kenanakis, G., Jan, M., Sidek, B. ;, Kulinich, S., Svetlichnyi, V. A., Kuchmizhak, A., & Honda, M. (2021). Utilization of Eco-Friendly Waste Generated Nanomaterials in Water-Based Drilling Fluids; State of the Art Review. *Materials 2021, Vol. 14, Page 4171*, *14*(15), 4171. https://doi.org/10.3390/MA14154171

Kelessidis, V. C., and G. Mpandelis. 2004. "Measurements and Prediction of Terminal Velocity of Solid Spheres Falling through Stagnant Pseudoplastic Liquids." Powder Technology 147 (1–3): 117–25. https://doi.org/10.1016/j.powtec.2004.09.034.

Khan, R., Kuru, E., Tremblay, B., & Saasen, A. (2007). Extensional Viscosity of Polymer Based Fluids as a Possible Cause of Internal Cake Formation.

Http://Dx.Doi.Org/10.1080/00908310600626630, *29*(16), 1521–1528. https://doi.org/10.1080/00908310600626630

Khan, R., Kuru, E., Tremblay, B., & Saasen, A. (2004). An Investigation of the Extensional Viscosity of Polymer Based Fluids as a Possible Mechanism of Internal Cake Formation. *Proceedings - SPE International Symposium on Formation Damage Control*, 375–389. https://doi.org/10.2118/86499-MS

Lomba, R. F. T., Martins, A. L., Soares, C. M., Brandao, E. M., Magalhaes, J. V. M., & Ferreira, M. V.D. (2002). Drill-In Fluids: Identifying Invasion Mechanisms. *Proceedings - SPE International Symposium on Formation Damage Control*, 131–142. https://doi.org/10.2118/73714-MS

Malhotra, Sahil, and Mukul M. Sharma. 2012. "Settling of Spherical Particles in Unbounded and Confined Surfactant-Based Shear Thinning Viscoelastic Fluids: An Experimental Study." Chemical Engineering Science 84 (January): 646–55. https://doi.org/10.1016/j.ces.2012.09.010.

Malhotra, S., Lehman, E. R., & Sharma, M. M. (2013). Proppant placement using Alternate-Slug fracturing. Society of Petroleum Engineers - SPE Hydraulic Fracturing Technology Conference 2013, 405–420. https://doi.org/10.2118/163851-MS

Maxey, J. (2010). A Rheological Approach to Differentiating Muds by Gel Structure. *AADE Fluids Conference and Exhibition*

Mezger, T. G. (2006). The rheology handbook: For users of rotational and oscillatory rheometers. 3rd Edition. Vincentz Network. Hannover, Germany. ISBN 978-3-86630-890-9

Miura, H., Takahashi, T., Ichikawa, J., Kawase, Y. (2001). Bed expansion in liquid-solid two-phase fluidized beds with Newtonian and non-Newtonian fluids over the wide range of Reynolds numbers. Powder Tech., 117(3), 239–246. https://doi.org/10.1016/S0032-5910(00)00375-2

Okesanya, T., Kuru, E., & Sun, Y. (2020). A New Generalized Model for Predicting the Drag Coefficient and the Settling Velocity of Rigid Spheres in Viscoplastic Fluids. SPE Journal, 25(06), 3217–3235. https://doi.org/10.2118/196104-PA.

Ofei, T. N., Cheng, I., Lund, B., Saasen, A., & Sangesland, S. (2020). On the Stability of Oil-Based Drilling Fluid: Effect of Oil-Water Ratio. *Proceedings of the International Conference on Offshore Mechanics and Arctic Engineering - OMAE*, *11*. https://doi.org/10.1115/OMAE2020-19071

Poole, R. (2012). The Deborah and Weissenberg numbers. The British Society of Rheology - Rheology Bulletin. 53. 32-39.

Powell, J. W., Parks, C. F., and Seheult, J. M. (1991). Xanthan and Welan: The Effects of Critical Polymer Concentration on Rheology and Fluid Performance. International Arctic Technology Conference. Society of Petroleum Engineers. https://doi.org/10.2118/22066-MS.

Rabenjafimanantsoa, H. A., Rune, W. T. and Saasen, A. (2005). Flow regimes over particle beds experimental studies of particle transport in horizontal pipes. Annual Transactions of the Nordic Rheology Society.

Rushd, S., Hassan, I., Sultan, R. A., Kelessidis, V. C., Rahman, A., Hasan, H. S., and Hasan, A. (2018). Terminal settling velocity of a single sphere in drilling fluid. Particulate Science and Technology. Taylor & Francis, 0(0), pp. 1–10. DOI: 10.1080/02726351.2018.1472162.

Salehi, S. (2015). *SPE-174273-MS Study of Filtrate and Mud Cake Characterization in HPHT: Implications for Formation Damage Control*. http://onepetro.org/SPEEFDC/proceedings-pdf/15EFDC/All-15EFDC/SPE-174273-MS/1438069/spe-174273-ms.pdf/1

Saasen, A., Tengbreg-Hansen, H., Marken C., and Stavland A.: "Influence of linear Viscoelastic Properties on Invasion of Drilling Fluid Filtrate into a Porous Formation", Oil Gas European Magazine, Vol.4, 1990.

Saasen, A. and Løklingholm, G. (2002). The Effect of Drilling Fluid Rheological Properties on Hole Cleaning. IADC/SPE Drilling Conference. Dallas, Texas, 26-28 February, SPE-74558-MS, DOI: 10.2118/74558-MS.

Sayindla, S., Lund, B., Ytrehus, J. D., & Saasen, A. (2017). Hole-cleaning performance comparison of oil-based and water-based drilling fluids. Journal of Petroleum Science and Engineering, 159, 49-57. https://doi.org/10.1016/j.petrol.2017.08.069.

Shah, Subhash N, Youness E El-Fadili, and R P Chhabra. 2007. "New Model for Single Spherical Particle Settling Velocity in Power Law (Visco-Inelastic) Fluids" 33: 51–66. https://doi.org/10.1016/j.ijmultiphaseflow.2006.06.006.

Shahi, Shivam, and Ergun Kuru. 2015. “An Experimental Investigation of Settling Velocity of Natural Sands in Water Using Particle Image Shadowgraph.” Powder Technology 281: 184–92. https://doi.org/10.1016/j.powtec.2015.04.065.

Shahi, S., & Kuru, E. (2016). Experimental investigation of the settling velocity of spherical particles in Power-law fluids using particle image shadowgraph technique. International Journal of Mineral Processing, 153, 60–65. https://doi.org/10.1016/J.MINPRO.2016.06.002.

The Centre for Industrial Rheology (2022). Die Swell Effect. Hampshire. www.rheologylab.com

Veerabhadrappa, S. K., Doda, A., Trivedi, J. J., & Kuru, E. (2013). On the Effect of Polymer Elasticity on Secondary and Tertiary Oil Recovery. *Industrial and Engineering Chemistry Research*, *52*(51), 18421–18428. https://doi.org/10.1021/IE4026456

Werner, B., Myrseth, V., & Saasen, A. (2017). Viscoelastic properties of drilling fluids and their influence on cuttings transport. Journal of Petroleum Science and Engineering, 156, 845-851. https://doi.org/10.1016/j.petrol.2017.06.063.

Wilson, K. C., Horsley, R. R., Kealy, T., Reizes, J. and Horsley, M. (2003) ‘Direct prediction of fall velocities in non-Newtonian materials’, International Journal of Mineral Processing, 71(1–4), pp. 17–30. DOI: 10.1016/S0301-7516(03)00027-9.

Zamir, A., & Ahmad Siddiqui, N. (2017). *Investigating and Enhancing Mud Cake Reduction Using Smart Nano Clay Based WBM*. *8*, 1. https://doi.org/10.4172/2157-7463.1000315

Zamora, M., Broussard, P. N., & Stephens, M. P. (2000). The Top 10 Mud-Related Concerns in Deepwater Drilling Operations. *SPE International Petroleum Conference and Exhibition in Mexico, IPCEM*. https://doi.org/10.2118/59019-MS

Zang, Y. H., Muller, R., & Froelich, D. (1987). Influence of molecular weight distribution on viscoelastic constants of polymer melts in the terminal zone. New blending law and comparison with experimental data. Polymer, 28(9), 1577–1582. https://doi.org/10.1016/0032-3861(87)90362-4.

CHAPTER 3 Experimental Program

3.1 Test Materials

This section provides the detailed information about test materials used in this thesis study which includes the spherical particles used for conducting particle settling experiment and the polymer additives used for preparing viscoelastic fluids.

3.1.1 Spherical Particles

Particles with the perfect spherical shape made of silicon nitride, zirconium ceramic, aluminum, and titanium were used to conduct the terminal velocity measurements. The dimensions and densities of particles used are listed in Table 3-1. The perfect spherical shape of particles were utilized in this study because this certain shape bear least resistance from the fluid media during settling; therefore, the terminal velocity measurement represent the worst case scenario as far as the drilling fluids' particle suspension ability is concerned (Okesanya et al., 2020).

Table 3-1 Physical Properties of Spherical Particles Used in This Study

Particle No.	Material	Diameter (mm)	Density (Kg/m^3)
1	Aluminum	1.2	2700
2	Aluminum	1.5	2700
3	Aluminum	2.0	2700
4	Aluminum	4.0	2700
5	Aluminum	5.0	2700
6	Silicon Nitride	1.2	3200

7	Silicon Nitride	1.6	3200
8	Silicon Nitride	2.0	3200
9	Silicon Nitride	3.0	3200
10	Silicon Nitride	4.0	3200
11	Titanium	1.0	4500
12	Titanium	2.0	4500
13	Titanium	3.0	4500
14	Titanium	4.0	4500
15	Zirconia Ceramic	1.2	6000
16	Zirconia Ceramic	1.6	6000
17	Zirconia Ceramic	2.0	6000
18	Zirconia Ceramic	3.0	6000
19	Zirconia Ceramic	4.0	6000

3.1.2 Polymer Additives

Various polymer additives were utilized in this study, including PHPA and Flowzan (a biopolymer derivative of Xanthan Gum). This section gives the detailed information about these polymer additives.

3.1.2.1 PHPA Polymer

A commonly used synthetic polymer in oil and gas development, called PHPA (or HPAM), is utilized for preparing viscoelastic fluids in this study. It is also referred as partially hydrolyzed polyacrylamide, which is formed from the monomers of acrylic and acrylamide. The rheological behavior of PHPA is mainly dependent on the average molecular weight and degree of hydrolysis

(Arnipally and Kuru, 2018; Dehghanpour and Kuru, 2011). The detailed information for controlling PHPA solution's viscoelasticity and shear thinning characteristics can be found in 2.3 section. Various blends of four types of PHPA polymers with different molecular weights were used in this study to produce fluids with different viscoelastic properties. The average molecular weight of PHPA polymers is shown in Table 3-2.

Table 3-2 Average Molecular Weight of Four PHPA Polymers Used in This Study

Viscosifier	Average molecular weight (10^6 g/g mol)
PHPA 3630	20
PHPA 3330	8
PHPA 3130	5
PHPA AB005V	0.5

3.1.2.2 Flowzan Polymer

Flowzan polymer was utilized in this study to prepare visco-inelastic fluids to provide comparison with various different level of viscoelasticity, and ultimately observe the influence of viscoelasticity on the performance of different critical drilling activities.

Flowzan is a high-purity, high performance Xanthan Gum biopolymer utilizing unique, patented dispersion chemistry which significantly enhances product dispersion and solubility and reduces the formation of fisheyes; it features the thermal stability up to positive or negative 270 degree Fahrenheit in fresh water, and 320 degree Fahrenheit in saturated salt water (Chevron Phillips Chemical, 2022).

Typically, Flowzan exhibit shear thinning characteristics with negligible viscoelasticity; the shear viscosity of Flowzan solution can be simply controlled by varying the weight concentration of additives in the base solution. The level of shear viscosity is usually dependent on specific shear rate, flow consistency index and flow behavior index. (Eq 2.3)

3.2 Polymer Fluid Preparation

The mixing procedure of the experimental fluids was similar to the methodology recommended by Foshee et al., (1976). The de-ionized water was used as the base fluid, the liquid had the majority of the mineral ions removed; therefore, mitigating the possibility of potential chemical reaction, that might ruin the result of measurements. The detailed mixing procedure involves the following three steps:

1. Measure the appropriate amount of each polymer and de-ionized water and pre-shear the base solution with a magnetic mixer at 300 RPM.

2. Slowly pour the polymer blend through the vortex edge to prevent forming dissolvable chunks. After adding the viscosifier, change the mixing speed to 150 RPM and continuously mix for 2 hours; a lower mixing speed is selected to avoid mechanical degradation of the polymers, which can severely damage the internal structure of the prepared fluid.

3. After mixing for 2 hours, if the solution is transparent with no visible polymer powder, it will be sealed and allowed to stay quiescent for 24 hours; the reason for doing this is to release the bubbles entrapped in the solution and allow it to reach a homogeneous state.

3.3 Rheological Characterization of Test Fluids

This section will provide explanations and functionality of four different rheological tests including controlled shear rate, amplitude sweep, funnel viscometry and API viscometry tests.

3.3.1 Controlled Shear Rate Test

The controlled shear rate test was conducted using advanced Anton Parr MCR102e Rheometer with the cone and plate geometry (Fig 3.1); it has a cone diameter of 50mm, and the angle of geometry is 1 degree. Furthermore, the rheometer is also equipped with the evaporation blocker system which can efficiently mitigate the polymer evaporation when conducting long time-scale experiments.

Figure 3.1 Anton Parr MCR 102e Rheometer(Anton Parr,2022)

The controlled shear rate test was conducted for each test fluid with a shear rate range of 0.1 1/s to 1200 1/s. A typical rheogram for shear thinning fluid is shown in Fig 3.2. The fluids exhibiting shear-thinning (pseudo-plastic type fluids) behavior can be characterized with power law relationship (Eq 2.3). The level of shear viscosity is dependent on the specific shear rate, flow consistency index and flow behavior index.

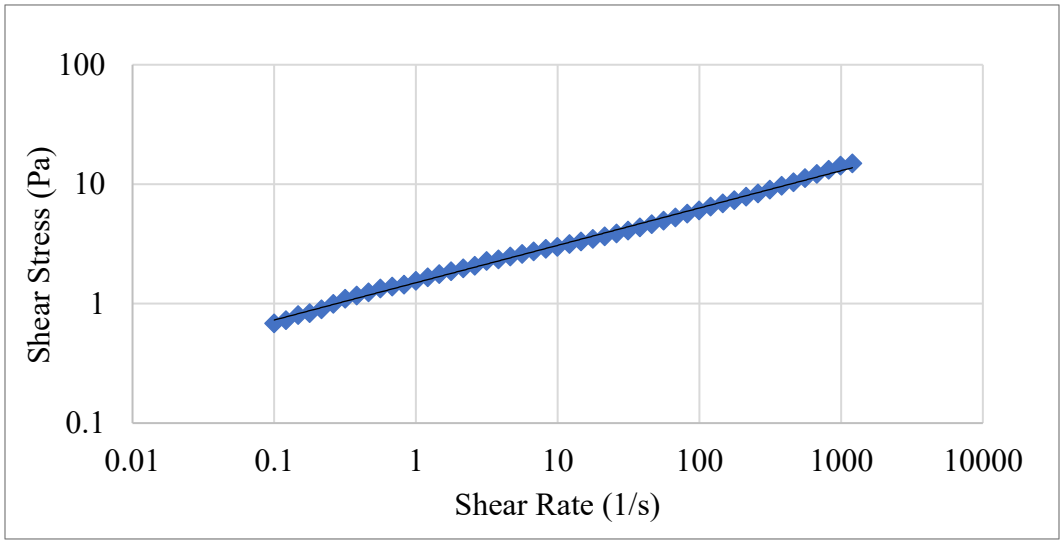

Figure 3.2 Typical Controlled Shear Rate Test Rheogram

3.3.2 Amplitude Sweep Test

The amplitude sweep test was conducted using advanced Anton Parr MCR102e Rheometer with the cone and plate geometry (Fig 3.1). The diameter of the cone is 50mm, and the angle of geometry is 1 degree. Furthermore, the rheometer is also equipped with the evaporation blocker system which can efficiently mitigate the polymer evaporation when conducting long time-scale experiments.

Viscoelastic characteristics of a fluid can be determined by using amplitude sweep test data. The amplitude sweep test was conducted for each test fluid with an oscillation strain range of 0.1 to 800% at oscillation frequency of 10 rad/s. Typical amplitude sweep data obtained from oscillatory rheometer tests are shown in Figures 3.3 and 3.4, where variations of the elastic modulus (G') and loss modulus (G") measurements were plotted as a function of the oscillation strain and oscillation stress, respectively.

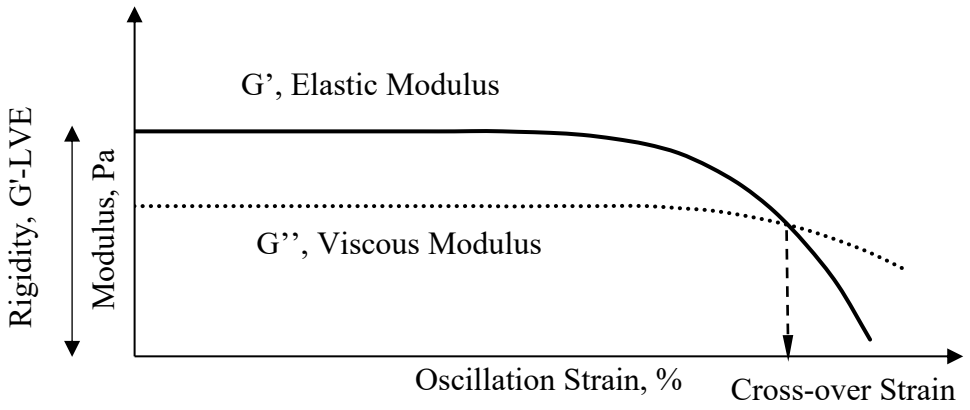

Figure 3.3 Typical Amplitude Sweep Test Result Shown as a Function of Oscillation Strain

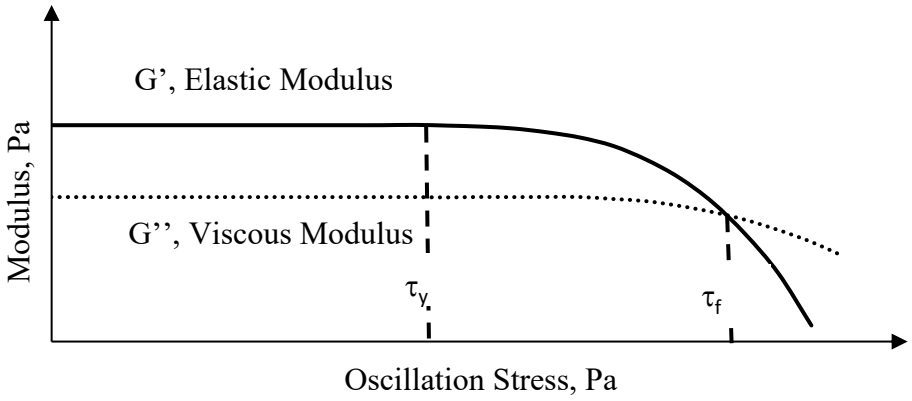

Figure 3.4 Typical Amplitude Sweep Test Result Shown as a Function of Oscillation Stress

The elastic modulus, G', corresponds to the constant plateau value in the linear viscoelastic region (LVE), where the deformation of the fluid-structure under stress is reversible, and the fluid can fully recover from the deformation once the stress is released. The crossover strain defines the maximum strain that can be applied before the viscous modulus (G") surpasses the elastic modulus (G'). After the cross-over point, the viscous behavior dominates over the elastic behavior, and the sample would experience permanent deformation under stress. The fluid viscoelasticity is generally quantified either by using the fluid rigidity (i.e., Elastic Modulus (G') in the LVE region) or stretchiness (i.e., strain value at the crossover of G' and G") values, and both parameters can be obtained from the Amplitude Sweep Test results (Fig 3.3). Both the rigidity and stretchiness parameters can serve as the indicator of the strength of the viscoelasticity to some extent; however, from the practical point of view, neither the rigidity nor the stretchiness can fully demonstrate the level of fluid elasticity. Two viscoelastic fluids with the same rigidity (G') values but with different stretchiness do not necessarily have identical performance under the same deformation process. More specifically, (within the scope of this experimental study) the resistance (i.e., drag) imposed by the two viscoelastic fluids on the settling particles will not be the same if the two fluids have the same rigidity but different stretchiness values. Since neither of these two parameters can be used to fully characterize fluid viscoelastic behavior, a more comprehensive approach is needed for the more realistic assessment of fluid elasticity.

Maxey (2010) claimed that the fluid viscoelasticity could be better described by using the concept of Energy Dissipation (E_D), which entails the minimum energy required for transferring liquid from elastic state to viscous state. In a physical sense, E_D describes the threshold energy needed to break the internal structure of the viscoelastic fluid. Generally, fluids with higher elasticity will require more energy dissipation per unit volume to transfer from elastic to the

viscous state of flow. Having obtained the stress versus strain relationship of a fluid from a typical amplitude sweep test data (i.e., the combination of data shown in Figs. 3.3 and 3.4); the energy dissipation can be conveniently assessed by simple integration of the oscillation shear stress as a function of the oscillation strain (Eq 2.7).

Maxey (2010) also suggested that the energy dissipation can be estimated by using the crossover point (also known as gel point or flow point) in a typical amplitude sweep test data (Figs. 3.3 and 3.4) as a reference point, i.e., cross-over strain (Fig 3.3) is the upper limit of the integral in Eq 2.7. The detailed description of the Maxey (2010) technique to determine energy dissipation is given in section 2.4 of Chapter 2.The flow point in an amplitude sweep test indicates the maximum stress-strain values (and hence the total energy) required for a fluid to transfer from an elastic state to a viscous state. Therefore, it is plausible to determine the energy dissipation at this specific point.

3.3.3 Funnel Viscometry

Funnel viscometer is used to measure the viscosity of a drilling fluid (Fig 3.5). The calibration of the funnel viscometer uses the outflow of one quart (946 cm3) of fresh water at a temperature of 70 ± 5°F (21 ± 3°C) in 26 ± 0.5 seconds. The funnel viscometer test measures the discharge time required for 1 quart (946 cm3) of drilling fluid to flow through the funnel vertically. The funnel viscosity measurement is reported in seconds. People often connect funnel viscosity with drilling fluid's apparent viscosity; however, we have shown that possessing viscoelasticity can have huge impact on the funnel viscosity. More detailed information can be found in Chapter 5 (A Generalized Model for the Field Assessment of Drilling Fluid Viscoelasticity).

Figure 3.5 Funnel Viscometer/Marsh Funnel (Vidhya Enterprises,2022)

3.3.4 API Viscometry

The rotational viscometer measures the rheological properties of the drilling fluids per API 13B-1 and 13B-2 (Fig 3.6). The viscometer readings obtained at six different rotational speeds (i.e., 600, 300, 200, 100, 6, and 3 rev/min) are generally used to determine the rheological behavior of the drilling fluids.

Figure 3.6 Rotational Viscometer (Shale Tech, 2022)

One of the study objectives is to determine if there is any correlation between the funnel viscosity and the other rheological properties measured by a rotational viscometer. Recently, Sedaghat (2017) presented an equation for determining the shear rate of non-Newtonian fluids relevant to flow through funnel viscometer (Eq 3.1).

$$\gamma = \frac{1}{2}\left(\frac{h}{H}\right)\left(\frac{3n'+1}{4n'}\right)\frac{4Q}{\pi R^3} \qquad 3.1$$

Where:

γ = shear rate, 1/sec

h = height of the fluid level in the Funnel, cm

H = length of the tube section of the Funnel, cm

n' = flow behavior index of the fluid

Q = volume flow rate, cc/s

R = radius of tube section of the funnel viscometer, cm

Using the shear rate relationship given by Eq 3.1 and the various drilling fluid formulations used in this study, initial screening tests were conducted to determine shear rates relevant to the flow of various drilling fluids through the funnel viscometer. In addition, we measured the flow rates of various fluids coming out of the funnel viscometer varying as a function of time. The shear rate corresponding to the 600 rev/min reading of a rotational viscometer (i.e., 1021.8 1/sec) was found to be the most representative shear rate for characterizing the viscous characteristics of drilling fluids through a funnel viscometer.

According to 13B-1, estimation of a drilling fluid's apparent viscosity takes one-half of the 600 rev/min reading from a rotational viscometer (Eq 3.2). The design of the rotational viscometer geometry helps determine the apparent viscosity directly from a 600 rev/min reading in millipascal-second. Note that one millipascal-second is equivalent to one centipoise (cp), which is a commonly used field unit for drilling fluid viscosity.

$$AV = \Theta_{600}/2 \qquad 3.2$$

Where:

AV = apparent viscosity, cp

Θ_{600} = shear stress reading at 600-rpm, lbs./100ft^2

Following the results from the screening studies, the apparent viscosity (AV) measurements of drilling fluids using a rotational viscometer were correlated with the funnel viscosity measurements.

3.4 Settling Velocity Measurement

This section explains the testing system used for particles' settling velocity measurement and give details on procedure for measuring settling velocity.

3.4.1 Experimental Set-up

A transparent acrylic square column was used in this experimental study. The width and the height of the column were 15 centimeters 70 centimeters, respectively. The largest particle diameter used in this study was 4 millimeters ensuring the width of the square column is 37.5 times

more than the particle diameter. Typically, the wall effect can be avoided if the size of the container is 20 to 30 times larger than the particle diameter in Newtonian fluids (Zang et al., 2015). Zhang et al., (2015) also reported that the shear-thinning characteristics of non-Newtonian fluids reduced the wall retardation effect. Therefore, the dimension of the acrylic column is assumed to be large enough to ensure the particle's settling behavior is not influenced by the wall effect. A schematic diagram depicting the principle of the experimental measurement technique is shown in Fig 3.7.

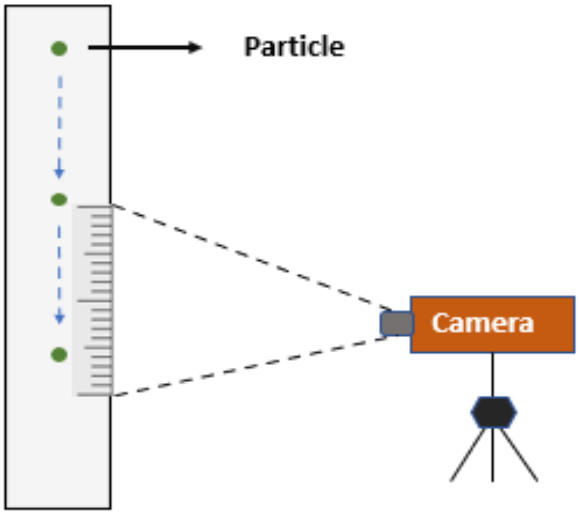

Figure 3.7 Schematic Diagram Showing the Principle of Experimental Measurement Technique

3.4.2 Procedure for Measuring Particle's Settling Velocity

When conducting particle settling experiments, a particle was first immersed in the test fluid to allow the formation of a thin layer around the particle, which would prevent any potential surface tension effect and make sure that there were no air bubbles attached to the particle during settling. The particle was then released to settle after being entirely placed under the fluid surface so that there would be no initial acceleration, which might influence the quality of the measured

data. The fluid was allowed to relax for 20 minutes after each particle settled through the entire fluid column vertically. This ensured the viscoelastic fluid fully reaches the homogeneous state as there might be a possible shear history effect, which would make the particle settling in the same path experience less resistance from the fluid.

To ensure the data accuracy and repeatability; three sets of terminal velocity measurements were made for each particle. The final settling velocity value was determined by averaging the results of the three measurements. The measurement was considered accurate if there was no more than a 5 percent difference between the average settling velocity value and the individual test results. If the data did not fulfill the criteria, another set of measurements was conducted.

3.4.3 Verification of the Measurement Accuracy

Verification tests were conducted to ensure the accuracy of the technique used for particle settling velocity measurements. Three different size particles were allowed to settle in a Newtonian fluid (Glycerin). The particle Reynolds number was calculated using Eq 3.3.

$$Re_p = \frac{\rho_f V_t d}{\mu} \tag{3.3}$$

The theoretical drag coefficients were computed by using the model proposed for particles settling in Newtonian fluids using Eq 3.4 (Morrison and Faith, 2013).

$$C_{D-uni} = \frac{24}{Re_p} + \frac{2.6\left(\frac{Re_p}{5}\right)}{1+\left(\frac{Re_p}{5}\right)^{1.52}} + \frac{0.411\left(\frac{Re_p}{263000}\right)^{-7.94}}{1+\left(\frac{Re_p}{263000}\right)^{-8.00}} + \frac{0.25\left(\frac{Re_p}{10^6}\right)}{1+\left(\frac{Re_p}{10^6}\right)} \tag{3.4}$$

By plotting the particle Reynolds number versus the theoretical drag coefficient, the universal curve for particles settling in Newtonian fluids can be obtained. Experimental drag coefficients were determined by using the theoretical definition given as Eq 3.5:

$$C_{D-exp} = \frac{4g(\rho_s - \rho_f)d}{3V_t^2 \rho_f} \qquad 3.5$$

The experimental drag coefficients were then plotted onto the universal CD vs Rep curve for comparison (Fig 3.8). The difference between the measured values and universal curve was within 5 %, confirming the accuracy of the measurement technique for further use.

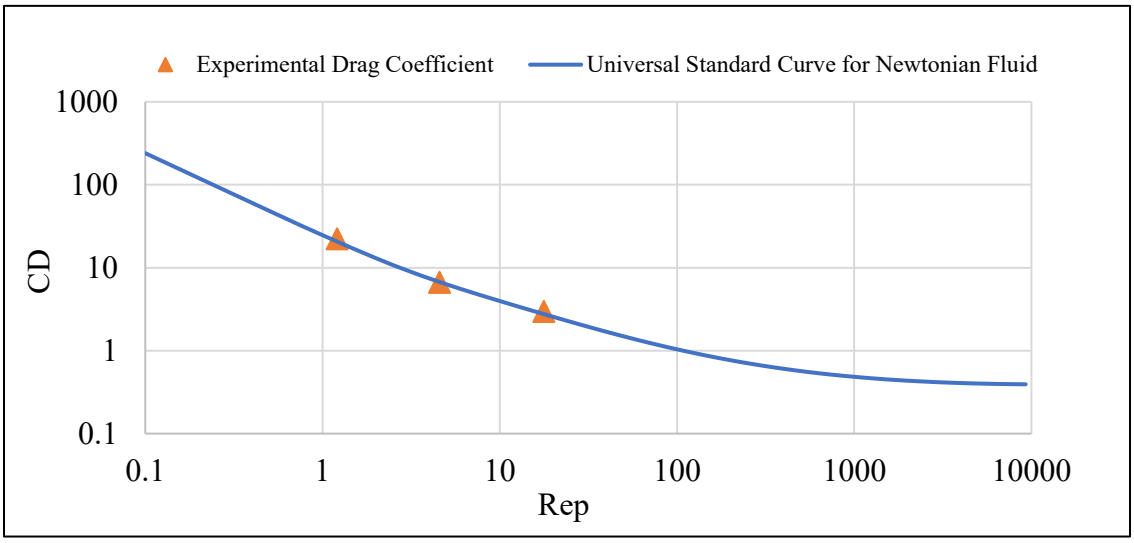

Figure 3.8 The Experimental Drag Coefficient Projected on the Universal Particle Reynolds Number vs. Drag Coefficient Curve Given for Newtonian Fluids

3.5 Core flooding Experiments

This section explains the testing system and the procedure used for core flooding experiments.

3.5.1 Experimental Set-up for Core Flooding Experiment

The apparatus for conducting the core flooding experiment is shown in Fig 3.9. A syringe pump with a pressure capacity of up to 7500 psi is used to inject the polymer fluid through the core. The controlled flow rate model was used to ensure the accuracy of flow rate measurement. A pressure transducer with a sampling rate of 10 samples per second, is connected to the inlet of the core holder for computing the pressure drop across the core, the outlet of the cell is open to atmospheric pressure. A confining pressure control system is installed to make sure the fluid flows through the core's permeable media instead of slipping through by the side of the core. Berea Sandstone core samples with 1 in diameter and 1 inch length were used for core flooding experiments. Berea sandstone was selected because the sandstone formation is generally more susceptible to fluid loss problem because of their high permeability, also high permeability sample will make the results have a noticeable difference, make it more suitable for observing the effects of two rheological properties on filtration loss properties.

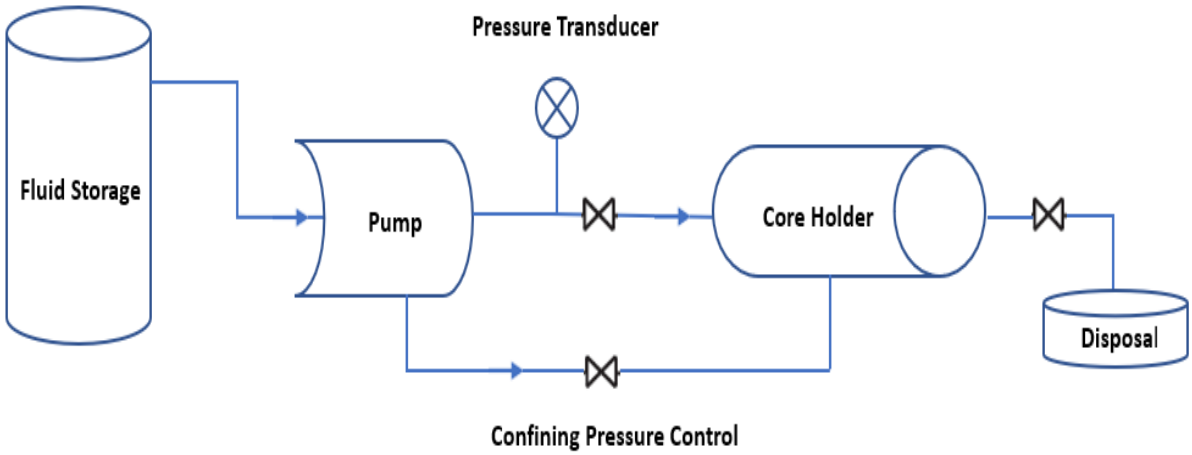

Figure 3.9 Core Flooding Experimental Apparatus

3.5.2 Test Procedure for Core Flooding Experiment

There were three major steps implemented to conduct the core flooding experiment. Before starting the test, the Berea sandstone was placed in the core holder, and the confining pressure of 450 psi was applied to make sure the fluid only went through the porous media of the core. Each experiment starts with a new sample core and a cleaned system with no polymer residue; all measurements were taken at steady-state, when the inlet pressure stabilizes and does not change for at least 15 minutes. The experimental procedure includes the following steps:

Step-1: The de-ionized water is pressurized to go through the core holder at five different flow rates to compute the absolute permeability of undamaged Berea sandstone; if no significant difference is observed in the calculated permeability, the average of five values will be used as the absolute permeability.

Step-2: The selected polymer solution is pumped through the core holder at five different flow rates; the pressure drop at each flow rate is recorded.

Step-3: The polymer flooded core is flushed with de-ionized water for 24 hours to remove the polymer residue inside the core; another permeability measurement is taken to determine the damaged permeability due to polymer flooding.

3.6 Static Filtration Test System

The static filtration loss tests were conducted to understand the influence of shear viscosity and viscoelasticity on filtration loss characteristics. API standard test procedure was used in this case. Experimental apparatus used is API filter press (Fig 3.10). The nitrogen tank was allowed to

pressurize the holding chamber to 100 psia; the fluids were kept at room temperature; lower permeability filter papers were used instead of standard API filter paper (Advantec GA5590 Grade Glass fiber filters with 0.6-micron pore size), for better observing the effect of two rheological properties on static filtration loss rate.

Figure 3.10 API Filter Press

3.7 References

API RP 13B-1, Recommended Practice for Field Testing Water-based Drilling Fluids. (2019). Washington, DC United States: API.

API RP 13B-2, Recommended Practice for Field Testing Oil-based Drilling fluids. (2014). Washington, DC United States: API.

Anton Paar, (2022), MCR102e Rheometer with cone and plate geometry. https://www.anton-paar.com/ca-en/products/details/rheometer-mcr-102-302-502/

Arnipally, S. K., & Kuru, E. (2018). Settling velocity of particles in viscoelastic fluids: A comparison of the shear-viscosity and elasticity effects. SPE Journal, 23(5), 1689–1705. https://doi.org/10.2118/187255-PA

Chevron Phillips Chemical. (2022). Flowzan Bio polymer. www.cpchem.com

Dehghanpour, H. and Kuru, E. (2011). Effect of viscoelasticity on the filtration loss characteristics of aqueous polymer solutions. Journal of Petroleum Science and Engineering, 76(1–2), 12–20. https://doi.org/10.1016/J.PETROL.2010.12.005

Foshee, W. C., Jennings, R. R., & West, T. J. (1976). Preparation and Testing of Partially Hydrolyzed Polyacrylamide Solutions. SPE-6202-MS. Paper presented at the SPE Annual Fall Technical Conference and Exhibition, New Orleans, LA. https://doi.org/10.2118/6202-MS.

Maxey, J. (2010). A Rheological Approach to Differentiating Muds by Gel Structure. AADE-10-DF-HO-27, AADE 2010 Fluids Conference, Houston, TX

Morrison, Faith A., 2013. Data Correlation for Drag Coefficient for Spheres. An Introduction to Fluid Mechanics. Cambridge University Press, New York.

Okesanya, T., Kuru, E., & Sun, Y. (2020). A New Generalized Model for Predicting the Drag Coefficient and the Settling Velocity of Rigid Spheres in Viscoplastic Fluids. SPE Journal, 25(06), 3217–3235. https://doi.org/10.2118/196104-PA.

Sedaghat, A. (2017). A novel and robust model for determining rheological properties of Newtonian and non-Newtonian fluids in a marsh funnel. Journal of Petroleum Science and Engineering, 156, 896–916. https://doi.org/10.1016/j.petrol.2017.06.057

Shale Tech Solutions Drilling Manual, Model 35 Viscometer, www.shaletechsolutions.com

Vidhya Enterprises Marsh Funnel, For Industrial, 1, Rs 9500 /unit | ID: 19218478648. (2022). https://www.indiamart.com/proddetail/marsh-funnel-19218478648.html

CHAPTER 4 A Generalized Model for the Field Assessment of Drilling Fluid Viscoelasticity

4.1 Abstract

Recent studies highlight the significant role of drilling fluid elasticity in particle suspension and hole cleaning during drilling operations. Traditional methods to quantify fluid elasticity require the use of advanced rheometers not suitable for field applications. The main objectives of this study were to investigate the factors influencing drilling fluid viscoelasticity in the field and develop a generalized model for determining the viscoelasticity of a drilling fluid using standard field-testing equipment.

Ninety-three fluid formulations used in this study included field samples of oil-based drilling fluids as well as laboratory samples of water-based, invert emulsion and other oil-based fluids. Basic rheological characterizations of these fluids were done by using a funnel viscometer and a rotational viscometer. Elastic properties of the drilling fluids (quantified in terms of the energy required to cause an irreversible deformation in the fluid's structure) were obtained from oscillatory tests conducted by using a research grade rheometer with double gap concentric cylinder geometry. Using an empirical approach, a non-iterative model for quantifying drilling fluid elasticity was developed by correlating test results from a funnel viscometer and a rotational viscometer to energy required to cause an irreversible deformation of the fluid's elastic structure, furthermore the model was modified to account for the density effect of the drilling fluid, making the methodology more practical

The generalized models for the unweighted and weighted viscoelastic drilling fluids were able to predict the elasticity of drilling fluids with a mean absolute error of 4.67% and 5.28%,

respectively. In addition, the models offer practical versatility by requiring only standard drilling fluid testing equipment to predict viscoelasticity. Experimental results showed that non-aqueous fluid (NAF) viscoelasticity is inversely proportional to the oil-water ratio and the presence of clay greatly debilitates the elasticity of the drilling fluids while enhancing their viscosity.

The paper presents new models for estimating unweighted and weighted drilling fluid elasticity using standard drilling fluid field-testing equipment. Furthermore, it proposes a prudent approach for quantifying the viscoelastic property of a drilling fluid by measuring the amount of energy required to irreversibly deform a unit volume of viscoelastic fluid. The new methodology, combined with the recommended use of energy dissipation concept, provides a practical tool that can be used for developing optimum drilling fluid formulations and hydraulic programs for effective hole cleaning operations, improved ECD management, and mitigating barite sag problems.

4.2 Introduction

Drilling fluids serve many important functions: controlling formation pressure and providing well control, removing cuttings from the wellbore, minimizing formation damage by sealing permeable formations encountered while drilling, cooling and lubricating the bit, transmitting hydraulic energy to downhole tools and the bit, and maintaining wellbore stability. (Williamson, 2013).

Cuttings transport efficiency is critical to the success of hole cleaning operation, failure to remove cuttings can potentially cause pipe stuck, especially in high inclination and horizontal well drilling wells (Werner et al., 2017). Equivalent circulation density (ECD) is a key parameter during drilling through formations where the margin between the pore pressure and the fracture pressure

is narrow. Strict control of the ECD is required to control the formation pressure and prevent kicks (Abdelgawad et al., 2018) as well as maintain wellbore stability and avoid lost circulation (Al Bahrani et al., 2022). Barite is used as one of the most common weighting agent when designing fluids for drilling in high pressure formations. Failure to suspend barite sufficiently creates a problem known as "Barite Sag", which may lead to severe operational problems such as loss of well control and wellbore instability (Amighi et al., 2010). Controlling filtration loss characteristics of drilling fluids is considered as one of the most critical tasks when designing optimum drilling fluid formulations for best drilling performance while preserving the original reservoir rock properties and minimizing the formation damage (Chesser et al., 1994).

Optimization of drilling fluid rheological properties is the key task for tackling most of these major challenges encountered in drilling operations. Shear viscosity, yield point, low shear rate viscosity (LSRV), and the gel strength are the main drilling fluid rheological properties that have been traditionally controlled and optimized for achieving trouble free drilling. In addition to this traditional approach used for drilling fluid formulations, recently viscoelastic properties of drilling fluids have drawn much attention in the drilling industry because of the critical role they play in the evaluation of frictional pressure loss, particle settling velocity, and cuttings transport efficiency.

Powell et al. (1991) related the gel-like behavior of biopolymer fluids to their viscoelasticity and reported that fluid elasticity improved the solid suspension ability of these fluids. Zamora et al. (1993) investigated cuttings transport performance of biopolymer fluids under laminar flow conditions and stated that superior drill cuttings suspension ability and hole-cleaning

performance of biopolymer fluids in laminar flow could be attributed to the viscoelastic characteristics of these fluids.

Based on their field experiences from North Sea operations, Saasen and Loklingholm (2002) concluded that the gel forming as a result of the interaction of cuttings bed and viscoelastic polymer-based drilling fluids would be one of the main factors causing the observed poor hole cleaning performance of these fluids. Similar results were also reported by Rabenjafimanantsoa et al. (2005), where they observed that the polymer-water mixture forms a gel, which resulted particles to be glued together and, as a result, the cuttings bed became more consolidated.

Cuttings transport experiments conducted by Sayindla et al. (2017) and Werner et al. (2017) have shown that oil-based fluids have superior cuttings transport abilities as compared to water-based fluids with similar viscometric properties but different viscoelastic properties. Werner et al. (2017) also reported that the water-based drilling fluids used in their study had no yield stress but a 50 to100% higher elasticity than the oil-based drilling fluids, indicating the lower viscoelasticity of the oil-based fluids would be one of the main reasons behind their favorable cuttings transport performance.

Arnipally and Kuru (2018) reported that models not taking the fluid elasticity effect into account could over predict the settling velocity of particles in a viscoelastic fluid by as much as 14 to 50 times.

Recent laboratory investigations (Bizhani and Kuru, 2018; Hirpa and Kuru, 2020) have shown that much higher critical flow rates were required for the initiation of bed erosion/hole cleaning when using viscoelastic drilling fluids. Bizhani and Kuru (2018) concluded that additional

elastic normal forces arising from the variable normal stress differences of viscoelastic fluids could be responsible for delaying the onset of the bed erosion.

All these previous field experience and lab data strongly suggest that fluid elastic properties are important in hole cleaning and should be given due consideration together with the viscous properties to assess the solids transport ability of a drilling fluid.

Despite the impact of fluid viscoelasticity on the drilling hydraulics design has been well recognized, currently there is no standard field technique available for measuring the fluid viscoelastic properties. The viscoelastic properties can only be measured in the lab by using advanced rheometers, which are not suitable for field applications. There is a need for development of a methodology that can be used in the field to determine the viscoelastic properties of drilling fluids using standard field-testing equipment. The development of a generalized model for quantifying viscoelasticity by using field testing equipment has, therefore, been set as one of the main objectives of this study. The work presented in this paper consists of two parts: 1) Investigation of the factors affecting the elastic properties of a drilling fluid; 2) Development of a generalized model for determining viscoelasticity of a drilling fluid using standard field-testing equipment.

4.2.1 Assessment of Fluid Viscoelasticity

Viscoelastic behavior of a fluid can be characterized by using amplitude sweep test data. Figures 4.1 and 4.2 show typical amplitude sweep results obtained from an oscillatory rheometer test where variations of the storage modulus (G') and loss modulus (G") measurements are recorded as a function of the shear strain and shear stress, respectively.

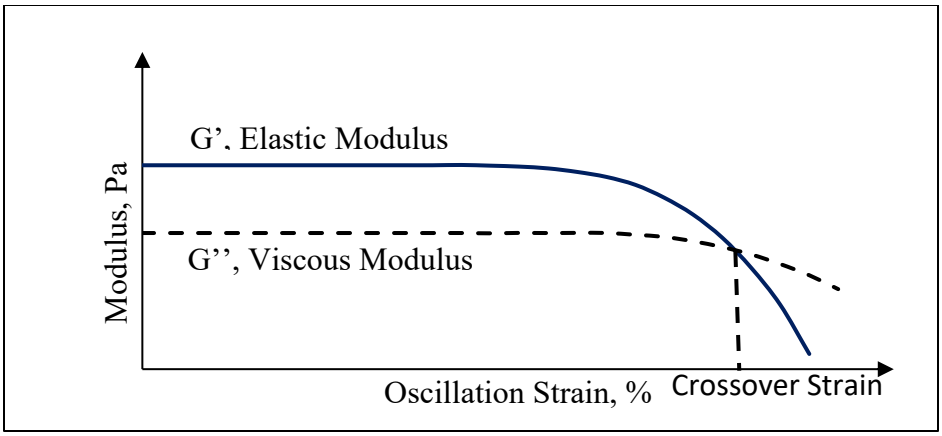

Figure 4.1 Amplitude Sweep Test Result with Oscillation Strain as x-axis

The strain at the crossover point in Fig 4.1 (i.e., the strain at which elastic modulus, G', and viscous modulus, G'', are equal) represents the maximum deformation that can be applied to the viscoelastic fluid without permanently damaging the fluid's internal structure. The corresponding stress at crossover strain is called the flow point stress (Fig 4.2), which is also construed as the minimum stress required for initiating the flow.

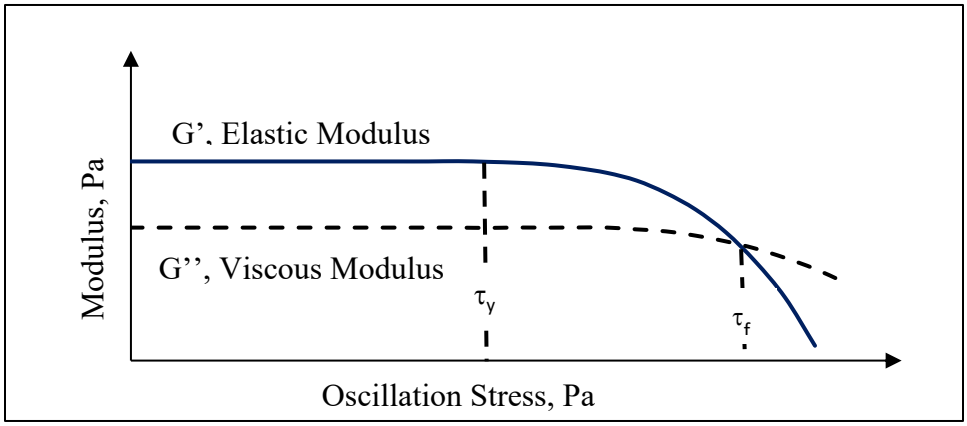

Figure 4.2 Amplitude Sweep Test Result with Oscillation Stress as x-axis

Maxey (2010) suggested using the "Energy Dissipation" concept for assessing fluid elasticity. The energy dissipation per unit volume, E_D, represents the amount of energy needed to

transfer fluid from the elastic state to the viscous state. It is a measure of the threshold energy needed to break the internal structure of the viscoelastic fluid. Generally, the higher the energy dissipation per unit volume is, the more elastic the fluid will be. Once the stress versus strain relationship of a fluid is available from a typical amplitude sweep test data, the energy dissipation can be determined by simply integrating the shear stress as a function of strain (Eq 4.1).

$$E_D = \int \tau \, d\gamma \qquad 4.1$$

Where:

E_D = energy dissipation per unit volume, J/m^3

τ = shear stress, Pa

γ = strain, Fraction

Maxey (2010) recommended that the gel point (also known as crossover point) in a typical amplitude sweep test data (Figs 4.1 and 4.2), can be used as a reference point to assess the energy dissipation. The cross-over point in an amplitude sweep test indicates the maximum stress-strain values (and hence the total energy) required for the transition from an elastic state to a viscous state; therefore, it is reasonable to assess the energy dissipation at this critical point.

Energy dissipation, E_D, can be determined by using a two-step procedure as follows: 1-) Plot shear stress versus strain data obtained from amplitude sweep test until the gel point (Fig 4.3); 2-) Compute the area under the curve, which is equal to the integral of the oscillation shear stress over the oscillation shear strain (Eq 4.1).

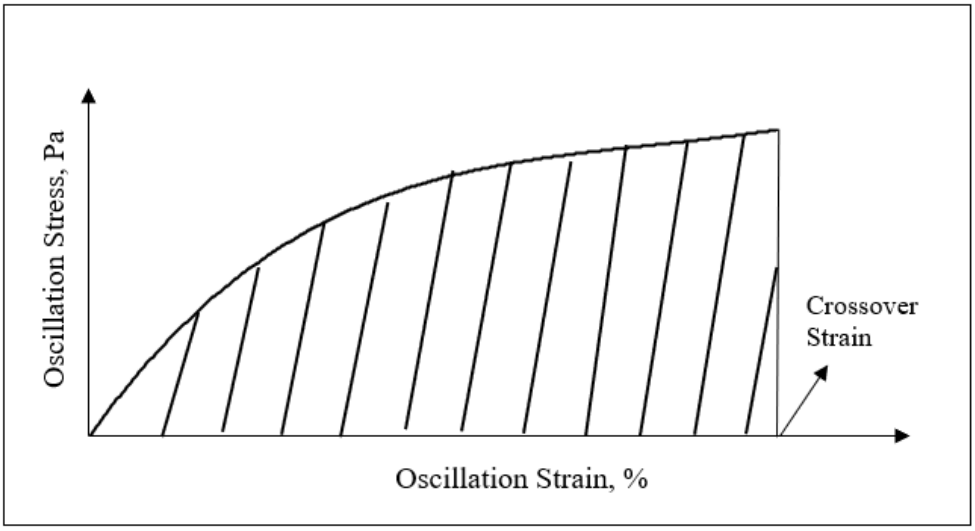

Figure 4.3 Plot of Oscillation Shear Stress versus Oscillation Strain Until the Cross-Over Point

4.3 Materials and Methods

4.3.1 Test Fluid Preparation

This section provides the information for preparing the test fluids used in this study.

4.3.1.1 Material Selection

In total, 93 fluids (including 5 field samples) were used in this study to ensure that viscoelastic behaviors of the wide variety of drilling fluids were considered in the model development. Test fluids are categorized into 5 groups: water-based fluids, oil-based fluids, invert emulsion fluids, oil-based field samples and weighted drilling fluids. The generic description of the different polymers used for drilling fluid formulations are given as follows:

HMO : Hydrotreated Mineral Oil

NVO : Novel Viscoelastic Organellar

PDAO : Petroleum Distillate Aromatic Base Oil

HPAM : Hydrolyzed Polyacrylamide

PAA : Polyacrylic Acid

XG : Xanthan Gum

Forty-eight water-based fluids samples were prepared with the following formulations:

HPAM1 (0.15%, 0.2%, 0.25% 0.36%, 0.37% and 0.385%)

HPAM2 (0.1%, 0.15%, 0.17%, 0.2%, 0.25% and 0.3%)

HPAM3 (0.25%, 0.30%, 0.35%, 0.40%, 0.45% and 0.50%)

HPAM4 (0.15%, 0.2%, 0.22%, 0.25%, 0.3%, and 0.35%)

PAA1 (0.05%, 0.06%, 0.065%, 0.07%, 0.075% and 0.09%)

PAA2 (0.015%, 0.025%, 0.035%, 0.04%, 0.045% and 0.06%)

XG (0.15%, 0.2%, 0.25%, 0.027%, 0.3% and 0.35%)

Bentonite (4%, 5%, 6%, 7.5%, 8% and 8.5%)

HPAM is a common synthetic polymer used for various oilfield applications. It is formed from the monomers of acrylamide and acrylic acid. The viscous and elastic behavior of the polymer is dependent on the degree of hydrolysis and the average molecular weight. Four types of HPAM

polymer with different molecular weights were used to cover a broad range of viscoelasticity. For example, HPAM2 has an average molecular weight of 20 million grams per mole. Having the largest average molecular weight among the HPAM polymers used; HPAM2 exhibited the highest level of viscoelasticity. Molecular weights of the HPAM polymers are listed in Table 4-1.

Table 4-1 Molecular Weight of the HPAM Polymers

Viscosifier	Molecular weight (g/g mol)
HPAM1	5,000,000
HPAM2	20,000,000
HPAM3	8,000,000
HPAM4	3,600,000

Fourteen oil-based fluid samples were prepared with the following formulations:

NVO in PDAO (0.1%, 0.15%, 0.2%, 0.25%, 0.3%, 0.35% and 0.4%)

NVO in HMO (0.1%, 0.15%, 0.2%, 0.25%, 0.3%, 0.35% and 0.4%)

Eighteen invert emulsions samples were prepared with the following formulations:

NVO in 90/10 invert emulsion (0.1%, 0.15%, 0.2%, 0.2% with 2% bentonite, 0.25% and 0.3%)

NVO in 80/20 invert emulsion (0.1%, 0.15%, 0.2%, 0.2% with 2% bentonite, 0.25% and 0.3%)

NVO in 70/30 invert emulsion (0.1%, 0.15%, 0.2%, 0.2% with 2% bentonite, 0.25% and 0.3%)

Three unweighted field drilling fluid samples (containing drilled clay cuttings) were collected from different drilling fluid storage tanks. The field samples were used to test the model's capability to capture viscoelastic properties of typical oil-based fluids used in the field as well as to compare characteristics of field oil-based fluids to that of similar fluids prepared in the lab without containing drilled solids. This allowed us to investigate how the presence of drilled solids (shale cuttings) would influence the viscoelasticity of the drilling fluid.

Ten weighted drilling fluids including two field drilling samples were obtained to investigate the influence of density effect on quantifying viscoelasticity. Eight weighted drilling fluids samples were prepared with the following formulations:

XG (0.32% with 2.2% barite, 0.4% with 14.4% barite and 0.75% with 18.9% barite)

HPAM1 (0.2% with 7.8% barite, 0.3% with 12.3% barite, 0.34% with 4.5% barite, 0.39% with 14.4% barite and 0.48% with 17.8% barite)

The detailed composition of drilling fluids can be found in Appendix-A.

4.3.1.2 Mixing Procedure

The mixing procedure for the water-based drilling fluids was similar to the methodology developed by Foshee et al., (1976). The steps for preparing the test fluids include:

1. Take 1.2 liter of deionized water and stir at a constant speed of 300 rev/min.

2. Measure the appropriate amount of the additives and add them slowly through the edge of the vortex to prevent forming fisheyes.

3. After adding the additives, the solution was stirred at a reduced speed of 150 rev/min for 2 hours to avoid mechanical degradation of the polymers.

4. For PAA polymers: Following additives were dissolved in deionized water in Step #2; i)10 wt.% sodium hydroxide was used to adjust the pH to the desired level between 6.4 to 6.6, measured by using a benchtop pH meter, ii) PPA polymer was used to viscosify the solution by neutralization with sodium hydroxide. The degree of viscosity and elasticity is dependent on the neutralization process.

The mixing procedure for oil-based fluids and invert emulsion fluids are different from water-based fluids. Due to the low solubility of NVO polymer, a dispersant was used to help in the dissolution step and the oil-based or invert-emulsion fluids were stirred at 5,000 rev/min. After the addition of the additives, the fluids were stirred for 1 hour to ensure full dissolution. The samples taken from the mud tank cooled down to room temperature then pre-sheared at 300 rev/min to ensure homogenization before testing. For all the prepared samples, upon completion of the mixing process, the solution was sealed and allowed to settle for 24 hours to remove air bubbles and allow reaching a homogeneous state.

4.3.2 Field Measurements of Rheological Properties

Funnel viscometer and rotational viscometer measurements are regularly taken in the field to characterize the rheological properties of the drilling fluids.

4.3.2.1 Funnel Viscometer

Funnel viscometer is used to measure the viscosity of a drilling fluid relative to that of water. The calibration of the funnel viscometer uses the outflow of one quart (946 cm3) of fresh water at a temperature of 70 ± 5°F (21 ± 3°C) in 26 ± 0.5 seconds. The funnel viscometer test measures the discharge time required for 1 quart (946 cm3) of drilling fluid to flow through the funnel vertically. The funnel viscosity measurement is reported in seconds.

4.3.2.2 Rotational Viscometer

The rotational viscometer measures the rheological properties of the drilling fluids per API 13B-1 and 13B-2. The viscometer readings obtained at six different rotational speeds (i.e., 600, 300, 200, 100, 6, and 3 rev/min) are used to determine the rheological behavior of the drilling fluids.

One of the study objectives is to determine if there is any correlation between the funnel viscosity and the other rheological properties measured by a rotational viscometer. Recently, Sedaghat (2017) presented an equation for determining the shear rate of non-Newtonian fluids relevant to flow through funnel viscometer (Eq 4.2).

$$\gamma = \frac{1}{2}\left(\frac{h}{H}\right)\left(\frac{3n'+1}{4n'}\right)\frac{4Q}{\pi R^3} \qquad 4.2$$

Where:

γ = shear rate, 1/sec

h = height of the fluid level in the Funnel, cm

H = length of the tube section of the Funnel, cm

n' = flow behavior index of the fluid

Q = volume flow rate, cc/s

R = radius of tube section of the funnel viscometer, cm

Using the shear rate relationship given by Eq 4.2 and the various drilling fluid formulations used in this study, initial screening tests were conducted to determine shear rates relevant to the flow of various drilling fluids through the funnel viscometer. In addition, we measured the flow rates of various fluids coming out of the funnel viscometer varying as a function of time. The shear rate corresponding to the 600 rev/min reading of a rotational viscometer (i.e., 1021.8 1/sec) was found to be the most representative shear rate for characterizing the viscous characteristics of drilling fluids through a funnel viscometer.

According to 13B-1, estimation of a drilling fluid's apparent viscosity takes one-half of the 600 rev/min reading from a rotational viscometer (Eq 4.3). The design of the rotational viscometer geometry helps determine the apparent viscosity directly from a 600 rev/min reading in millipascal-second. Note that one millipascal-second is equivalent to one centipoise (cp), which is a commonly used field unit for drilling fluid viscosity.

$$AV = \Theta_{600}/2 \qquad 4.3$$

Where:

AV = apparent viscosity, cp

Θ_{600} = shear stress reading at 600-rpm, lbs./100ft^2

Following the results from the screening studies, the apparent viscosity (AV) measurements of drilling fluids using a rotational viscometer were correlated with the funnel viscosity measurements.

4.3.3 Laboratory Characterization of Fluid Viscoelastic Fluid Properties

4.3.3.1 Amplitude Sweep Test

To develop a generalized model considering the viscoelasticity of drilling fluid, it is necessary to measure the viscoelastic properties of the test fluid with accuracy. An amplitude sweep test investigates the viscoelastic properties of polymer fluids. The test subjects the fluid to a sinusoidal deformation and measures the resulting mechanical response as a function of time (Hyun et al. 2011). The amplitude sweep test uses a constant rate of oscillation while increasing the shear strain or shear stress. In this study, the amplitude sweep measurements were done by using the Discovery Hybrid-1 Rheometer (DHR) coupled with the standard Peltier concentric cylinder geometry (Fig 4.4). The rheometer has Peltier concentric cylinder geometry with a cup radius of 15 mm, and a DIN Rotor, which has a radius of 14 mm and a height of 42 mm. Amplitude sweep tests were conducted at room temperature using the controlled-shear stress mode of the rheometer.

Figure 4.4 Discovery Hybrid-1 Rheometer with Double Gap Concentric Cylinder Geometry

4.3.4 Experimental Procedure

The preferred sequence of conducting experiments was the amplitude sweep test first, then the funnel viscometer test, and the rotational viscometer test last. The reason for using the rotational viscometer as the last test was to avoid any effect of the high shear rate experienced by the fluid at 600 rev/min. The high shear rate may affect the internal structure of the drilling fluid or cause an undesired thixotropic effect while it may not influence the other test results. Results from these three tests were used to determine the viscous and elastic characteristics of a drilling fluid. The data obtained from these tests were used to develop a generalized model capable of determining the fluid viscoelasticity in the field.

4.4 Results and Discussion

4.4.1 Rheological Characterization of the Sample Fluids

The results of amplitude sweep tests (results are reported as energy dissipation in this case), funnel, and rotational viscometer measurements are summarized in Tables 4-2, 4-3, 4-4, 4-5 and 4-6. The water-based samples (Table 4-2) included both viscoelastic and visco-inelastic fluids (evaluated based on the energy dissipation concept), to ensure the model produces representative results. Thirteen oil-based samples (Table 4-3) had variations in polymer concentration (NVO) used for building viscosity and the type of base oil ensuring the model applies to viscoelastic oil-based drilling fluids typically used in the field. The invert-emulsion tests included 18 samples (Table 4-4) with different concentrations of polymer used for building viscosity (NVO) and the oil-water ratio to ensure the model is capable of predicting viscoelasticity of invert emulsion drilling fluids. Three field samples collected from the mud tanks (Table 4-5) containing clay helped to validate the model and further investigate the effect of clay on the viscoelasticity. Ten weighted drilling fluids (Table 4-6) were included to investigate the influence of density effect on quantifying viscoelasticity.

Table 4-2 Rheological Characterization of Water-Based Drilling Fluids

Sample No.	Viscosifier	Concentration	Apparent Viscosity	Funnel Viscosity	Energy Dissipation
		(wt.%)	(cp)	(s)	(J/m^3)
1	HPAM1	0.15	9	60	7.23
2	HPAM1	0.2	12	77	8.64
3	HPAM1	0.25	14	97	10.89

4	HPAM1	0.3	16	122	13.65
5	HPAM1	0.35	22	171	16.54
6	HPAM1	0.385	25	245	24.11
7	HPAM2	0.1	3	50	15.35
8	HPAM2	0.15	4	63	17.65
9	HPAM2	0.17	4.5	68	18.23
10	HPAM2	0.2	5	76	19.86
11	HPAM2	0.25	6.5	93	22.13
12	HPAM2	0.3	8.5	115	24.65
13	HPAM3	0.1	2.75	42	12.10
14	HPAM3	0.12	3	45	13.45
15	HPAM3	0.15	3.25	52	14.35
16	HPAM3	0.2	3.5	56	15.12
17	HPAM3	0.25	4	60	18.24
18	HPAM3	0.3	4.5	68	19.36
19	HPAM4	0.25	4	43	7.65
20	HPAM4	0.3	4.5	46	8.65
21	HPAM4	0.35	4.75	50	10.39
22	HPAM4	0.4	5	53	11.96
23	HPAM4	0.45	5.5	56	12.36
24	HPAM4	0.5	5.75	60	13.94
25	PAA1	0.05	15	54	0.69
26	PAA1	0.06	24	79	1.06
27	PAA1	0.065	28	94	2.13

28	PAA1	0.07	34	116	2.65
29	PAA1	0.075	40	143	2.89
30	PAA1	0.09	49	180	3.69
31	PAA2	0.015	11	41	0.11
32	PAA2	0.025	14	49	0.15
33	PAA2	0.035	20	65	0.35
34	PAA2	0.04	27.5	84	0.39
35	PAA2	0.045	35	103	0.49
36	PAA2	0.06	48	139	0.56
37	XG	0.15	9	41	1.87
38	XG	0.2	11	52	3.21
39	XG	0.25	12.5	58	3.56
40	XG	0.27	13.5	64	3.98
41	XG	0.3	14.5	69	4.19
42	XG	0.35	19.5	90	5.36
43	Bentonite	4	7	33	0.26
44	Bentonite	5	10	40	0.49
45	Bentonite	6	13	49	0.71
46	Bentonite	7.5	17	61	1.39
47	Bentonite	8	22.5	74	1.67
48	Bentonite	8.5	26	85	2.19

Table 4-3 Rheological Properties of Oil-Based Drilling Fluids

Sample No.	Additives	Base Oil	Concentration	Apparent Viscosity	Funnel Viscosity	Energy Dissipation
			(wt.%)	(cp)	(s)	(J/m^3)
49	NVO	PDAO	0.1	14	53	0.99
50	NVO	PDAO	0.15	18	66	1.21
51	NVO	PDAO	0.2	21.5	79	1.64
52	NVO	PDAO	0.25	24	102	2.97
53	NVO	PDAO	0.3	27.5	120	3.80
54	NVO	PDAO	0.35	30	182	10.84
55	NVO	PDAO	0.4	33.5	264	15.69
56	NVO	HMO	0.1	9	49	2.16
57	NVO	HMO	0.15	14	69	3.59
58	NVO	HMO	0.2	18.5	90	4.36
59	NVO	HMO	0.25	23	110	4.97
60	NVO	HMO	0.3	27	130	7.16
61	NVO	HMO	0.35	42	197	8.34
62	NVO	HMO	0.4	53	245	9.64

Table 4-4 Rheological Properties of Invert Emulsion Drilling Fluids

Sample No.	Additives	Oil-Water Ratio	Concentration	Apparent Viscosity	Funnel Viscosity	Energy Dissipation
			(wt.%)	(cp)	(s)	(J/m^3)
63	NVO	90-10	0.1	19	68	1.34
64	NVO	90-10	0.15	23	87	1.45
65	NVO	90-10	0.2	27	112	2.36
66	NVO	90-10	0.25	35	139	3.87
67	NVO	90-10	0.3	40	172	5.09
68	NVO	80-20	0.1	24	83	1.29
69	NVO	80-20	0.15	28	98	1.87
70	NVO	80-20	0.2	34	126	2.79
71	NVO	80-20	0.25	39	156	4.08
72	NVO	80-20	0.3	45	194	5.28
73	NVO	70-30	0.1	27	93	1.29
74	NVO	70-30	0.15	31	109	2.09
75	NVO	70-30	0.2	36	126	3.16
76	NVO	70-30	0.25	43	160	3.84
77	NVO	70-30	0.3	49	215	5.89
78	NVO/Bentonite	90-10	0.20/2.0	30	90	0.13
79	NVO/Bentonite	80-20	0.20/2.0	40	116	0.16
80	NVO/Bentonite	70-30	0.20/2.0	47	135	0.28

Table 4-5 Rheological Properties of Drilling Fluid Samples Collected from the Field

Sample No.	Presence of Clay	Apparent Viscosity (cp)	Funnel Viscosity (s)	Energy Dissipation (J/m^3)
81	Yes	18.5	60	0.05
82	Yes	21	68	0.12
83	Yes	33.5	100	0.24

Table 4-6 Rheological Properties of Weighted Drilling Fluid Samples

Sample No.	Fluid Composition	Concentration (%)	Density (kg/m^3)	Apparent Viscosity (cp)	Funnel Viscosity (s)	Energy Dissipation (J/m^3)
84	Field Fluid	-	1325	61	78	0.29
85	Field Fluid	-	1500	39.5	55	0.54
86	XG + Barite	0.32/2.2	1100	16	40	0.79
87	XG + Barite	0.40/14.4	1650	25	41	1.08
88	XG + Barite	0.75/18.9	1850	50	57	1.47
89	HPAM1 + Barite	0.34/4.5	1200	21	150	15.75
90	HPAM1 + Barite	0.20/7.8	1350	12	70	8.64
91	HPAM1 + Barite	0.3/12.3	1550	16	96	13.65
92	HPAM1 + Barite	0.39/14.4	1650	25	162	24.11
93	HPAM1 + Barite	0.48/17.8	1800	35	245	33.14

4.4.2 Factors Affecting the Viscoelasticity of Drilling Fluids

Bentonite is a common clay type used as a viscosifier and filtration loss control additive in drilling fluids. In-situ or native clays also exist in downhole formations and can intermix into the drilling fluid during drilling. Invert emulsion drilling fluids with varying oil-water ratios (OWR) and clay content were used to investigate the effects of OWR and the clay concentration on the drilling fluid viscoelasticity. Rheological properties of OBM fluids (of 3 different OWR) with and without clay presence are shown in Tables 4-7 and 4-8, respectively. The OBM samples in Group 1 (Table 4-7) have a magnitude higher energy dissipation than that of the ones in Group 2 (Table 4-8). This is an indication of the fact that the presence of clay reduces the viscoelasticity of invert-emulsion type drilling fluids. It was also noticeable that the magnitude of the change in energy dissipation due to the clay effect was not constant.

Table 4-7 Group 1 Data (OBM without clay) Extracted from Table 4-4

Sample No.	Additives	Oil-Water Ratio	Concentration	Apparent Viscosity	Funnel Viscosity	Energy Dissipation
			(wt.%)	(cp)	(s)	(J/m^3)
65	NVO	10-90	0.2	27	112	2.36
70	NVO	80-20	0.2	34	126	2.79
75	NVO	70-30	0.2	36	126	3.16

Table 4-8 Group 2 Data (OBM with Clay) Extracted from Table 4-4

Sample No.	Additives	Oil-Water Ratio	Concentration	Apparent Viscosity	Funnel Viscosity	Energy Dissipation
			(wt.%)	(cp)	(s)	(J/m^3)
78	NVO/Bentonite	10-90	0.20/2.0	30	90	0.13
79	NVO/Bentonite	80-20	0.20/2.0	40	116	0.16
80	NVO/Bentonite	70-30	0.20/2.0	47	135	0.28

For all drilling fluid samples in Group 1 and 2, the energy dissipation decreased as the OWR increased indicating that the viscoelasticity of invert-emulsions is inversely proportional to the OWR (Fig 4.5).

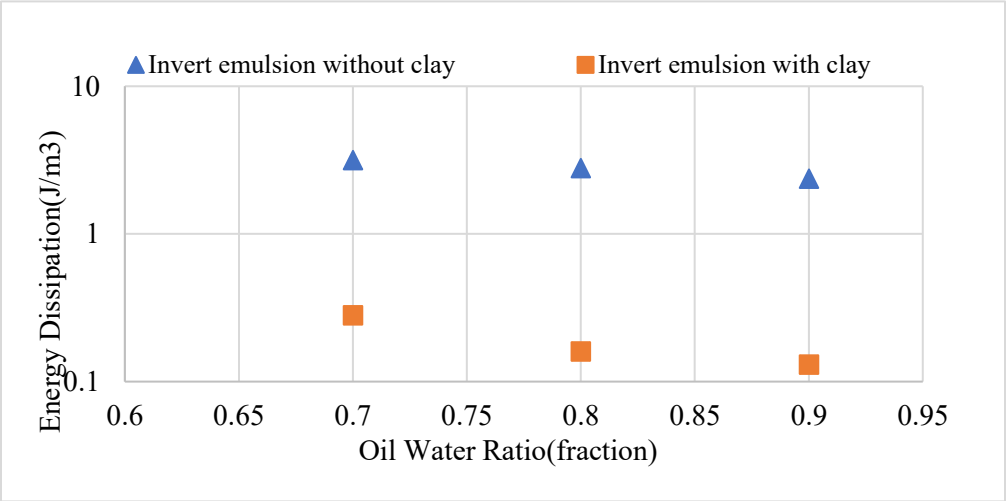

Figure 4.5 Energy Dissipation versus Oil-Water Ratio for Group 1 (without clay) and Group 2 samples (with clay)

Rheological properties presented in Table 4-9 belong to OBM fluids collected from the field. The field oil-based drilling fluids were formulated by using NVO polymer as viscosifier in the base oil (PDAO) and contained clay (i.e., drilled solids from shale formations). Using the same

formulation as the field OBM fluids, we have prepared laboratory samples of OBM fluids, which have the similar apparent viscosity (AV) as the field OBMs but without any clay content and the rheological properties of these fluids are presented in Table 4-10.

Table 4-9 Group 3 Data Extracted from Table 4-5 (OBM fluids collected from the field)

Sample No.	Apparent Viscosity (cp)	Energy Dissipation (J/m^3)	G'-LVE (Pa)	Flow Point Strain (%)
81	18.5	0.05	5.4	34
82	21	0.12	7.3	41
83	33.5	0.24	10.8	47

Table 4-10 Group 4 Data Extracted from Table 4-3 (OBM fluids prepared in the lab)

Sample No.	Apparent Viscosity (cp)	Energy Dissipation (J/m^3)	G'-LVE (Pa)	Flow Point Strain (%)
50	18	1.21	4.3	284
51	21.5	1.64	6.5	335
54	30	10.84	9.7	463

Figure 4.6 shows the amplitude sweep test results of sample 81(i.e. Field OBM fluid containing clay and AV=18.5 cp) and sample 50 (i.e. OBM fluid containing no clay and AV=18.0 cp). The comparison illustrates the effect of clay and/or drilled solids on the fluid viscoelastic properties. Sample 81, with clay and/or drilled solids, has a higher G'-LVE value (5.4 Pa) than sample 50, without clay and/or drilled solids, which has a G'-LVE of 4.3 Pa. The results indicate that a drilling fluid with clay and/or drilled solids has higher viscoelasticity in terms of rigidity (i.e., storage modulus G'). The increase in the rigidity may be due to the increased concentration

of solids, which may increase the internal friction within the liquid and the fluid requires more external stress to deform and lead to an increment in G'-LVE.

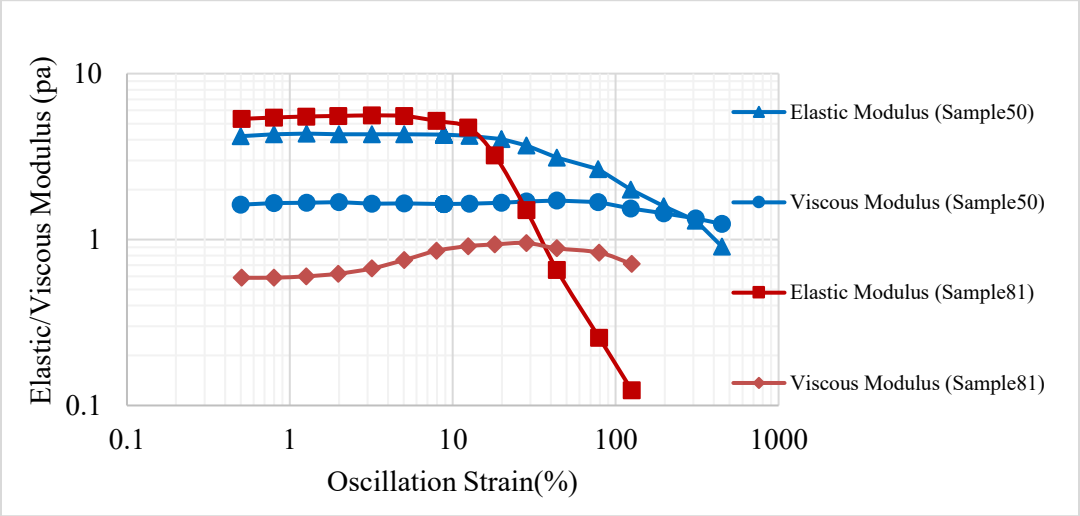

Figure 4.6 Amplitude Sweep Test Results for Samples 50 (without clay and drilled solids) and 81 (containing clay and drilled solids)

The stretchiness (oscillation strain % at the crossover point of G' and G" curves) can also be used to assess the viscoelasticity of a fluid. Sample 50 has a higher crossover point strain value of 284% (Fig 4.6, Table 4-10) than that of sample 81, which has a crossover strain of 34% (Fig 4.6, Table 4-9). The results indicate that if we only consider the stretchiness, sample 50 is more viscoelastic than sample 81. The decreasing stretchiness may result from the increasing concentration of clay and/or drilled solids that potentially interrupt the polymer chains from interacting with each other and causes a reduction of the overall elasticity. These results indicate that neither the rigidity (G') nor the stretchiness (oscillation strain % at the crossover point of G' and G" curves) can be used alone to characterize the viscoelastic properties of a drilling fluid. Therefore, in this study, we propose to use the energy dissipation concept for a more accurate (and comprehensive) characterization of fluid viscoelastic properties.

Figure 4.7 shows the comparison of the energy dissipation versus apparent viscosity plots of samples 50, 51, and 54 (Group 4 in Table 4-10) with samples 81, 82, and 83 (Group 3 in Table 4-9. The two groups of samples exhibit the same trend where the energy dissipation (Fig 4.7) is proportional to their apparent viscosity. Although the apparent viscosities were similar in both groups of fluids, the energy dissipation was different; indicating that the presence of clays in the field fluids (Group 3) might affect the energy dissipation. The results indicate that the presence of additional clay could reduce the viscoelasticity of oil-based drilling fluids. It is, therefore, important to be aware of the formation lithology and understand the effect of in-situ clay or using clays as a viscosifier on the drilling fluid viscoelasticity.

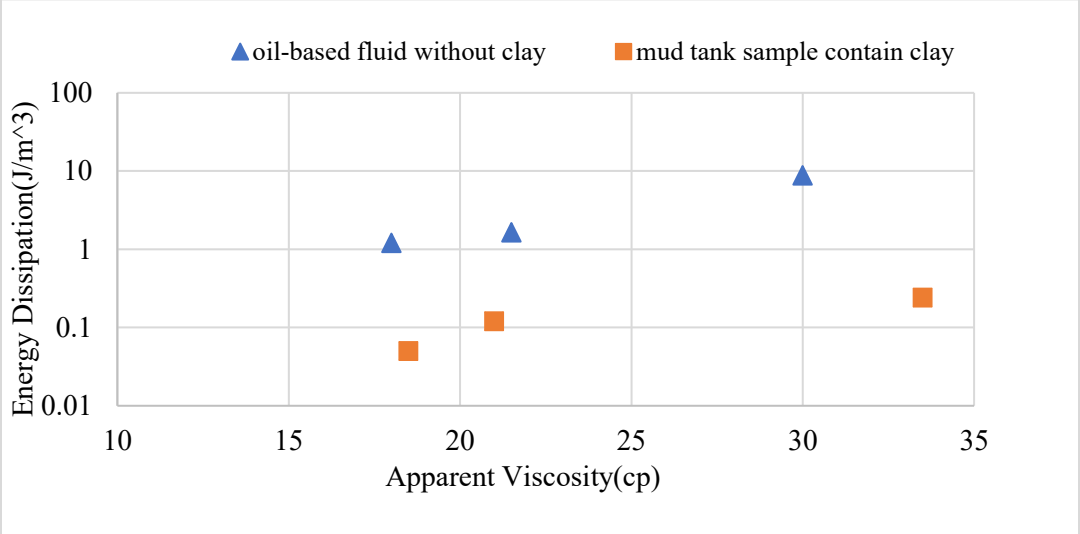

Figure 4.7 Energy Dissipation versus Apparent Viscosity for Group 3 and Group 4 Samples

4.4.3 Field Assessment of Drilling Fluid Viscoelasticity-Model Development

Previous research studies (Pitt, 201) and our initial screening studies have shown that the relationship between the drilling fluid apparent viscosity and funnel viscosity would show

different trends depending on whether the drilling fluid is unweighted or weighted. We have, therefore, developed two different models for assessing viscoelasticity of the unweighted and weighted drilling fluids.

4.4.3.1 Development of Field Energy Dissipation Model for Unweighted Drilling Fluids

It is generally assumed that the funnel viscometer reading is directly related to the drilling fluid shear viscosity. In this study, we introduce a new argument that the flow of drilling fluid through a funnel viscometer is a function of both the fluid shear viscosity and the fluid viscoelasticity. Comparisons of the funnel viscosities of drilling fluid samples with similar apparent viscosity but different elasticity (i.e., energy dissipation) are shown in Table 4-11. Here, the samples in Group 5 are water-based drilling fluids, the samples in Group 6 are oil-based drilling fluids, and the samples in Group 7 are invert-emulsion drilling fluids.

Table 4-11 Comparison of Funnel Viscosity of Samples with Similar Apparent Viscosity and Different Elasticity (Energy Dissipation)

	Sample No.	Base Oil	Oil-Water Ratio	Viscosifier	Concentration (wt.%)	Apparent Viscosity (cp)	Funnel Viscosity (s)	Energy Dissipation (J/m^3)
Group 5	43	-	-	Bentonite	4	7	33	0.26
	11	-	-	HPAM2	0.25	6.5	93	22.13
Group 6	50	PDAO	-	NVO	0.15	18	66	1.21
	58	HMO	-	NVO	0.2	18.5	90	4.36
Group 7	73	PDAO	70-30	NVO	0.1	27	93	1.29
	65	PDAO	10-90	NVO	0.2	27	112	2.36

Groups 5, 6, and 7 include a pair of samples, which have similar apparent viscosities within the group but exhibit different funnel viscosities as well as different Energy Dissipation (elasticity) values. It appears that the viscoelastic property of the drilling fluid affects the funnel viscosity measurement. Cross-correlation of the rheological properties of the fluids within Groups 5, 6, and 7 indicate that the funnel viscosity can be a function of both the viscosity and the elasticity. To understand the relationship between the funnel viscosity and the viscoelasticity of drilling fluid, we first investigated the funnel viscosity changes with the apparent viscosity of visco-inelastic fluids. Figure 4.8 shows funnel viscosity versus apparent viscosity plot of fluids exhibiting very little or no viscoelastic characteristics as indicated by their very low energy dissipation. The detailed information about the fluids used to generate the correlation can be found in Table 4-12.

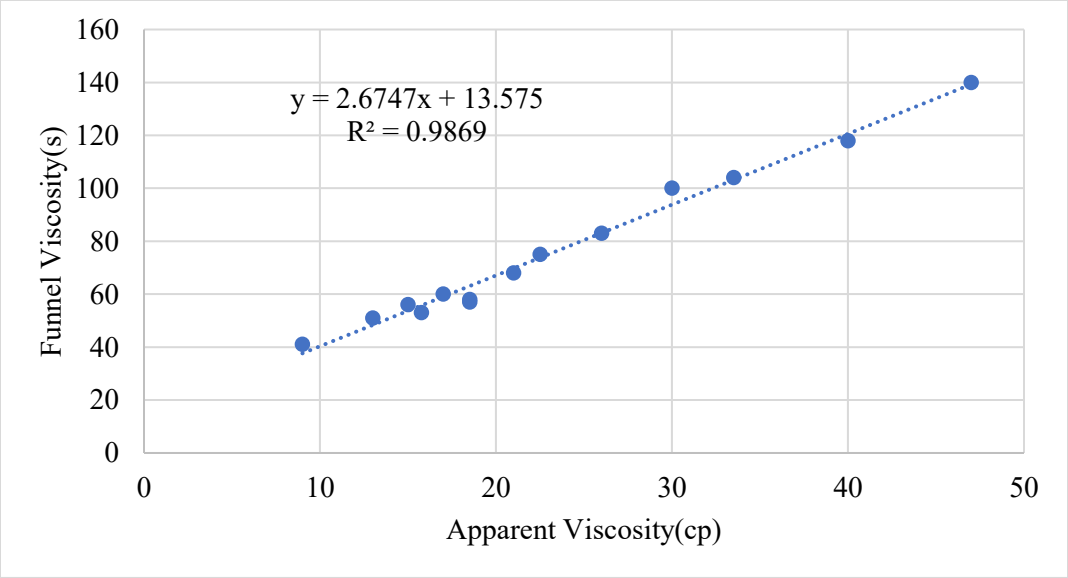

Figure 4.8 Funnel Viscosity versus Apparent Viscosity of Visco-Inelastic Fluids

Table 4-12 Visco-Inelastic Fluids Used to Generate the Relationship between Funnel Viscosity and Apparent Viscosity

Sample No.	Additive	OWR	Concentration (%)	Apparent Viscosity (cp)	Funnel Viscosity (s)	E_D (J/m^3)
37	XG	-	0.15	9	41	1.87
38	XG	-	0.2	11	52	3.21
45	Bentonite	-	6	13	49	0.71
46	Bentonite	-	7.5	17	61	1.39
47	Bentonite	-	8	22.5	74	1.67
48	Bentonite	-	8.5	26	85	2.19
49	NVO	-	0.1	14	53	0.99
78	NVO/BENTONITE	90-10	0.2/2.0	30	90	0.13
79	NVO/BENTONITE	80-20	0.2/2.0	40	116	0.16
80	NVO/BENTONITE	70-30	0.2/2.0	47	135	0.28
81	Field Sample	-	-	18.5	60	0.05
82	Field Sample	-	-	21	68	0.12
83	Field Sample	-	-	33.5	100	0.24

As shown in Fig 4.8, there is a linear correlation between the funnel viscosity and the apparent viscosity of these fluids, which also explains why the funnel viscometer measurement is a reliable tool to measure the fluid apparent viscosity. Using regression analyses of the data presented in Fig 4.8, we have developed an empirical model for estimating the funnel viscosity as a function of the apparent viscosity of visco-inelastic fluids (Eq 4.4).

$$PFV = 2.67*AV + 13.575 \quad (4.4)$$

Where:

PFV = Predicted funnel viscosity, sec

AV = Apparent viscosity, cp

The data shown in Table 4-11 suggests that the funnel viscosity of a fluid is a function of both the viscous and elastic fluid properties. A three-step methodology was followed to develop the relationship among the apparent viscosity, viscoelasticity, and the funnel viscosity.

Step-1: Determine the apparent viscosity of the fluid using a rotational viscometer (Eq 4.3), assuming the fluid is visco-inelastic, predict the corresponding funnel viscosity (PFV) by using Eq 4.4.

Step-2: Measure the actual funnel viscosity (MFV) of the fluid and compare it with the predicted value from Step-1. If the fluid was viscoelastic, the predicted funnel viscosity would not be the same as the direct measurement from the funnel viscometer. In that case, calculate the percentage of deviation (PD) between the predicted and measured funnel viscosity values using Eq 4.5.

$$PD = (MFV-PFV)/PFV*100 \quad (4.5)$$

Where:

PD = percentage of deviation, %

MFV = measured funnel viscosity, sec

PFV = predicted funnel viscosity, sec

Step-3: Plot the percentage of deviation (PD) versus energy dissipation (ED) of the test fluid (Fig 4.9).

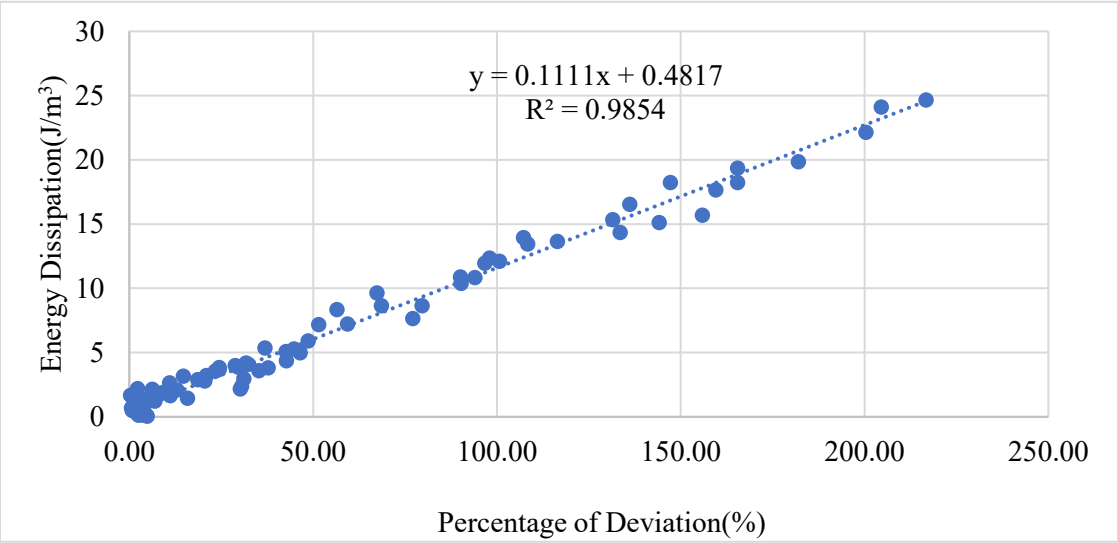

Figure 4.9 Energy Dissipation versus Percentage of Deviation of Funnel Viscosity between Viscoelastic and Visco-Inelastic Fluids

As shown in Fig 4.9, there is a linear relationship between the percentage of deviation (i.e., deviation between measured and predicted funnel viscosity values) and the fluid viscoelasticity measured in terms of energy dissipation (J/m^3). For visco-inelastic fluids, the percentage of deviation will be very low (close to zero) since the funnel viscosity is not inflated by the viscoelasticity. The low-energy-dissipation, low-percentage of deviation samples are shown near the origin in Fig 4.9. For viscoelastic fluids, depending on the degree of viscoelasticity, the sample would exhibit a correspondingly higher level of funnel viscosity, which would result in a higher percentage of deviation between the measured and predicted funnel viscosity values. The higher the percentage deviation of funnel viscosity is, the higher the energy dissipation and the more

elastic a fluid will be. The correlation between the energy dissipation (ED) and the percentage of deviation (PD) is explicitly illustrated by Eq 4.6.

$$\text{Energy Dissipation } (J/m^3) = 0.1111 * PD + 0.4817 \quad (4.6)$$

Finally, by introducing Equations 4.4 and 4.5 into Equation 4.6, a unified model for predicting the energy dissipation of drilling fluid was obtained (Eq 4.7). As discussed earlier in the introduction section, energy dissipation(E_D) is an excellent measure of the fluid elasticity. Equation 4.7 describes an explicit model that can be used to determine the energy dissipation (and, hence the elasticity) of drilling fluid as a function of the funnel viscosity (MFV) and the apparent viscosity (AV), both are obtained from direct field measurements.

$$\text{Energy Dissipation } (J/m^3) = 11.11*[(MFV-PFV)/PFV]+0.4817 \quad (4.7)$$

Where:

MFV = measured funnel viscosity, sec

PFV = predicted funnel viscosity, sec

The new model is capable of predicting energy dissipation based on the field measured values of funnel and apparent viscosity of the unweighted viscoelastic fluids. Two examples showing the application of the model (Eq 4.7) are presented in the Appendix-B.

Note that the drilling fluids (including field samples) used for the development of the Field Energy Dissipation model (Eq 4.7) were all unweighted fluids. In the following section, we will present the results of our analyses using weighted drilling fluid samples and provide a new model that can be used for predicting Field Energy Dissipation of weighted drilling fluids.

4.4.3.2 Development of Field Energy Dissipation Model for Weighted Drilling Fluids

Majority of drilling activities require the use of weighted drilling fluid for ECD management. In order to account for the density effect on the field energy dissipation, ten weighted drilling fluids (five visco-inelastic fluids and five viscoelastic fluids) with a density range of 1200 to 1800 kg/m3 were used for further analyses.

Pitt (2001) developed a model (Eq 4.8) correlating apparent viscosity with the funnel viscosity and density of the drilling fluids. Rearranging the Eq 4.8, drilling fluid funnel viscosity can be written in terms of apparent viscosity and density as shown in Eq 4.9.

$$AV = \exp\left[\frac{ln(\frac{PFV-24.5}{0.58})}{1.2} + ln(\rho)\right] \quad 4.8$$

$$PFV = 0.58*\exp[1.2[\ln(AV)-\ln(\rho)]]+24.5 \quad 4.9$$

Where:

PFV = predicted funnel viscosity, sec

AV = Apparent viscosity, cp

ρ = density, g/cm^3

We have used direct measurements of apparent viscosity, funnel viscosity and density of 5 visco-inelastic fluids to verify the accuracy of the model (Eq 4.9) prediction. Detailed properties of the fluids used for model verification and results from the comparisons of the predicted and the measured funnel viscosity values are summarized in Table 4-13.

Very low energy dissipation (E_D) values of the fluids confirmed that these fluids can be considered as visco-inelastic. The difference between predicted and measured funnel viscosity values were less than 5%, indicating reasonable accuracy of the Pitt (2001) model for predicting funnel viscosity of the visco-inelastic fluids.

Table 4-13 The API Viscometry, Funnel Viscometry, and Amplitude Sweep Test Results for 5 Weighted Visco-Inelastic Fluids

Sample No.	Fluid Composition	Concentration (%)	Density (kg/m^3)	AV (cp)	E_D (J/m^3)	PFV (s)	MFV (s)	Difference(%)
84	Field Fluid	-	1325	61	0.29	82	78	4.8
85	Field Fluid	-	1500	39.5	0.54	54	55	2.1
86	XG + Barite	0.32 / 2.2	1100	16	0.79	39	40	2.8
87	XG + Barite	0.4 / 14.4	1650	25	1.08	40	41	3.4
88	XG + Barite	0.75 / 18.9	1850	50	1.47	55	57	4.0

Five viscoelastic fluids with various density were used to conduct API viscometry, Funnel viscometry and amplitude sweep measurement tests and the results are summarized in Table 4-14.

Table 4-14 The API Viscometry, Funnel Viscometry, and Amplitude Sweep Test Results for 5 Weighted Viscoelastic Fluids

Sample No.	Additive	Concentration (%)	Density (kg/m^3)	E_D (J/m^3)	AV (cp)	MFV (s)	PFV (s)	Percentage of deviation (%)
89	HPAM1 + Barite	0.34 / 4.5	1200	15.75	21	150	43	248.8
90	HPAM1 + Barite	0.2 / 7.8	1350	8.64	12	70	34	105.9
91	HPAM1 + Barite	0.3 / 12.3	1550	13.65	16	96	35	174.3
92	HPAM1 + Barite	0.39 / 14.4	1650	24.11	25	162	40	305.0
93	HPAM1 + Barite	0.48 / 17.8	1800	33.14	35	245	44	456.8

The energy dissipation values of these fluids were very high, confirming the viscoelastic nature of these fluids. Percentage of deviation of measured funnel viscosity (calculated using Eq 4.5) from the predicted funnel viscosity of these fluids were noticeably high. Knowing that the Pitt model(2021) was developed for visco-inelastic fluids, these high percentage of deviations of measured funnel viscosity values of viscoelastic fluids from the predicted values were not unexpected. A plot of energy dissipation of the weighted viscoelastic fluids versus percentage deviation proves that a reasonable correlation exists between these two variables (Fig 4.10). By curve fitting the trend line observed in Fig 4.10, we have obtained a new correlation between energy dissipation of the viscoelastic fluids and the percentage deviation (Eq 4.10). The percentage deviation can be computed by introducing measured and predicted funnel viscosity

values into Eq 4.5, where the predicted funnel viscosity here is defined by Eq 4.9, which considers the density effect.

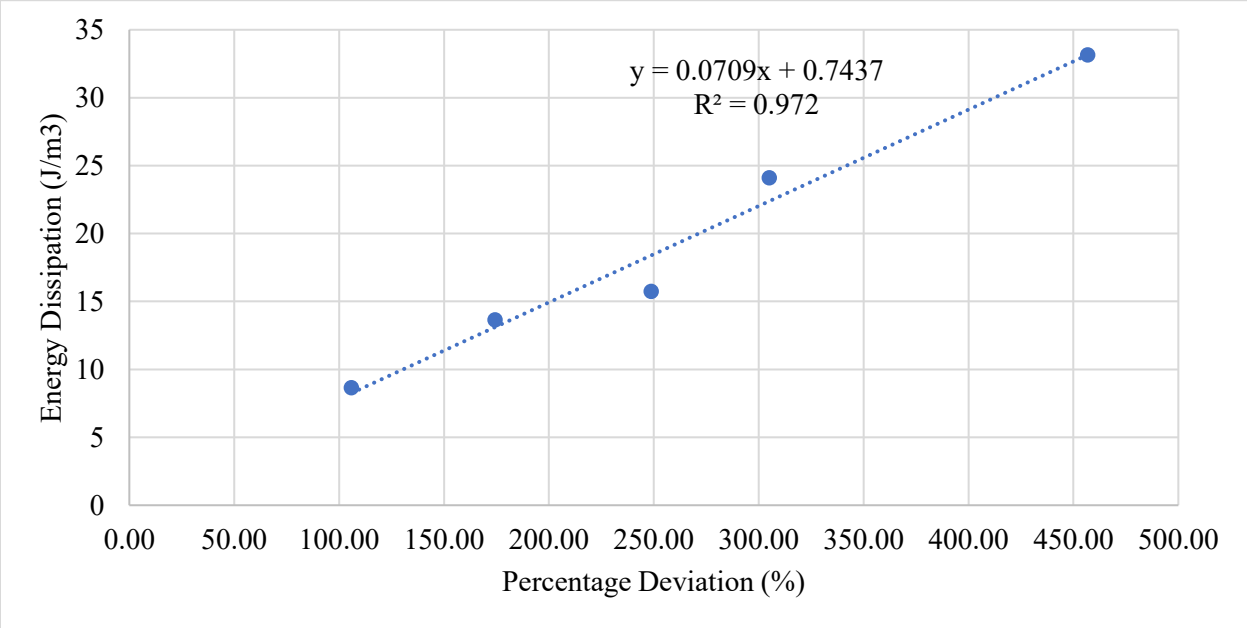

Figure 4.10 Energy Dissipation versus Percentage Deviation for 5 Weighted Viscoelastic Fluids

$$\text{Energy Dissipation } (J/m^3) = 0.0709 * PD + 0.7437 \qquad 4.10$$

The new model is capable of predicting energy dissipation based on the field measured values of density, funnel, and apparent viscosity of the weighted viscoelastic fluids. An example showing the application of the model (Eq 4.10) is presented in the Appendix-C.

4.4.3.3 Statistical Evaluation of the Model Accuracy

Statistical analyses were conducted to assess the accuracy of the model prediction of energy dissipation. The root mean square error (RMSE) is frequently used to measure the deviation between the predicted value and actual values (Eq 4.11). The mean absolute percentage error

(MAPE) is a measure of the prediction accuracy of a forecasting method (Eq 4.12). MAPE depicts the expected percentage error associated with a specific model. Generally, the lower the RMSE and MAPE values more accurate is the model prediction.

$$RMSE= \sqrt{\frac{\sum_1^n (E_{Dp}-E_{Da})}{n}} \quad 4.11$$

$$MAPE=\frac{1}{n} * \sum_1^n \left|\frac{(E_{Da}-E_{Dp})}{E_{Da}}\right| \quad 4.12$$

Where:

n = total number of samples

E_{Da} = actual energy dissipation values of the fluids as measured in the lab, J/m^3

E_{Dp} = energy dissipation values of the fluids predicted by using the model, J/m^3

The RMSE and MAPE of the model for unweighted viscoelastic fluids was 0.167 J/m^3 and 4.67%, respectively. The RMSE and MAPE of the model for weighted viscoelastic fluids was 0.547 J/m^3 and 5.28%, respectively.

4.4.4 Discussions

The focus of the work efforts presented in this paper was to understand the factors influencing the drilling fluid's viscoelasticity and develop a generalized model for assessing the viscoelasticity (measured in terms of energy dissipation) of drilling fluids by using the data from direct field measurements such as funnel viscosity and apparent viscosity.

It has been well documented that drilling fluid viscoelastic properties strongly influence gel-strength, barite-sag (Bui et al., 2012), filtration-loss characteristics of the drilling fluids (Dehghanpour and Kuru, 2011), particle settling velocity (Arnipally and Kuru, 2018), hole cleaning and cuttings transport (Bizhani and Kuru, 2018; Hirpa and Kuru, 2020).

Dehghanpour and Kuru, (2011) reported that static filtration loss of the drilling fluids can be effectively reduced by increasing fluid viscoelasticity. Drill-in fluids with extended viscoelasticity can be formulated to minimize the dynamic filtration losses into the reservoir rock (by increasing the resistance of fluid flow into the reservoir rock and, hence, effectively building internal cake) and, thereby reduce potential formation damage problems that may be caused by drilling operations, especially when drilling long horizontal well sections.

Arnipally and Kuru, (2018) demonstrated that the settling velocity of particles can be reduced up to 50 times when the effect of the fluid elasticity is included in drilling fluid formulation. Viscoelasticity can, therefore, be effectively used to improve solids suspension ability of the drilling fluids, which will enhance cuttings transport ability of fluids in vertical sections as well as mitigating Barite sag issues in the horizontal sections of the wells.

Other recent studies (Bizhani and Kuru, 2018; Hirpa and Kuru, 2020) also showed that viscoelastic fluids require much higher flow rates than that of water to initiate the cuttings bed erosion (i.e., need to dissipate more turbulent energy and exert higher drag force). Formation of stationary cuttings bed deposits is inevitable when drilling long horizontal and extended reach wells. Operational problems arise such as low ROP, excessive torque and drag, bridging, pack-off, hole fill and pipe stuck. Occasionally drilling must stop to clean the well, this costs time and money. Therefore, hole cleaning must be performed in timely and cost-effective manner. Results of hole

cleaning studies using viscoelastic fluid suggests that viscoelasticity delays the onset of bed erosion; therefore, fluids used for hole cleaning in long horizontal and extended reach wells should be of visco-inelastic nature. From the practical point of interest, fluids used for hole cleaning process can be formulated by using viscosifier comprised of low molecular weight, short-chain length polymers such as polyanionic cellulose (e.g., PAC) rather than using high molecular weight, long chain polymers such as derivatives of hydrolyzed polyacrylamides (e.g., PHPA).

Results from previous studies clearly suggested the viscoelastic properties of the drilling fluids are very important and should be given due consideration when preparing drilling fluid and hydraulic design programs of drilling operations. Although the impact of drilling fluid viscoelasticity on the various elements of drilling hydraulics design has been well recognized; the field implementation these research findings have been hampered mainly because there has not been any standard field technique available for measuring the fluid viscoelastic properties. The development of a generalized model for quantifying viscoelasticity by using field testing equipment would help to fill this knowledge gap and; hence, open the ways for developing optimum drilling fluid formulations by considering viscoelastic properties. Availability of such practical methodology for field evaluation of drilling fluid viscoelasticity is expected to facilitate design and development of improved drilling hydraulics programs.

The main objective of the current paper is to provide a generalized, field-measurement based methodology and the proof of the concept for assessing the viscoelasticity of the drilling fluids. Validity of the new models have been confirmed by presenting sample assessments of the viscoelasticity of unweighted and weighted drilling fluid samples as shown in Appendix-B and C, respectively. Design and development of the optimum drilling hydraulics program utilizing

viscoelastic drilling fluids would require extensive field case study works and is, therefore, beyond the scope of this study.

4.5 Conclusion

Paper presents a new methodology to determine the viscoelasticity of the drilling fluids using funnel viscosity and apparent viscosity, which are commonly measured using conventional field-testing equipment (i.e., funnel viscometer and rotational viscometer).

The new method uses the energy dissipation concept to quantify the drilling fluid viscoelasticity and correlates it to the apparent viscosity and the funnel viscosity of drilling fluids. Statistical assessments confirm that the model for unweighted drilling fluids can predict the energy dissipation of the viscoelastic fluid with a RMSE of 0.167 J/m^3 and a MAPE of 4.67%. The model for weighted drilling fluids can predict the energy dissipation a RMSE of 0.547 J/m^3 and MAPE of 5.28%.

Paper also provides results of investigations on how the change in oil-water ratio and the presence of clays/drilled solids would affect the elasticity of the drilling fluids.

Based on the results from this study following additional conclusions can be offered:

- Neither the rigidity modulus (G') nor the stretchiness (oscillation strain % at the crossover point of G' and G" curves) can solely characterize the viscoelastic property of the drilling fluid. More comprehensive assessment on the viscoelastic characteristics of the drilling fluid can be done using the "energy dissipation" concept.

- For the same concentration of a viscosifying additive and the type of base oil, the fluid's viscoelasticity shows to be inversely proportional to the oil-water ratio.

- Viscoelasticity oil-based drilling fluids show a reduction with additions of clays.

- Since the presence of clays influences the viscoelasticity, it is important to consider the effect of natural clay and drill solids as they intermix with the drilling fluid.

With the development of the new model, drilling fluid viscoelasticity can now be evaluated at the well site by using commonly measured apparent viscosity and funnel viscosity data. A better understanding of the drilling fluid viscoelastic properties would help field engineers to develop optimum drilling fluid formulations and hydraulic programs for effective hole cleaning operations, improved ECD management, and mitigating barite sag problems.

4.6 Acknowledgements

This project is financially supported through the funds provided by the Natural Sciences and Engineering Research Council of Canada (NSERC RGPIN-2016-04647 Kuru, NSERC EGP 543455-19 Kuru). The authors would also like to acknowledge the technical support provided by Newpark Canada Inc.

4.7 References

Abdelgawad, K., Elzenary, M., Elkatatny, S. et al (2018). New approach to evaluate the equivalent circulating density (ECD) using artificial intelligence techniques. Journal of Petroleum Exploration and Production Technology. 9. 10.1007/s13202-018-0572-y.

AlBahrani, H., Alsheikh, M., Wagle, V., and Aqeel A. Designing Drilling Fluids Rheological Properties with a Numerical Geomechanics Model for the Purpose of Improving Wellbore Stability. Paper presented at the IADC/SPE International Drilling Conference and Exhibition, Galveston, Texas, USA, March 2022. doi: https://doi.org/10.2118/208753-MS

Allahvirdizadeh, P., & Kuru, E. (2015). A Comparative Study of Cuttings Transport Performance of Water versus Polymer-Based Fluids in Horizontal wells. https://www.researchgate.net/publication/276354306

API RP 13B-1, Recommended Practice for Field Testing Water-based Drilling Fluids. (2019). Washington, DC United States: API.

API RP 13B-2, Recommended Practice for Field Testing Oil-based Drilling fluids. (2014). Washington, DC United States: API.

Amighi, M. R. and Khalil S. "Effective Ways to Avoid Barite Sag and Technologies to Predict Sag in HPHT and Deviated Wells." Paper presented at the SPE Deep Gas Conference and Exhibition, Manama, Bahrain, January 2010. doi: https://doi.org/10.2118/132015-MS

Arnipally, S. K., Kuru, E. (2018). Settling Velocity of Particles in Viscoelastic Fluids: A Comparison of the Shear Viscosity vs Elasticity Effect. SPE J. 23 (05):1689–1705.https://doi.org/10.2118/187255-PA.

Bizhani, M. and Kuru, E. (2018). Particle Removal From Sandbed Deposits in Horizontal Annuli Using Viscoelastic Fluids. SPE J. 23 (2018): 256–273. doi: https://doi.org/10.2118/189443-PA

Bui, B., Saasen, A., Maxey, J., Ozbayoglu, E., Miska, S., Yu, M. (2012). Viscoelastic properties of oil-based drilling fluids. Annual Trans Nordic Rheol Soc. 20. 33-47.

Chesser, B. G., Clark, D. E., and W. V. Wise. "Dynamic and Static Filtrate-Loss Techniques for Monitoring Filter-Cake Quality Improves Drilling-Fluid Performance." SPE Drill & Compl 9 (1994): 189–192. doi: https://doi.org/10.2118/20439-PA

Dehghanpour, H., & Kuru, E. (2011). Effect of viscoelasticity on the filtration loss characteristics of aqueous polymer solutions. Journal of Petroleum Science and Engineering, 76(1–2), 12–20. https://doi.org/10.1016/J.PETROL.2010.12.005

Foshee, W. C., Jennings, R. R., & West, T. J. (1976). Preparation and Testing of Partially Hydrolyzed Polyacrylamide Solutions. SPE-6202-MS. Paper presented at the SPE Annual Fall Technical Conference and Exhibition, New Orleans, LA. https://doi.org/10.2118/6202-MS.

Hirpa, M.M. and Kuru, E. (2020). Hole Cleaning in Horizontal Wells Using Viscoelastic Fluids: An Experimental Study of Drilling-Fluid Properties on the Bed-Erosion Dynamics. SPE J. 25 (2020): 2178–2193. doi: https://doi.org/10.2118/199636-PA

Maxey, J. (2010). A Rheological Approach to Differentiating Muds by Gel Structure. AADE-10-DF-HO-27, AADE 2010 Fluids Conference, Houston, Texas, April 6-7, 2010.

Pitt, M. J.. "The Marsh Funnel and Drilling Fluid Viscosity: A New Equation for Field Use." SPE Drill & Compl 15 (2000): 3–6. doi: https://doi.org/10.2118/62020-PA

Powell, J. W., Parks, C. F., and Seheult, J. M. (1991). Xanthan and Welan: The Effects of Critical Polymer Concentration on Rheology and Fluid Performance. International Arctic Technology Conference. Society of Petroleum Engineers. https://doi.org/10.2118/22066-MS.

Rabenjafimanantsoa, H. A., Rune, W. T. and Saasen, A. (2005). Flow regimes over particle beds experimental studies of particle transport in horizontal pipes. Annual Transactions of the Nordic Rheology Society.

Saasen, A. and Løklingholm, G. (2002). The Effect of Drilling Fluid Rheological Properties on Hole Cleaning. IADC/SPE Drilling Conference. Dallas, Texas, 26-28 February, SPE-74558-MS, DOI: 10.2118/74558-MS.

Sayindla, S., Lund, B., Ytrehus, J. D., & Saasen, A. (2017). Hole-cleaning performance comparison of oil-based and water-based drilling fluids. Journal of Petroleum Science and Engineering, 159, 49-57. https://doi.org/10.1016/j.petrol.2017.08.069.

Sedaghat, A. (2017). A novel and robust model for determining rheological properties of Newtonian and non-Newtonian fluids in a marsh funnel. Journal of Petroleum Science and Engineering, 156, 896–916. https://doi.org/10.1016/j.petrol.2017.06.057

Werner, B., Myrseth, V., & Saasen, A. (2017). Viscoelastic properties of drilling fluids and their influence on cuttings transport. Journal of Petroleum Science and Engineering, 156, 845-851. https://doi.org/10.1016/j.petrol.2017.06.063.

Williamson, D. (2013). Drilling fluid basics. Oilfield Review, 25(1), 63–64. http://www.slb.com/resources/oilfield_review/en/2013/or2013_spr.aspx

Zamora, M., Jefferson, D. T., Powell, J. W. (1993). Hole-Cleaning Study of Polymer-Based Drilling Fluids. Society of Petroleum Engineers. doi:10.2118/26329-MS.

Appendix-A Composition and Nomenclature for Drilling Fluids Utilized in This Study

Sample No.	Viscosifier	Drilling Fluid Type	Concentration (%)	Oil-Water Ratio	Base Solution	Clay Presence
1	HPAMB	WBM	0.15	-	De-ionized water	No
2	HPAMB	WBM	0.2	-	De-ionized water	No
3	HPAMB	WBM	0.25	-	De-ionized water	No
4	HPAMB	WBM	0.3	-	De-ionized water	No
5	HPAMB	WBM	0.35	-	De-ionized water	No
6	HPAMB	WBM	0.385	-	De-ionized water	No
7	HPAM3630	WBM	0.1	-	De-ionized water	No
8	HPAM3630	WBM	0.15	-	De-ionized water	No
9	HPAM3630	WBM	0.17	-	De-ionized water	No
10	HPAM3630	WBM	0.2	-	De-ionized water	No
11	HPAM3630	WBM	0.25	-	De-ionized water	No
12	HPAM3630	WBM	0.3	-	De-ionized water	No
13	HPAM3330	WBM	0.1	-	De-ionized water	No
14	HPAM3330	WBM	0.12	-	De-ionized water	No

15	HPAM3330	WBM	0.15	-	De-ionized water	No
16	HPAM3330	WBM	0.2	-	De-ionized water	No
17	HPAM3330	WBM	0.25	-	De-ionized water	No
18	HPAM3330	WBM	0.3	-	De-ionized water	No
19	HPAM3130	WBM	0.25	-	De-ionized water	No
20	HPAM3130	WBM	0.3	-	De-ionized water	No
21	HPAM3130	WBM	0.35	-	De-ionized water	No
22	HPAM3130	WBM	0.4	-	De-ionized water	No
23	HPAM3130	WBM	0.45	-	De-ionized water	No
24	HPAM3130	WBM	0.5	-	De-ionized water	No
25	Carbopol 940	WBM	0.05	-	De-ionized water	No
26	Carbopol 940	WBM	0.06	-	De-ionized water	No
27	Carbopol 940	WBM	0.065	-	De-ionized water	No
28	Carbopol 940	WBM	0.07	-	De-ionized water	No
29	Carbopol 940	WBM	0.075	-	De-ionized water	No
30	Carbopol 940	WBM	0.09	-	De-ionized water	No
31	Carbopol 2020	WBM	0.015	-	De-ionized water	No

32	Carbopol 2020	WBM	0.025	-	De-ionized water	No
33	Carbopol 2020	WBM	0.035	-	De-ionized water	No
34	Carbopol 2020	WBM	0.04	-	De-ionized water	No
35	Carbopol 2020	WBM	0.045	-	De-ionized water	No
36	Carbopol 2020	WBM	0.06	-	De-ionized water	No
37	Xanthan Gum	WBM	0.15	-	De-ionized water	No
38	Xanthan Gum	WBM	0.2	-	De-ionized water	No
39	Xanthan Gum	WBM	0.25	-	De-ionized water	No
40	Xanthan Gum	WBM	0.27	-	De-ionized water	No
41	Xanthan Gum	WBM	0.3	-	De-ionized water	No
42	Xanthan Gum	WBM	0.35	-	De-ionized water	No
43	Bentonite	WBM	4	-	De-ionized water	Yes
44	Bentonite	WBM	5	-	De-ionized water	Yes
45	Bentonite	WBM	6	-	De-ionized water	Yes
46	Bentonite	WBM	7.5	-	De-ionized water	Yes

47	Bentonite	WBM	8	-	De-ionized water	Yes
48	Bentonite	WBM	8.5	-	De-ionized water	Yes
49	GEL8	OBM	0.1	100-0	Diesel Oil	No
50	GEL8	OBM	0.15	100-0	Diesel Oil	No
51	GEL8	OBM	0.2	100-0	Diesel Oil	No
52	GEL8	OBM	0.25	100-0	Diesel Oil	No
53	GEL8	OBM	0.3	100-0	Diesel Oil	No
54	GEL8	OBM	0.35	100-0	Diesel Oil	No
55	GEL8	OBM	0.4	100-0	Diesel Oil	No
56	GEL8	OBM	0.1	100-0	Mineral Oil	No
57	GEL8	OBM	0.15	100-0	Mineral Oil	No
58	GEL8	OBM	0.2	100-0	Mineral Oil	No
59	GEL8	OBM	0.25	100-0	Mineral Oil	No
60	GEL8	OBM	0.3	100-0	Mineral Oil	No
61	GEL8	OBM	0.35	100-0	Mineral Oil	No
62	GEL8	OBM	0.4	100-0	Mineral Oil	No
63	GEL8	Invert Emulsion	0.1	10-90	Diesel Oil +De-ionized water	No
64	GEL8	Invert Emulsion	0.15	10-90	Diesel Oil +De-ionized water	No

65	GEL8	Invert Emulsion	0.2	10-90	Diesel Oil +De-ionized water	No
66	GEL8	Invert Emulsion	0.25	10-90	Diesel Oil +De-ionized water	No
67	GEL8	Invert Emulsion	0.3	10-90	Diesel Oil +De-ionized water	No
68	GEL8	Invert Emulsion	0.1	80-20	Diesel Oil +De-ionized water	No
69	GEL8	Invert Emulsion	0.15	80-20	Diesel Oil +De-ionized water	No
70	GEL8	Invert Emulsion	0.2	80-20	Diesel Oil +De-ionized water	No
71	GEL8	Invert Emulsion	0.25	80-20	Diesel Oil +De-ionized water	No
72	GEL8	Invert Emulsion	0.3	80-20	Diesel Oil +De-ionized water	No
73	GEL8	Invert Emulsion	0.1	70-30	Diesel Oil +De-ionized water	No
74	GEL8	Invert Emulsion	0.15	70-30	Diesel Oil +De-ionized water	No
75	GEL8	Invert Emulsion	0.2	70-30	Diesel Oil +De-ionized water	No
76	GEL8	Invert Emulsion	0.25	70-30	Diesel Oil +De-ionized water	No
77	GEL8	Invert Emulsion	0.3	70-30	Diesel Oil +De-ionized water	No
78	GEL8/Bentonite	Invert Emulsion	0.20/2.0	10-90	Diesel Oil +De-ionized water	Yes

79	GEL8/Bentonite	Invert Emulsion	0.20/2.0	80-20	Diesel Oil +De-ionized water	Yes
80	GEL8/Bentonite	Invert Emulsion	0.20/2.0	70-30	Diesel Oil +De-ionized water	Yes
81	Field Fluid	OBM	-	100-0	Diesel Oil	Yes
82	Field Fluid	OBM	-	100-0	Diesel Oil	Yes
83	Field Fluid	OBM	-	100-0	Diesel Oil	Yes
84	Field Fluid	OBM	-	100-0	Diesel Oil	Yes
85	Field Fluid	OBM	-	100-0	Diesel Oil	Yes
86	Flowzan + Barite	WBM	0.32/2.2	-	De-ionized water	Yes
87	Flowzan + Barite	WBM	0.40/14.4	-	De-ionized water	Yes
88	Flowzan + Barite	WBM	0.75/18.9	-	De-ionized water	Yes
89	HPAMB + Barite	WBM	0.34/4.5	-	De-ionized water	Yes
90	HPAMB + Barite	WBM	0.20/7.8	-	De-ionized water	Yes
91	HPAMB + Barite	WBM	0.30/12.3	-	De-ionized water	Yes
92	HPAMB + Barite	WBM	0.39/14.4	-	De-ionized water	Yes
93	HPAMB + Barite	WBM	0.48/17.8	-	De-ionized water	Yes

Appendix-B Example Field Assessment of Unweighted Drilling Fluid Viscoelasticity

Procedure

The following procedure can be used to determine the energy dissipation of a drilling fluid in the field:

1. Measure the funnel viscosity (MFV) of the drilling fluid using a funnel viscometer.

2. Measure the 600 rev/min reading (Θ600) using the rotational viscometer.

3. Determine the apparent viscosity (AV) of the drilling fluid, AV=Θ600/2.

4. Predict the funnel viscosity (PFV) of the drilling fluid using Eq 4.4 or Eq 4.7, depending on if the drilling fluids has been weighted or not.

5. Determine the energy dissipation of the drilling fluid using Eq 4.7 or Eq 4.10, depending on if the drilling fluid has been weighted or not.

Two sample calculations were performed to demonstrate that the generalized model works both for WBM and OBM.

The 1st example uses the rheological properties of sample #54(OBM) from Table 4-3.

1. The measured funnel viscosity (MFV) is 182 s.

2. The measured 600 rev/min reading from the rotational viscometer is 60 cp.

3. The apparent viscosity (AV) uses Eq 4.3.

AV = Θ600/2 = 60/2 = 30 cp

4. Predicted funnel viscosity uses Eq 4.4.

PFV = 2.67*AV + 13.575 = 2.67*30 + 13.575 = 93.68 sec

5. The energy dissipation of the drilling fluid uses Eq 4.7.

Energy Dissipation (J/m3) = 11.11*[(MFV-PFV)/PFV] + 0.4817

Energy Dissipation (J/m3) = 11.11*[(182-93.68)/93.68] + 0.4817 = 10.96 J/m3

The measured energy dissipation of sample #54 was 10.84 J/m^3. The difference between the measured energy dissipation and predicted energy dissipation is 0.12 J/m^3 (the difference is less than 1.2%). Results indicate that the new model prediction of the drilling fluid viscoelasticity is sufficiently accurate for OBM, and the model can be used for the assessment of the oil-based drilling fluid viscoelasticity in the field.

The 2nd example uses the rheological properties of sample #10(WBM) from Table 4-2.

1. The measured funnel viscosity (MFV) is 76 s.

2. The measured 600 rev/min reading from the rotational viscometer is 10 cp.

3. The apparent viscosity (AV) uses Eq 4.3.

AV = Θ600/2 = 10/2 = 5 cp

4. Predicted funnel viscosity uses Eq 4.4.

PFV = 2.67*AV + 13.575 = 2.67*5 + 13.575 = 26.93 sec

5. The energy dissipation of the drilling fluid uses Eq 4.7.

Energy Dissipation (J/m3) = 11.11*[(MFV-PFV)/PFV] + 0.4817

Energy Dissipation (J/m3) = 11.11*[(76-26.93)/26.93] + 0.4817 = 20.73 J/m3

The measured energy dissipation of sample #10 was 19.86 J/m^3. The difference between the measured energy dissipation and predicted energy dissipation is 0.866 J/m^3 (the difference is less than 4.2%). Results indicate that the new model prediction of the drilling fluid viscoelasticity is sufficiently accurate for WBM, and the model can be used for the assessment of the water-based drilling fluid viscoelasticity in the field.

Appendix-C Example Field Assessment of Weighted Drilling Fluid Viscoelasticity

The following procedure can be used to determine the energy dissipation of a weighted drilling fluid in the field:

1. Measure the funnel viscosity (MFV) of the drilling fluid using a funnel viscometer.

2. Measure the 600 rev/min reading (Θ 600) using the rotational viscometer.

3. Determine the apparent viscosity (AV) of the drilling fluid, AV= Θ600/2.

4. Predict the funnel viscosity (PFV) of the drilling fluid using Eq 4.9

5. Determine the energy dissipation of the drilling fluid using Eq 4.10

A sample calculation was performed to verify the validity of the model for assessing the viscoelasticity of a weighted drilling fluid.

Properties of the newly formulated weighted viscoelastic drilling fluid are as shown below:

Fluid	Concentration (%w/w)	Density (kg/m^3)	E_D (J/m^3)	AV (cp)	MFV (s)
HPAM1 + Barite	0.25 /15.6	1700	11.28	13.5	80

1. The measured funnel viscosity (MFV) is 80 s.

2. The measured 600 rev/min reading from the rotational viscometer is 27 $lbs./100ft^2$.

3. The apparent viscosity (AV) uses Eq 4.3.

$AV = \Theta 600/2 = 27/2 = 13.5$ cp

4. Predicted funnel viscosity uses Eq 4.9.

$PFV = 0.58*\exp[1.2[\ln(AV)-\ln(\rho)]]+24.5 = 31.5$ s

5. The energy dissipation of the drilling fluid uses Eq 4.10.

Energy Dissipation (J/m3) = 7.09*[(MFV-PFV)/PFV] + 0.7437

Energy Dissipation (J/m3) = 7.09*[(80-31.5)/31.5] + 0.7437 = 11.66 J/m3

The measured energy dissipation of the weighted drilling fluid was 11.28 J/m^3. The difference between the measured energy dissipation and predicted energy dissipation is 0.38 J/m3

(the difference is less than 3.4%). Results indicate that the new model prediction of the weighted drilling fluid viscoelasticity is sufficiently accurate.

CHAPTER 5 A Generalized Model for Field Assessment of Particle Settling Velocity in Viscoelastic Fluids

5.1 Abstract

It has been long known that drilling fluid viscoelastic properties have a significant impact on various elements of drilling hydraulics design (e.g., assessment of frictional pressure loss, particle settling velocity, hole cleaning, etc.). However, efforts for considering the viscoelastic fluid properties in drilling hydraulics design are traditionally hindered by the fact that there was no practical methodology to measure these critical fluid properties in the field.

Previous studies have highlighted the advantages of using the concept of "energy dissipation" for the quantitative evaluation of fluid elasticity. Energy dissipation theory provides a more comprehensive description of the fluid elasticity by considering the two characteristics of the fluid simultaneously; stretchiness (oscillation strain % at the crossover point of G' and G" curves) and the stress corresponding to crossover point (i.e., flow point). In a recent study, we have shown that the "energy dissipation" of viscoelastic fluids can be correlated to fluid physical properties such as apparent viscosity and funnel viscosity, which can be conveniently measured using standard field-testing equipment (i.e., Rotational Viscometer and Funnel viscometer). Based on these findings, a new methodology for the field assessment of drilling fluid viscoelasticity has been developed, opening new opportunities to develop improved hydraulics models.

In this paper, using the new methodology developed in a recent study, we present a new generalized model for the field assessment of the particle settling velocity in viscoelastic fluids. The main objectives of the study were to: 1) Develop a generalized model for the field assessment

of particle settling velocity in shear-thinning viscoelastic fluids by using the energy dissipation concept as an indicator of the fluid viscoelasticity; 2) Investigate the significant factors that influence the particle settling velocity to help provide a solution to the potential problem encountered in field drilling operations.

We prepared ten different fluids, which were divided into two groups based on their shear viscosity values. In each group, five fluids were having similar shear viscosity and variable elasticity values. Nineteen different spherical particles were used to conduct particle settling experiments with a density range from 2700 kg/m^3 to 6000kg/m^3 and a diameter range from 1mm to 4mm. Rheological characterizations of the fluids have been conducted by using funnel viscometer, API Rotational viscometer, controlled shear rate, and amplitude sweep test measurements.

Based on the experimental results and theory of the particle settling in non-Newtonian fluids, we developed a new model that can be used for predicting particle settling velocity in viscoelastic fluids. The statistical analyses had shown that the root means square error and mean absolute percentage error of model predictions were 0.0032 m/s and 4.1 percent, respectively.

Keywords: Terminal Velocity, Fluid Viscoelasticity, Funnel Viscosity, Energy Dissipation, Amplitude sweep tests

5.2 Introduction

Viscoelastic properties of drilling fluids have drawn much attention in the drilling industry because of the critical role they play in the evaluation of frictional pressure loss, particle settling velocity, and cuttings transport efficiency (Powell et al., 1991; Zamora et al., 1993; Saasen and

Loklingholm, 2002; Bui et al., 2012; Sayindla et al., 2017; Werner et al., 2017; Arnipally and Kuru, 2018; Bizhani and Kuru, 2018; Hirpa and Kuru, 2020).

Researchers investigating the proppant transport efficiency of fracturing fluids recommended that both shear viscosity and viscoelasticity of the fracturing fluid need to be considered to determine optimum fracturing fluid rheological properties for effective proppant transportation (Malhotra et al., 2012; Biheri and Imqam, 2021). Particle settling velocity is one of the key variables required for optimum hydraulic design of fluid-solid transport systems that have been used in various oil field operations such as proppant transport in hydraulic fracturing (Shah et al., 2007) and cuttings transport in drilling (Baldino et al., 2015; Altindal et al., 2017).

Settling behavior of particles in Newtonian (Clift et al., 1978; Turton and Levenspiel, 1986; R. Chhabra, 2006; Shahi and Kuru, 2015) and non-Newtonian fluids (Chien, 1994; Miura et al., 2001; Wilson, 2003; Kelessidis, and Mpandelis, 2004; Shah et al., 2007; Arabi et al., 2016; Shahi and Kuru, 2016; Rushd et al., 2018 and Okesanya et al., 2020) have been extensively investigated in the past. However, in addition to showing non-Newtonian rheological behavior, most fluids used in the oil field also have elastic characteristics (Bui et al., 2012 and Agwu et al., 2018).

Results of the previous lab investigations and field observations strongly suggest that fluid elastic properties need to be considered together with the viscous properties for a more accurate prediction of solids' transport ability of drilling fluids. Investigating the effect of fluid elasticity on the particle settling velocity independent from shear viscosity has been a real challenge in theoretical developments as well as in experimental studies, which complicates the accurate assessment of the particle settling velocity in viscoelastic fluids (Malhotra and Sharma, 2012; Arnipally and Kuru, 2018 and Okesanya et al., 2020).

Researchers used the concept of polydispersity index to resolve this conundrum, which enables the formulation of viscoelastic fluids, which have similar shear thinning characteristics while having different elasticity (Dehghanpour and Kuru, 2011; Arnipally and Kuru, 2018). By doing so, the effect of viscoelasticity could be better monitored and eventually correlated with the additional resistance experienced by the particles settling in shear-thinning viscoelastic fluids.

Although the importance of the fluid viscoelastic properties on the cuttings transport and other drilling hydraulics-related design problems have been well recognized, there has not been any standard procedure available for determining the fluid viscoelastic properties in the field. The viscoelastic fluid properties are usually measured in the lab using advanced rheometers, which are not suitable for field applications. It is, therefore, important to develop a methodology for the field assessment of the terminal settling velocity of particles in the viscoelastic fluids, which would allow field personnel to conveniently monitor the performance of drilling fluids in terms of their particle suspension ability in drilling operations. Recently, a new generalized model for the field assessment of drilling fluid viscoelasticity has been presented (Chen et al., 2021). In this study, using the new methodology presented by Chen et al., (2021), we developed a generalized model for the field assessment of the particle settling velocity in shear-thinning viscoelastic fluids.

5.2.1 Characterization of Fluid Viscoelastic Behavior

Viscoelastic characteristics of a fluid can be determined by using amplitude sweep test data. Typical amplitude sweep data obtained from oscillatory rheometer tests are shown in Figures 5.1 and 5.2, where variations of the elastic modulus (G') and loss modulus (G") measurements were plotted as a function of the oscillation strain and oscillation stress, respectively.

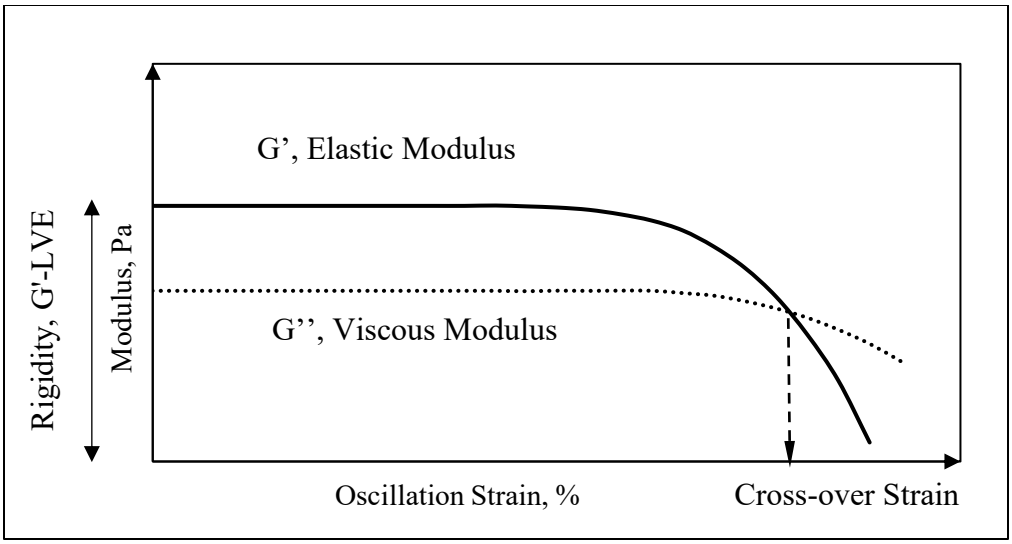

Figure 5.1 Typical Amplitude Sweep Test Result Shown as a Function of Oscillation Strain

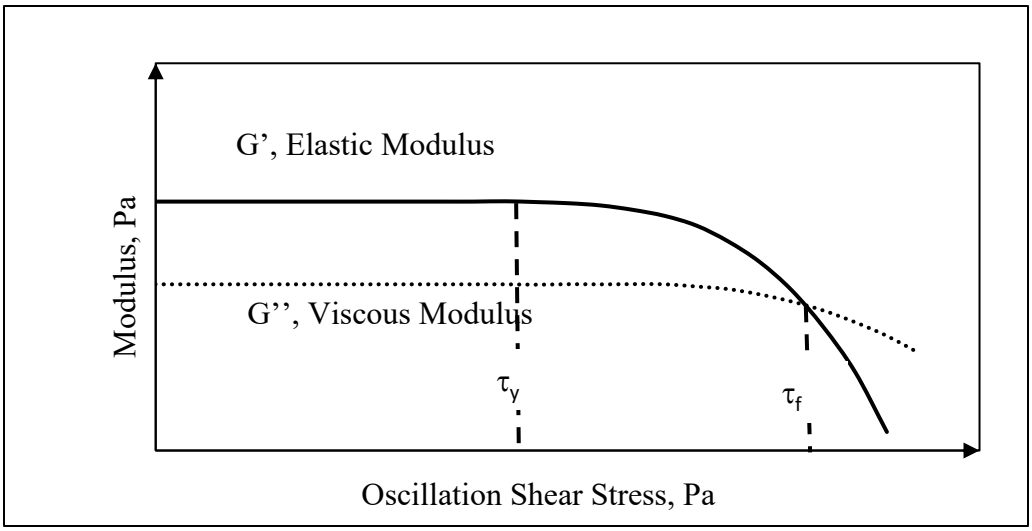

Figure 5.2 Typical Amplitude Sweep Test Result Shown as a Function of Oscillation Shear Stress

The elastic modulus, G', corresponds to the constant plateau value in the linear viscoelastic region (LVE), where the deformation of the fluid-structure under stress is reversible, and the fluid can fully recover from the deformation once the stress is released. The crossover strain defines the maximum strain that can be applied before the viscous modulus (G") surpasses the elastic modulus

(G'). After the cross-over point, the viscous behavior dominates over the elastic behavior, and the sample would experience permanent deformation under stress. The fluid viscoelasticity is generally quantified either by using the fluid rigidity (i.e., Elastic Modulus (G') in the LVE region) or stretchiness (i.e., strain value at the crossover of G' and G") values, and both parameters can be obtained from the Amplitude Sweep Test results (Fig 5.1). Both the rigidity and stretchiness parameters can serve as the indicator of the strength of the viscoelasticity to some extent; however, from the practical point of view, neither the rigidity nor the stretchiness can fully demonstrate the level of fluid elasticity. Two viscoelastic fluids with the same rigidity (G') values but with different stretchiness do not necessarily have identical performance under the same deformation process. More specifically, (within the scope of this experimental study) the resistance (i.e., drag) imposed by the two viscoelastic fluids on the settling particles will not be the same if the two fluids have the same rigidity but different stretchiness values. Since neither of these two parameters can be used to fully characterize fluid viscoelastic behavior, a more comprehensive approach is needed for the more realistic assessment of fluid elasticity.

Maxey (2010) claimed that the fluid viscoelasticity could be better described by using the concept of Energy Dissipation (E_D), which entails the minimum energy required for transferring liquid from elastic state to viscous state. In a physical sense, E_D describes the threshold energy needed to break the internal structure of the viscoelastic fluid. Generally, fluids with higher elasticity will require more energy dissipation per unit volume to transfer from elastic to the viscous state of flow. Having obtained the stress versus strain relationship of a fluid from a typical amplitude sweep test data (i.e., the combination of data shown in Figs. 5.1 and 5.2), the energy dissipation can be conveniently assessed by simple integration of the oscillation shear stress as a function of the oscillation strain (Eq 5.1).

$$E_D = \int \tau \, d\gamma \quad (5.1)$$

Maxey (2010) also suggested that the energy dissipation can be estimated by using the crossover point (also known as gel point or flow point) in a typical amplitude sweep test data (Figs. 5.1 and 5.2) as a reference point, i.e., cross-over strain (Fig 5.1) is the upper limit of the integral in Eq 2.7. The flow point in an amplitude sweep test indicates the maximum stress-strain values (and hence the total energy) required for a fluid to transfer from an elastic state to a viscous state. Therefore, it is plausible to determine the energy dissipation at this specific point.

5.2.2 Field Evaluation of Energy Dissipation

Chen et al., (2021) proposed a methodology to determine field energy dissipation (EDF) by using measurements from standard field-testing equipment, namely, funnel viscometer and API rotational viscometer. Equation 5.2 predicts the funnel viscosity of a visco-inelastic fluid as a function of the apparent viscosity (AV=600Θ/2).

$$PFV = 2.67*AV+13.575 \quad (5.2)$$

Equation 5.3 determines the energy dissipation, EDF in terms of measured and predicted funnel viscosity values:

$$EDF = 11.11*[(MFV-PFV)/PFV]+0.4817 \quad (5.3)$$

Readers should refer to Chen et al., (2021) for a more detailed derivation of the model equations.

5.3 Materials and Methods

5.3.1 Physical Properties of Solid Particles

Particles with the perfect spherical shape made of silicon nitride, zirconium ceramic, aluminum, and titanium were used to conduct the terminal velocity measurements. The dimensions and densities of particles used are listed in Table 5-1.

Table 5-1 Physical Properties of Spherical Particles Used in This Study

Particle No.	Material	Diameter (mm)	Density (Kg/m^3)
1	Aluminum	1.2	2700
2	Aluminum	1.5	2700
3	Aluminum	2.0	2700
4	Aluminum	4.0	2700
5	Aluminum	5.0	2700
6	Silicon Nitride	1.2	3200
7	Silicon Nitride	1.6	3200
8	Silicon Nitride	2.0	3200
9	Silicon Nitride	3.0	3200
10	Silicon Nitride	4.0	3200
11	Titanium	1.0	4500
12	Titanium	2.0	4500
13	Titanium	3.0	4500
14	Titanium	4.0	4500
15	Zirconia Ceramic	1.2	6000

16	Zirconia Ceramic	1.6	6000
17	Zirconia Ceramic	2.0	6000
18	Zirconia Ceramic	3.0	6000
19	Zirconia Ceramic	4.0	6000

5.3.2 Test Fluids

A total of 10 viscoelastic fluids in two groups were prepared. The fluids in each group were prepared to have similar shear viscosity and variable elasticity. Polymer blends with the same weighted average molecular weight (Eq 5.4) can be used to formulate fluids with similar shear viscosity (Zang et al., 1987; Dehghanpour and Kuru, 2009 and Veerabhadrappa et al., 2013). The polydispersity index (Eq 5.5) is an indicator of the molecular weight distribution of the individual polymers in a polymer blend (Zang et al., 1987; Dehghanpour and Kuru, 2009 and Veerabhadrappa et al., 2013). As the polydispersity index value increases the heterogeneity in cross-linking, network formation, chain length, branching, hyper branching will also increase with more random arrangement, which are all expected to contribute to the fluid elasticity (Zang et al., 1987; Dehghanpour and Kuru, 2009 and Veerabhadrappa et al., 2013). Therefore, we used the polydispersity index (PI) as a relative measure of the degree of fluid elasticity for initial formulation and screening purposes of the different polymer blends. Generally, polymer blends of the same average molecular weight and different polydispersity index values can be used to formulate fluids with similar shear viscosity and variable elasticity (Zang et al., 1987; Dehghanpour and Kuru, 2009 and Veerabhadrappa et al., 2013).

$$M_{w,B,} = \sum_{i=1}^{n} \Omega_i M_{w,i} \qquad 5.4$$

$$I = \left(\sum_{i=1}^{n} \Omega_i M_{w,i} \right) \times \left(\sum_{i=1}^{n} \frac{\Omega_i}{M_{n,i}} \right) \quad 5.5$$

Average molecular weights of Hydrolyzed Polyacrylamide (HPAM) polymers used for fluid formulations are summarized in Table 5-2.

Table 5-2 Average Molecular Weight of Three HPAM Polymers Used in This Study

Polymer	Average Molecular Weight (g/g mol)
HPAM1	20000000
HPAM2	8000000
HPAM3	500000

Compositions of polymer blends used for formulating ten fluids are shown in Table 5-3. Note that concentrations of the polymer blend in Group 1 and 2 fluids were 0.1% and 0.06%, respectively. This allowed us to prepare two groups of fluids with different shear viscosity.

Table 5-3 Polymer Blend Composition of Group 1 and Group 2 Fluids

Group No.	Fluid No.	Wt.% of Polymer in each blend (%)			Wt.% of polymer blend in the fluid formulation (%)	Average MW of the polymer blend, g/g mol	I	Density (kg/m^3)
		HPAM 1	HPAM 2	HPAM 3				
1	1	0	100	0	0.100	$8*10^6$	1	1002
	2	22.4	70.2	7.4	0.100	$8*10^6$	2.5	1002
	3	44.6	40.7	14.7	0.100	$8*10^6$	4.5	1002

	4	58.5	22.2	19.3	0.100	$8*10^6$	6	1002
	5	70.6	6.1	23.3	0.100	$8*10^6$	7.5	1002
2	6	0	100	0	0.060	$8*10^6$	1	1002
	7	22.4	70.2	7.4	0.060	$8*10^6$	2.5	1002
	8	44.6	40.7	14.7	0.060	$8*10^6$	4.5	1002
	9	58.5	22.2	19.3	0.060	$8*10^6$	6	1002
	10	70.6	6.1	23.3	0.060	$8*10^6$	7.5	1002

5.3.3 Rheological Characterization

5.3.3.1 Assessment of Viscoelasticity Using Field Tests

Apparent viscosities (AV) of the fluids were estimated by using the 600 RPM readings obtained from a Fann35 Viscometer measurement. The funnel viscosities of the fluids were measured by using the Marsh funnel. The funnel viscosity of a visco-inelastic fluid mainly depends on the AV of the fluid.

For a viscoelastic fluid having the same shear viscosity as a visco-inelastic fluid, the elasticity will increase the time needed for the fluid to flow through the marsh funnel. By knowing the measured AV and the extended funnel viscometer time (MFV), the viscoelasticity of the fluids can be determined as "Field Energy Dissipation, E_{DF}" by using Eqs 5.2 and 5.3. Measured apparent viscosity, funnel viscosity and estimated Field Energy Dissipation (EDF) values of 10 viscoelastic fluids are listed in Table 5-4.

Table 5-4 Measured Apparent Viscosity, Funnel Viscosity and Estimated Field Energy Dissipation Values of Test Fluids

Group No.	Fluid No.	Funnel Viscosity (s)	Apparent Viscosity (cp)	Field Energy Dissipation (J/m^3)
1	1	50	10.5	2.72
	2	51	10	3.43
	3	53	10.5	3.52
	4	57	11	4.12
	5	59	11	4.63
2	6	33	7	0.73
	7	34	7	1.08
	8	36	7.5	1.27
	9	37	7.5	1.60
	10	39	8	1.77

5.3.3.2 Rheological Characterization Tests

Anton Parr MCR102e Rheometer with a cone and plate geometry (with 50 mm cone diameter and 1degree cone angle) was used for rheological characterization of test fluids.

5.3.3.2.1 Controlled Shear Rate Test

The shear-thinning characteristics of the test fluids were determined by conducting a controlled shear rate test with a range of shear rates varying between 0.1 1/s to 1200 1/s. Rheograms of the fluids in Groups 1 and 2 are shown in Figs 5.3 and 5.4, respectively. Results

indicate that all the test fluids can be characterized as pseudo-plastic (Power Law) type fluids (Eq 5.6):

$$\tau = k\dot{\gamma}^n \qquad 5.6$$

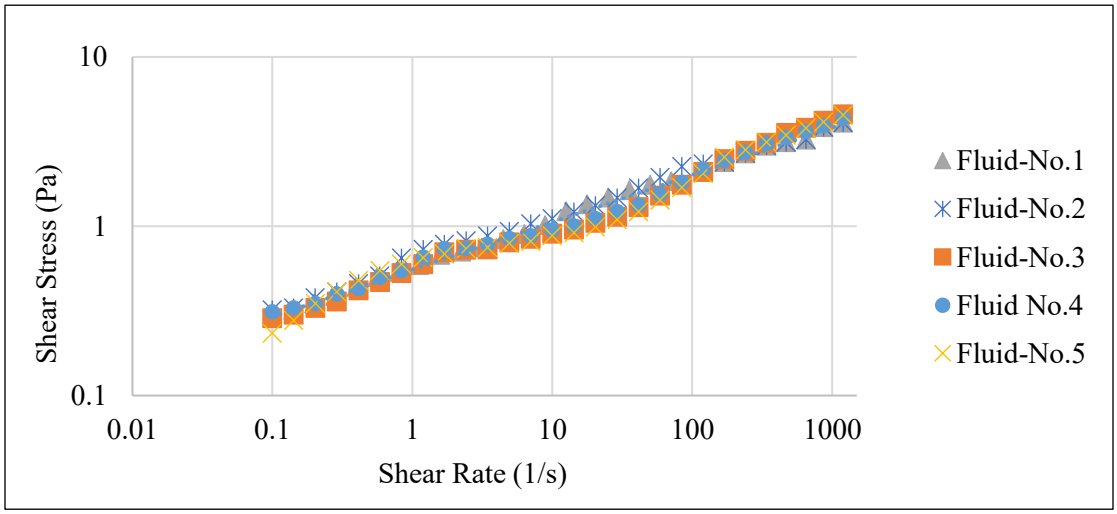

Figure 5.3 Rheograms of the 5 Fluids in Group #1, All Showing the Similar Shear Thinning Behavior

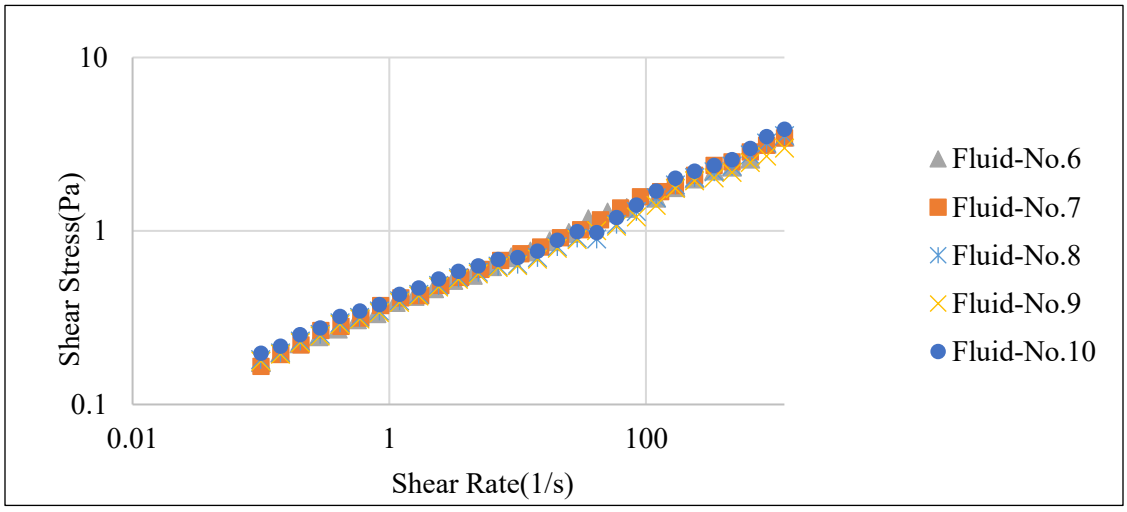

Figure 5.4 Rheograms of the 5 Fluids in Group #2, All Showing the Similar Shear Thinning Behavior

A summary of the flow behavior and consistency indices describing the rheological behavior of the test fluids is given in Table 5-5.

Table 5-5 Shear Thinning Characteristics of Fluids in Group #1 and #2

Group No.	Fluid No.	n (-)	k (Pa.s^n)
1	1	0.2808	0.5690
	2	0.2948	0.5435
	3	0.2931	0.5641
	4	0.2936	0.5676
	5	0.2832	0.5689
2	6	0.2964	0.3589
	7	0.3028	0.3698
	8	0.3047	0.3586
	9	0.3013	0.3524
	10	0.2907	0.3645

5.3.3.2.2 Amplitude Sweep Tests

The viscoelastic characteristics of the test fluids were determined by using strain-controlled amplitude sweep tests, which were conducted at four different angular frequency levels, 5 rad/s, 10 rad/s, 15 rad/s, and 20 rad/s. An example of the amplitude sweep test result is shown in Fig 5.5 Multiple angular frequencies were used because the viscoelastic behavior of the fluid is frequency-dependent.

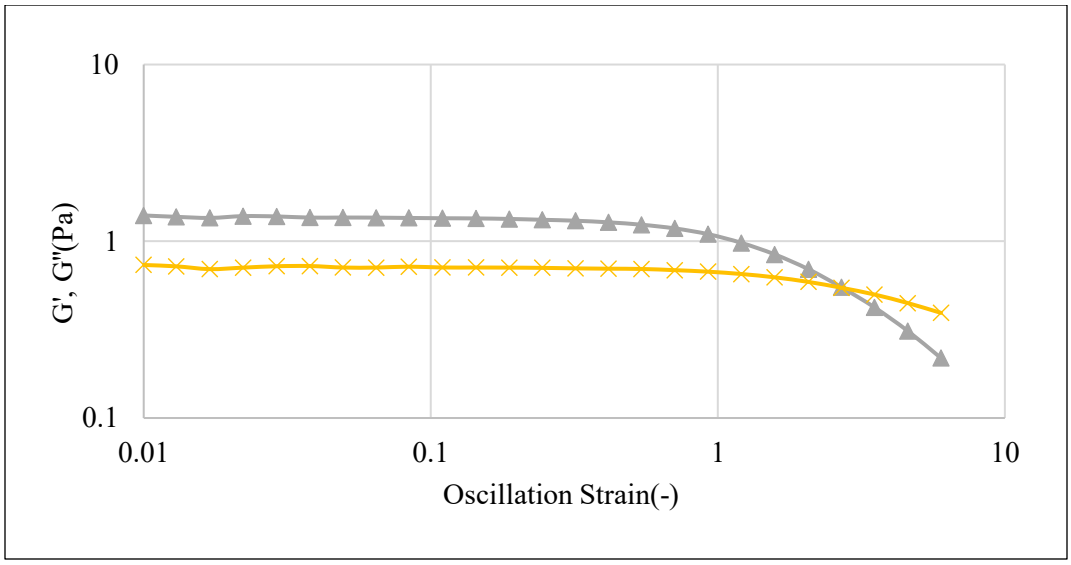

Figure 5.5 Amplitude Sweep Test Results for Fluid-1 at 10 Rad/s

In order to determine the effect of fluid elasticity on the particle settling velocity accurately, one needs to use the fluid elastic properties measured under specific conditions (e.g., fluid rheological properties, particle size/density, shear rate) relevant to the particle settling process. Particles settling with faster velocity will induce a higher shear rate (equivalent to a higher frequency effect) on the fluid than that of the particles settling at a slower velocity. It was, therefore, necessary to determine how the fluid elastic properties would change by conducting amplitude sweep tests using a wide range of frequencies. Ranges of strain rates used for the amplitude sweep tests varied between 0.1% to 600%. By using such a broader strain range, we were able to measure the stretchiness and flow point stress data required for the assessment of energy dissipation.

5.3.3.3 Assessment of True Energy Dissipation (E_{DT})

True Energy Dissipation (E_{DT}) values (i.e., E_D values at specific oscillation frequencies) can be obtained from the plot of oscillation shear stress versus oscillation strain data until the gel

point. In this case, E_{DT} is simply equal to the area under the curve. A summary of EDT values of all the test fluids obtained from amplitude sweep tests is given in Table 5-6. An example of such a characteristic plot is shown in Fig 5.6.

Table 5-6 True Energy Dissipation Values of all the Test Fluids Determined from Amplitude Sweep Tests Conducted at Different Oscillation Frequencies

Group No.	Fluid No.	E_{DT} @ 5rad/s (J/m^3)	E_{DT} @10rad/s (J/m^3)	E_{DT} @15rad/s (J/m^3)	E_{DT} @20rad/s (J/m^3)
1	1	3.31	2.73	2.23	1.98
	2	3.51	3.41	2.58	2.00
	3	3.68	3.52	2.65	2.05
	4	4.26	4.10	2.77	2.13
	5	4.98	4.63	2.95	2.20
2	6	1.20	1.01	0.85	0.76
	7	1.39	1.15	0.95	0.86
	8	1.56	1.24	1.08	0.97
	9	1.73	1.45	1.18	1.03
	10	1.94	1.65	1.31	1.11

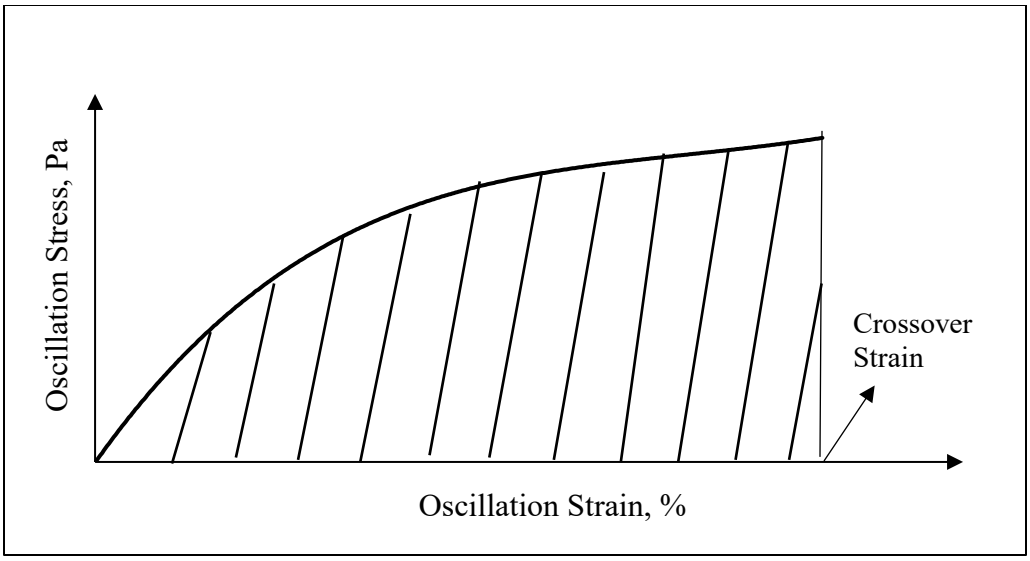

Figure 5.6 Oscillation Stress Versus Oscillation Strain Plot Used for the Assessment of Energy Dissipation

5.3.4 Particle Settling Velocity Measurement Tests

The description of the experimental program used for particle settling velocity measurements is given in the following sections.

5.3.4.1 Experimental Setup

A transparent acrylic square column was used in this experimental study. The width and the height of the column were 15 centimeters 70 centimeters, respectively. The largest particle diameter used in this study was 4 millimeters ensuring the width of the square column is 37.5 times more than the particle diameter. Typically, the wall effect can be avoided if the size of the container is 20 to 30 times larger than the particle diameter in Newtonian fluids (Zhang et al., 2015). Zhang et al., (2015) also reported that the shear-thinning characteristics of non-Newtonian fluids reduced the wall retardation effect. Therefore, the dimension of the acrylic column is assumed to be large

enough to ensure the particle's settling behavior is not influenced by the wall effect. A schematic diagram depicting the principle of the experimental measurement technique is shown in Fig 5.7.

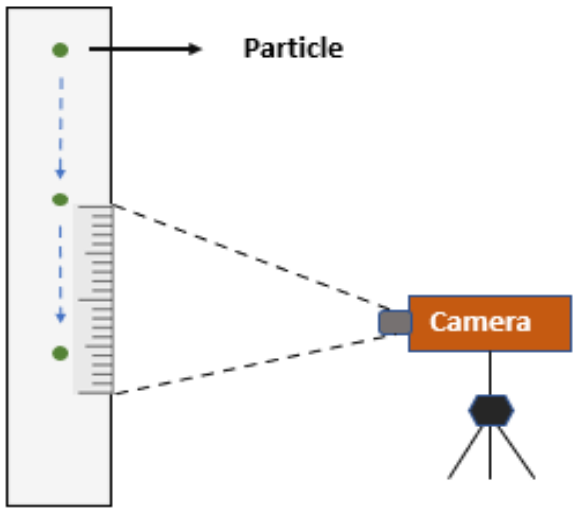

Figure 5.7 Schematic Diagram Showing the Principle of Experimental Measurement Technique

5.3.4.2 Experimental Procedure

When conducting particle settling experiments, a particle was first immersed in the test fluid to allow the formation of a thin layer around the particle, which would prevent any potential surface tension effect and make sure that there were no air bubbles attached to the particle during settling. The particle was then released to settle after being entirely placed under the fluid surface so that there would be no initial acceleration, which might influence the quality of the measured data. The fluid was allowed to relax for 20 minutes after each particle settled through the entire fluid column vertically. This ensured the viscoelastic fluid fully reaches the homogeneous state as there might be a possible shear history effect, which would make the particle settling in the same path experience less resistance from the fluid.

To ensure the data accuracy and repeatability, three sets of terminal velocity measurements were made for each particle. The final settling velocity value was determined by averaging the results of the three measurements. The measurement was considered accurate if there was no more than a 5 percent difference between the average settling velocity value and the individual test results. If the data did not fulfill the criteria, another set of measurements was conducted.

5.3.4.3 Verification of the Measurement Accuracy

Verification tests were conducted to ensure the accuracy of the technique used for particle settling velocity measurements. Three different size particles were allowed to settle in a Newtonian fluid (Glycerin). The particle Reynolds number was calculated using Eq 5.7.

$$Re_p = \frac{\rho_f V_t d}{\mu} \tag{5.7}$$

The theoretical drag coefficients were computed by using the model proposed for particles settling in Newtonian fluids (Morrison and Faith, 2013):

$$C_{D-uni} = \frac{24}{Re_p} + \frac{2.6\left(\frac{Re_p}{5}\right)}{1+\left(\frac{Re_p}{5}\right)^{1.52}} + \frac{0.411\left(\frac{Re_p}{263000}\right)^{-7.94}}{1+\left(\frac{Re_p}{263000}\right)^{-8.00}} + \frac{0.25\left(\frac{Re_p}{10^6}\right)}{1+\left(\frac{Re_p}{10^6}\right)} \tag{5.8}$$

By plotting the particle Reynolds number versus the theoretical drag coefficient, the universal curve for particles settling in Newtonian fluids can be obtained. Experimental drag coefficients were determined by using the theoretical definition given as Eq 5.9.

$$C_{D-exp} = \frac{4g(\rho_s - \rho_f)d}{3V_t^2 \rho_f} \tag{5.9}$$

The experimental drag coefficients were then plotted onto the universal C_D vs Re_p curve for comparison (Fig 5.8). The difference between the measured values and universal curve was within 5 %, confirming the accuracy of the measurement technique for further use.

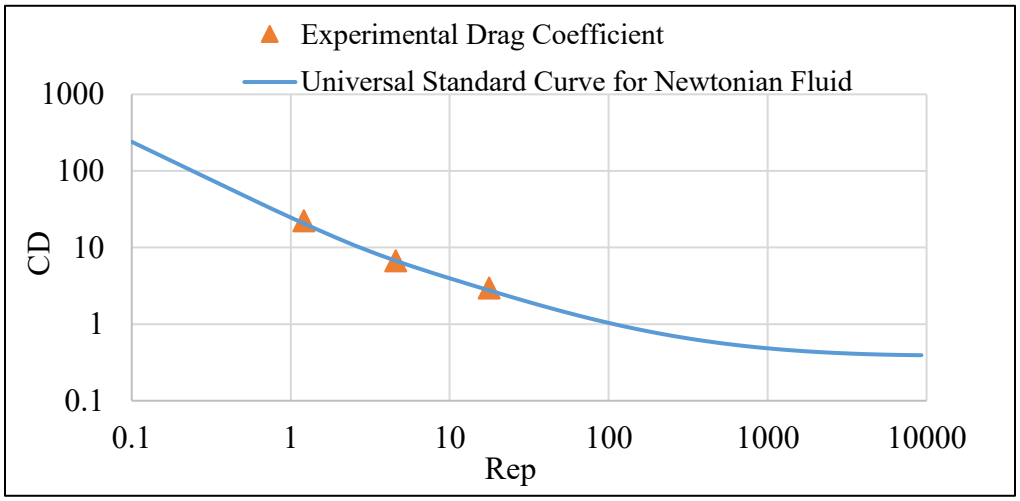

Figure 5.8 The Experimental Drag Coefficient Projected on the Universal Particle Reynolds Number Vs. Drag Coefficient Curve Given for Newtonian Fluids

5.4 Results and Discussion

A total of 190 sets of terminal velocity measurements were conducted using 10 shear-thinning viscoelastic fluids with different polymer blend compositions and polydispersity indices.

5.4.1 Model Development

The use of test fluids having similar shear viscosity, but different elasticity allowed us to investigate the effect of fluid elasticity on the terminal velocity of the particles settling in viscoelastic fluids, independent from the shear-thinning characteristics of the fluids. The particle settling experiments were then performed in each fluid to explore the underlying relationship between the resistance experienced by the particles during settling and the fluid elasticity.

A new model for predicting the particle settling velocity in the viscoelastic fluid was developed by modifying the generalized model developed for predicting particle settling velocity in shear-thinning visco-inelastic power-law type fluids (Okesanya et al., 2020).

5.4.1.1 Terminal Velocity of Particles Settling in Visco-Inelastic Power-Law Type Fluids

The terminal settling velocity in the shear-thinning visco-inelastic fluids can be determined by using the generalized model presented by Okesanya et al., (2020). The explicit model developed for particles settling in shear-thinning visco-inelastic fluids used the concept of mean surficial stress (Wilson et al., 2003). The mean surficial stress, $\bar{\tau}$, can be estimated by using Eq 5.10.

$$\bar{\tau} = \frac{dg\,(\rho_s - \rho_f)}{6} \tag{5.10}$$

With the known information about the shear stress developed by the settling particle and the shear thinning characteristics of the fluid, the corresponding shear rate can then be obtained by using the power-law relationship (Eq 5.6) as Eq 5.11.

$$\dot{\gamma} = \left(\frac{dg\,(\rho_s - \rho_f)}{6\,k}\right)^{1/n} \tag{5.11}$$

Effective fluid viscosity, μ, can then be determined by simply dividing the mean surficial stress by the shear rate as Eq 5.12.

$$\mu = \frac{\bar{\tau}}{\dot{\gamma}} \tag{5.12}$$

To determine the terminal velocity in shear-thinning visco-inelastic fluid, the particle Reynolds number needs to be computed by using the explicit model developed by Okesanya et al.,

(2020). The model uses the correlation proposed by Shah et al., (2007), which allows calculation of the term "$\sqrt{C_{D.}}Re_p$" independent from terminal settling velocity (V_t) as Eq 5.13.

$$\sqrt{C_{D.}}Re_p = \sqrt{\frac{4(\rho_s - \rho_f)d^3 g\rho_f}{3\mu^2}} \quad 5.13$$

Once the $\sqrt{C_{D.}}Re_p$ is evaluated, the particle Reynolds number, Re_p, can then be determined by using three empirical correlations developed by Okesanya et al., (2020):

$$\text{Region I } (10 > \sqrt{C_{D.}}Re_p): Re_p = 0.0289\left(\sqrt{\frac{4(\rho_s - \rho_f)d^3 g\rho_f}{3\mu^2}}\right)^{1.97} \quad 5.14$$

$$\text{Region II } (10 < \sqrt{C_{D.}}Re_p < 100): Re_p = 0.1147\left(\sqrt{\frac{4(\rho_s - \rho_f)d^3 g\rho_f}{3\mu^2}}\right)^{1.49} \quad 5.15$$

$$\text{Region III } (\sqrt{C_{D.}}Re_p > 100): Re_p = 0.9204\left(\sqrt{\frac{4(\rho_s - \rho_f)d^3 g\rho_f}{3\mu^2}}\right)^{1.06} \quad 5.16$$

Finally, the terminal velocity of particles settling in shear-thinning visco-inelastic fluids, V_{ti}, can be determined explicitly by introducing the known value of particle, Re_p, into Eq 5.17.

$$V_{ti} = \frac{\mu Re_p}{\rho_f d} \quad 5.17$$

5.4.1.2 Terminal Velocity of Particles Settling in Viscoelastic Power-Law Type Fluids

In order to obtain the model for predicting the terminal velocity of particles settling in shear-thinning viscoelastic fluids, Okesanya et al., (2020) model was modified by considering the magnitude of the viscoelasticity, which was assessed in terms of the Energy Dissipation.

5.4.1.2.1 Generalized Energy Dissipation Model Based on the Field Assessment

The model proposed by Chen et al., (2020) enables quantifying fluid viscoelasticity by using the funnel viscosity and AV values of the fluid measured by using field tests. The energy dissipation of a drilling fluid as determined by using the AV and funnel viscosity values (EDF) gives a general idea about the level of the fluid viscoelasticity.

5.4.1.2.2 Energy Dissipation Under the Shearing Effect of Settling Particles

An example of amplitude sweep test results showing the effect of oscillation frequency on the viscoelastic characteristic behavior of the fluid is shown in Fig 5.9.

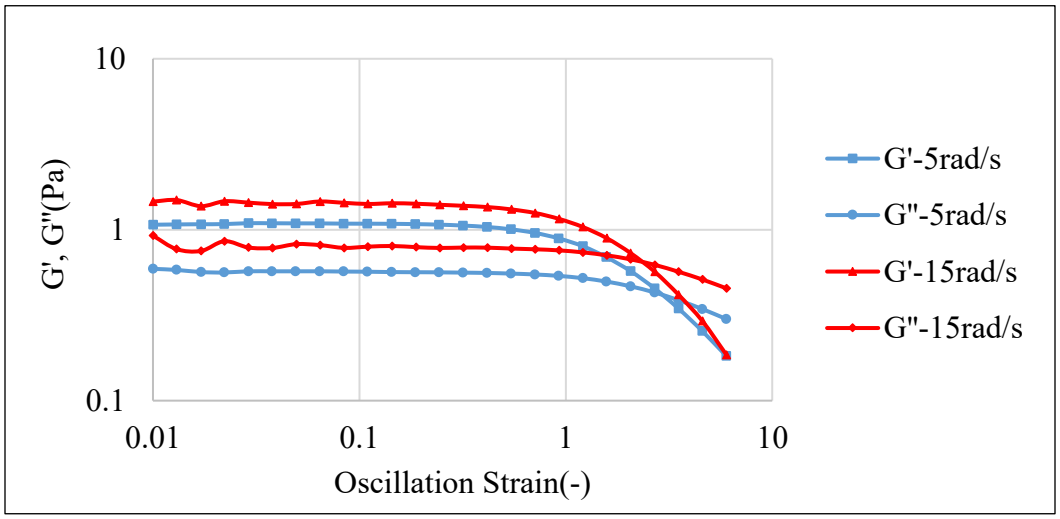

Figure 5.9 Amplitude Sweep Test Results for Fluid #1 at Oscillation Strain Rates of 5 Rad/s and 15 Rad/s

As shown in Fig 5.9, the stretchiness (i.e., oscillation strain at G'-G" cross-over point) of the fluid decreased when oscillation frequency increased from 5 rad/s to 15 rad/s, indicating that fluid would require less energy (i.e., lower flow point stress) to initiate the flow as the oscillation frequency increases. Consequently, lower energy dissipation is registered when the amplitude

sweep test is done using higher oscillation frequencies. Results shown in Figs 5.10 and 5.11 confirm the dependency of the energy dissipation (i.e., elasticity) of all fluids in group one and two on the oscillation frequency, respectively.

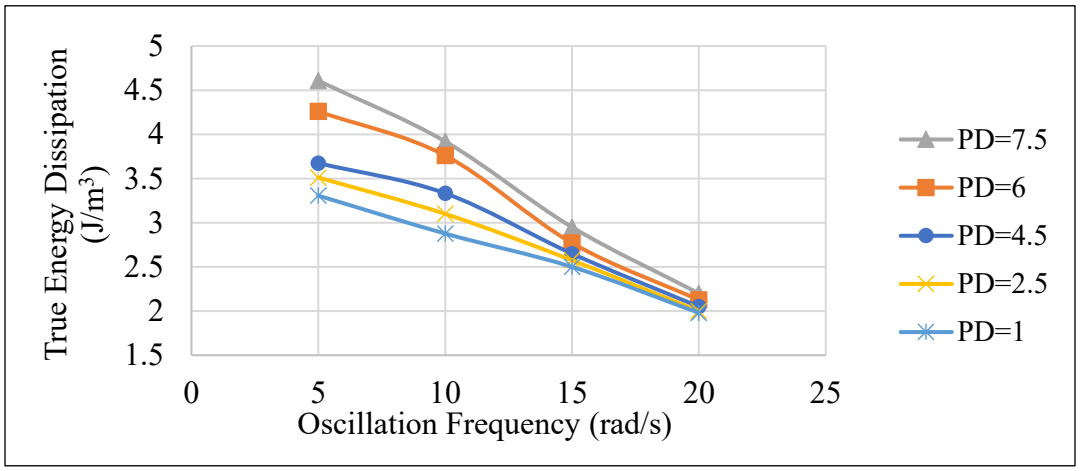

Figure 5.10 True Energy Dissipation of Group #1 Fluids Measured at Various Oscillation Frequency

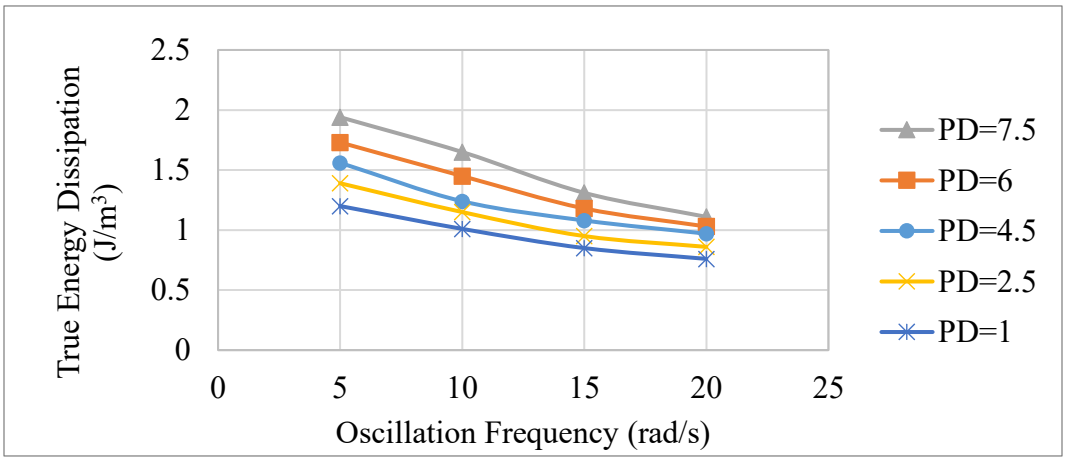

Figure 5.11 True Energy Dissipation of Group #2 Fluids Measured at Various Oscillation Frequency

Results shown in Figs 5.10 and 5.11 clearly indicate that the true energy dissipation (i.e., elasticity) of a fluid used in any industrial process should be determined by considering the local shear deformation conditions.

Note that amplitude sweep test measurements used for the development of the Chen et al., model (2021) were conducted at the standard oscillation rate of 10 rad/sec (i.e., tests were conducted under the effect of constant shear rate equivalent to 10 rad/s oscillation rate). Therefore, in order to determine the true elasticity of the fluid (E_{DT}), the viscoelasticity measured by using Chen et al., (2021) method needs to be modified according to the specific shear rate conditions of the process causing the fluid deformation (e.g., shear rate induced by particle settling in viscoelastic fluids).

5.4.1.2.3 Assessment of True Energy Dissipation

The Cox-Merz rule states that the shear-rate dependence of the steady-state viscosity is identical to the frequency dependence of the complex viscosity (May, 2013). Therefore, a change in shear rate can be considered to create an effect equivalent to a change in the oscillation frequency on the fluid elasticity (i.e., energy dissipation). Considering the observed dependency of fluid viscoelasticity on the oscillation frequency and following the Cox-Merz rule, it would be reasonable to assume that as the local shear rate in any industrial process changes, the elasticity of the fluid would also change. The effective energy dissipation (E_{DT}) observed under specific shear conditions will be referred as the "true energy dissipation" from this point on.

The local shear rate observed during a particle settling process varies depending on the particle density, diameter, and fluid rheological properties (Eq 5.11). A particle with a higher

density and larger diameter will tend to settle faster and induce a higher shear rate through the surrounding fluid. Therefore, the true energy dissipation of a fluid involved in the particle settling process will be considered as the energy dissipation found at the specific shear rate imposed on the fluid by the settling particle.

We measured the true energy dissipation, E_{DT}, values of all 10 test fluids under variable oscillation frequency conditions (Figs 5.10 and 5.11). Using the Cox-Merz rule (May, 2013), which suggests the equivalency of the oscillation frequency to the shear rate, we have converted the measured E_{DT} versus oscillation frequency results into E_{DT} versus shear rate data as shown in Figs. 5.12 and 5.13 for fluids in Group 1 and 2, respectively.

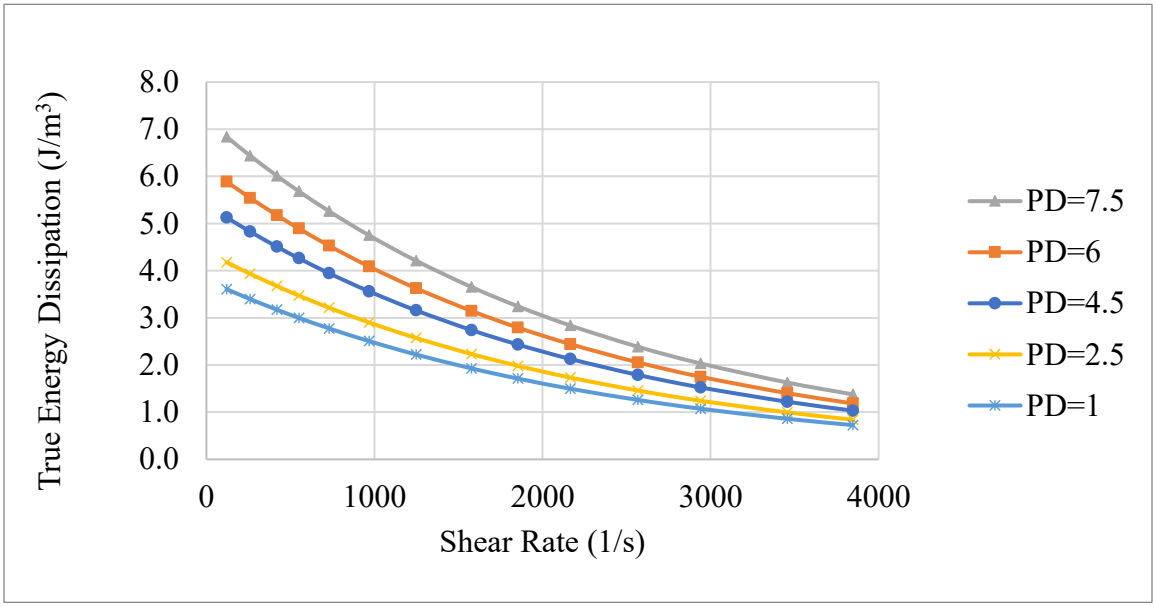

Figure 5.12 True Energy Dissipation of Group #1 Fluids at Various Shear Rate

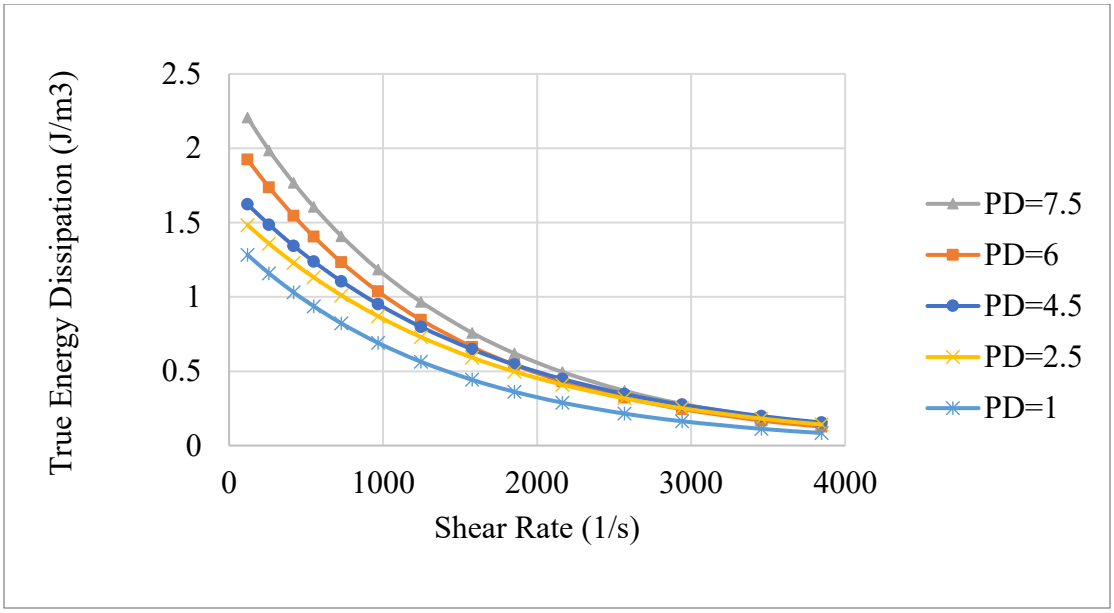

Figure 5.13 True Energy Dissipation of Group #2 Fluids at Various Shear Rate

Results shown in Figs. 5.12 and 5.13 were used to determine the True Energy Dissipation values at different shear rates (Eq 5.11) observed in each of the 190 particle settling experiments. The trend in figures 5.12 and 5.13 are slightly different because the local shear rate was computed using shear thinning characteristics of the fluids (Eq 5.11) and the fluids in two groups do not have the same n and k values.

5.4.1.2.4 Model Development for Particle Settling Velocity in Viscoelastic Fluid

Wilson et al., (2003) suggested that the shear velocity, V*, relevant to the particle settling process in static column of a fluid could be defined as the square root of the ratio of the surficial stress (Eq 5.10) to the fluid density. Following the Wilson et al., (2003) definition, an equation describing the shear velocity, V*, as functions of the particle diameter, the particle and the fluid density can be developed as Eq 5.18.

$$V^* = \sqrt{\frac{dg\,(\rho_s - \rho_f)}{6\rho_f}} \qquad 5.18$$

Knowing the shear velocity, V*, particle diameter, fluid density and viscosity values, the shear Reynolds number, Re*, as applied to particle settling in a stagnant fluid column, can then be defined as Eq 5.19.

$$Re^* = \frac{\rho_f V^* d}{\mu} \qquad 5.19$$

Note that the effective fluid viscosity in Eq 5.19 can be determined by using the Eq 5.12 defined earlier.

Knowing the measured apparent viscosity (AV) and the funnel viscosity (MFV), the viscoelasticity of the all the test fluids can be determined as "Field Energy Dissipation, E_{DF}" by using Eqs 5.2 and 5.3. Estimated Field Energy Dissipation (E_{DF}) values of 10 viscoelastic fluids are listed in Table 5-4.

True energy dissipation values, E_{DT}, of all the test fluids were determined experimentally (See discussion in Sections 5.4.1.2.2. and 5.4.1.2.3) and the data were summarized in Figs 5.12 and 5.13.

We have then plotted the experimentally obtained ratio of true energy dissipation to field energy dissipation (E_{DT}/E_{DF}) versus the shear Reynolds number. As illustrated in Fig 5.14, a unique correlation between E_{DT}/E_{DF} ratio and Re* was observed.

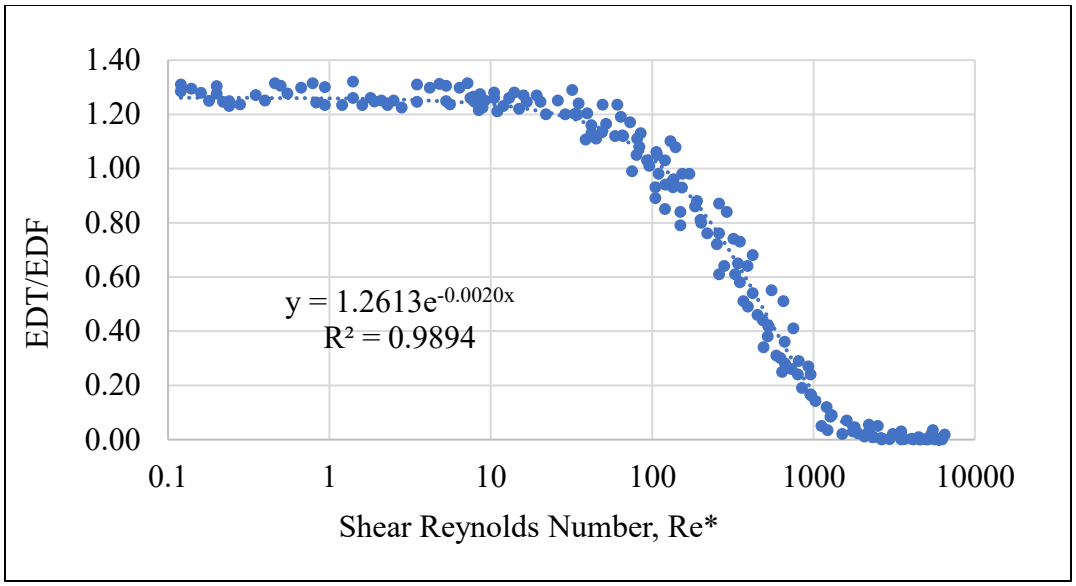

Figure 5.14 Correlation Between the Ratio of True Energy Dissipation to Field Energy Dissipation and Shear Reynolds Number

Based on the trend line of the data shown in Fig 5.14, an empirical correlation between E_{DT}/E_{DF} ratio and Re* was obtained as Eq 5.20.

$$E_{DT}/E_{DF} = 1.2613*e^{-0.002Re*} \quad 5.20$$

Equation 5.20 can be used to determine the true elasticity of the fluid under the shearing effect of a settling particle.

Knowing the true elasticity of the fluids, and the particle physical properties, the final step is now to develop a model for predicting the settling velocity of particles in viscoelastic fluids. Major steps for the development of the model for particle settling velocity in elastic fluids can be summarized as follows: i-) Using the properties of all the particle /fluid combinations tested in this study and the Okesanya et al., (2020) model, determine the particle settling velocity values in visco-inelastic fluids, V_{ti}; ii-) For all the particle/fluid combinations used in this study, measure

the true particle settling velocity values in viscoelastic fluids, V_{te}.; iii-) Determine the true energy dissipation (E_{DT}) values of all the test fluids under shear rate conditions relevant to particle settling velocity measurements conducted in this study (Figs 5.12 and 5.13); iv-) Plot the ratio of (V_{ti}-V_{te})/V_{ti} as a function of the E_{DT} (Fig. 5.15); v-) Observing the trend and by curve fitting of the data shown in Fig 5.15, develop a correlation (Eq 5.21), which can be used to determine particle settling velocity in a viscoelastic fluid.

$$V_{te} = V_{ti}\{1- [0.4752\ln(E_{DT})-0.0525]\} \quad 5.21$$

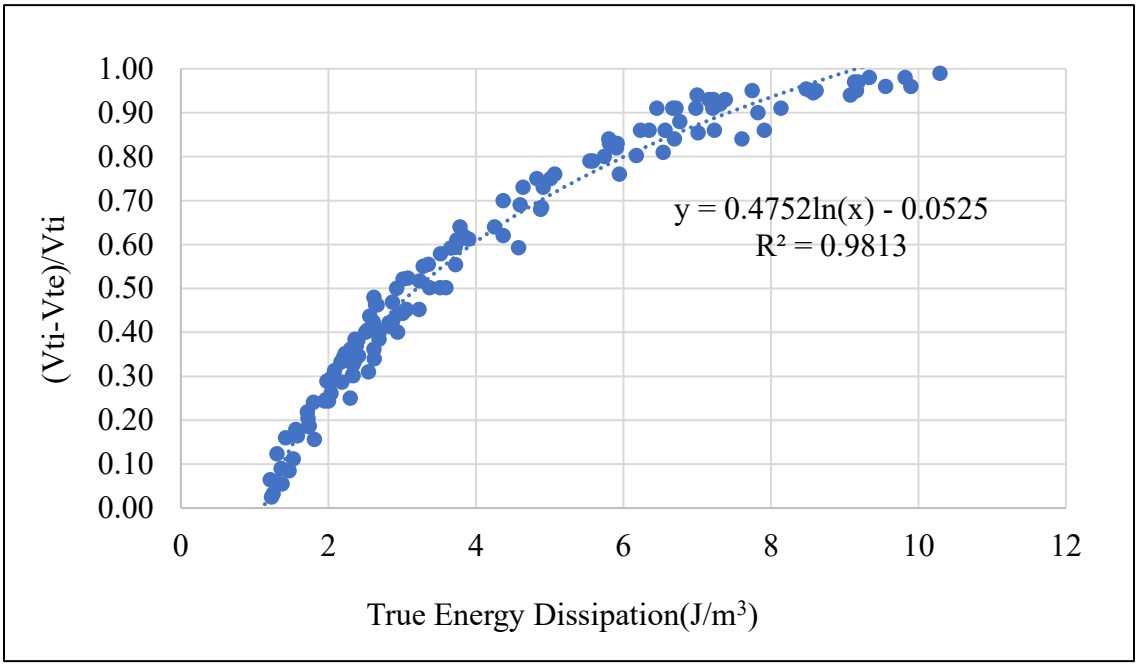

Figure 5.15 Difference Between Terminal Velocity in Viscoelastic and Visco-inelastic Fluid Vs. True Fluid Elasticity.

A detailed step-by-step procedure for assessing the particle settling velocity in elastic fluids together with an example calculation are given in Appendix-A.

5.4.2 Statistical Evaluation of the Accuracy of the Model Prediction

To determine the accuracy of the proposed model, mean absolute percentage error (MAPE) and root mean square error (RMSE) values of model predictions were evaluated using Eqs 5.22 and 5.23, respectively:

$$\text{MAPE}=\frac{1}{n}*\sum_{1}^{n}\left|\frac{(V_p-V_m)}{V_p}\right| \quad 5.22$$

$$\text{RMSE}=\sqrt{\frac{\sum_{1}^{n}(V_p-V_m)}{n}} \quad 5.23$$

MAPE and RMSE values were found to be 4.1% and 0.0032 m/s, respectively. Based on the results of statistical evaluations, the proposed model can be considered accurate enough for all practical purposes.

5.5 Conclusion

A generalized model for determining particle terminal settling velocity in shear-thinning viscoelastic fluids has been developed. The model uses the concept of energy dissipation to quantify fluid elasticity, which can be conveniently determined by using standard field measurements of apparent viscosity (AV) and funnel viscosity.

According to statistical evaluation of the proposed model, the model has a MAPE of 4.1 percent and RMSE of 0.0032 m/s indicating that the model predictions of particle settling velocity in viscoelastic fluids are sufficiently accurate for all practical purposes.

The new methodology provides a practical tool for determining particle terminal velocity in shear-thinning viscoelastic drilling fluids based on the standard field measurements of drilling fluid properties.

5.6 Acknowledgements

This project is financially supported through the funds provided by the Natural Sciences and Engineering Research Council of Canada (NSERC RGPIN-2016-04647 Kuru).

5.7 References

Altindal, M C, E Ozbayoglu, S Miska, M Yu, and N Takach. (2017). Impact of Viscoelastic Characteristics of Oil-Based Muds / Synthetic Based Muds on Cuttings Settling Velocities. OMAE2017-62129. ASME 2017 36th International Conference on Ocean, Offshore and Arctic Engineering. June 25–30, 2017. Trondheim, Norway.https://doi.org/10.1115/OMAE2017-62129.

Agwu, O. E., Akpabio, J.U, Alabi, S. B et al. 2018. Settling Velocity of Drill Cuttings in Drilling Fluids: A Review of Experimental, Numerical Simulations, and Artificial Intelligence Studies. Powder Tech.339: 728–46. https://doi.org/10.1016/j.powtec.2018.08.064.

Arabi, Ameneh S., Sean Sanders, R., 2016. Particle terminal settling velocities in non- Newtonian visco-plastic fluids. Can. J. Chem. Eng. 94 (6), 1092–1101. https://doi. org/10.1002/cjce.22496.

Arnipally, S. K., & Kuru, E. (2018). Settling velocity of particles in viscoelastic fluids: A comparison of the shear-viscosity and elasticity effects. SPE Journal, 23(5), 1689–1705. https://doi.org/10.2118/187255-PA

Baldino, S., R. E. Osgouei, E. Ozbayoglu, S. Miska, N. Takach, R. May, and D. Clapper. 2015. "Cuttings Settling and Slip Velocity Evaluation in Synthetic Drilling Fluids." In Offshore Mediterranean Conference and Exhibition, OMC 2015.

Biheri, G., & Imqam, A. (2021). Settling of Spherical Particles in High Viscosity Friction Reducer Fracture Fluids. Energies 2021, Vol. 14, Page 2462, 14(9), 2462. https://doi.org/10.3390/EN14092462

Bizhani, M. and Kuru, E. (2018). Particle Removal From Sandbed Deposits in Horizontal Annuli Using Viscoelastic Fluids. SPE J. 23 (2018): 256–273. DOI: https://doi.org/10.2118/189443-PA

Bui, B., Saasen, A., Maxey, J., et al. (2012). Viscoelastic properties of oil-based drilling fluids. Annual Trans Nordic Rheology Soc. 20. 33-47.

Chen H., Okesanya, T., Kuru, E., Heath, G., and Hadley, D. (2021). A Generalized Model for the Field Assessment of Drilling Fluid Viscoelasticity. Paper presented at the SPE ATCE, Dubai, UAE, September 2021. doi:https://doi.org/10.2118/205953-MS

Chhabra, R. P. (2007). Bubbles, Drops, and Particles in Non-Newtonian Fluids. Bubbles, Drops, and Particles in Non-Newtonian Fluids. CRC Press. Boca Raton, FL. https://doi.org/10.1201/9781420015386

Chien, S. F. (1994). Settling velocity of irregularly shaped particles. SPE Drill & Compl 9 (04): 281–289 https://doi.org/10.2118/26121-PA.

Clift, R, J R Grace, and M E Weber. 1978. Bubbles, Drops, and Particles., 2005. Dover Publications Inc. Mineola, New York. ISBN:0-486-44580-1.

Dehghanpour, H. and Kuru, E. (2011). Effect of viscoelasticity on the filtration loss characteristics of aqueous polymer solutions. Journal of Petroleum Science and Engineering, 76(1–2), 12–20. https://doi.org/10.1016/J.PETROL.2010.12.005

Kelessidis, V. C., and G. Mpandelis. 2004. Measurements and Prediction of Terminal Velocity of Solid Spheres Falling Through Stagnant Pseudoplastic Liquids. Powder Technology 147 (1–3): 117–25. https://doi.org/10.1016/j.powtec.2004.09.034.

Hirpa, M.M. and Kuru, E. (2020). Hole Cleaning in Horizontal Wells Using Viscoelastic Fluids: An Experimental Study of Drilling-Fluid Properties on the Bed-Erosion Dynamics. SPE J. 25 (2020): 2178–2193. DOI: https://doi.org/10.2118/199636-PA.

Malhotra, Sahil, and Mukul M. Sharma. 2012. "Settling of Spherical Particles in Unbounded and Confined Surfactant-Based Shear Thinning Viscoelastic Fluids: An Experimental Study." Chemical Eng. Sci. 84 (1:646–55). https://doi.org/10.1016/j.ces.2012.09.010.

Maxey, J. (2010). A Rheological Approach to Differentiating Muds by Gel Structure. AADE-10-DF-HO-27, AADE 2010 Fluids Conference, Houston, TX.

May, R., C. (2013). Rheological Behavior and Processing of Unvulgarized Rubber. The Science and Technology of Rubber. 4th Edition. Academic Press. https://doi.org/10.1016/B978-0-12-394584- 6.00006-6.

Miura, H., Takahashi, T., Ichikawa, J., Kawase, Y. (2001). Bed expansion in liquid-solid two-phase fluidized beds with Newtonian and non-Newtonian fluids over the wide range of Reynolds numbers. Powder Technology. 117(3), 239–246. https://doi.org/10.1016/S0032-5910(00)00375-2.

Morrison, Faith A., 2013. Data Correlation for Drag Coefficient for Spheres. An Introduction to Fluid Mechanics. Cambridge University Press, New York.

Okesanya, T., Kuru, E., & Sun, Y. (2020). A New Generalized Model for Predicting the Drag Coefficient and the Settling Velocity of Rigid Spheres in Viscoplastic Fluids. SPE Journal, 25(06), 3217–3235. https://doi.org/10.2118/196104-PA.

Powell, J. W., Parks, C. F., and Seheult, J. M. (1991). Xanthan and Welan: The Effects of Critical Polymer Concentration on Rheology and Fluid Performance. SPE Int. Arctic Technology Conference. Anchorage, Alaska. https://doi.org/10.2118/22066-MS.

Rushd, S., Hassan, I., Sultan, R. A., Kelessidis, V. C., Rahman, A., Hasan, H. S., and Hasan, A. (2018). Terminal settling velocity of a single sphere in drilling fluid. Particulate Science and Technology. Taylor & Francis, 0(0), pp. 1–10. DOI: 10.1080/02726351.2018.1472162.

Saasen, A. and Løklingholm, G. (2002). The Effect of Drilling Fluid Rheological Properties on Hole Cleaning. IADC/SPE Drilling Conf. Dallas, TX, 26-28 February, SPE-74558-MS, DOI: 10.2118/74558-MS.

Sayindla, S., Lund, B., Ytrehus, J. D., & Saasen, A. (2017). Hole-cleaning performance comparison of oil-based and water-based drilling fluids. Journal of Petroleum Science and Engineering, 159, 49-57. https://doi.org/10.1016/j.petrol.2017.08.069

Shah, S. N, El-Fadili, Y.E, and Chhabra, R.P. 2007. New Model for Single Spherical Particle Settling Velocity in Power Law (Visco-Inelastic) Fluids. International Journal of Multiphase Flow. 33: 51–66. https://doi.org/10.1016/j.ijmultiphaseflow.2006.06.006

Shahi, S., & Kuru, E. (2016). Experimental investigation of the settling velocity of spherical particles in Power-law fluids using particle image shadowgraph technique. International Journal of Mineral Processing, 153, 60–65. https://doi.org/10.1016/J.MINPRO.2016.06.002.

Turton.R, O. Levenspiel, A short note on the drag correlation for spheres, Powder Technology, Volume 47, Issue 1, 1986, Pages 83-86, ISSN 0032-5910, https://doi.org/10.1016/0032-5910(86)80012-2.

Veerabhadrappa, S. K., Doda, A., Trivedi, J. J., & Kuru, E. (2013). On the Effect of Polymer Elasticity on Secondary and Tertiary Oil Recovery. Industrial and Engineering Chemistry Research, 52(51), 18421–18428. https://doi.org/10.1021/IE4026456.

Werner, B., Myrseth, V., & Saasen, A. (2017). Viscoelastic properties of drilling fluids and their influence on cuttings transport. Journal of Petroleum Science and Engineering, 156, 845-851. https://doi.org/10.1016/j.petrol.2017.06.063.

Wilson, K. C., Horsley, R. R., Kealy, T., Reizes, J. and Horsley, M. (2003). Direct prediction of fall velocities in non-Newtonian materials. International Journal of Mineral Processing. 71(1–4), pp. 17–30. DOI: 10.1016/S0301-7516(03)00027-9.

Zang, Y. H., Muller, R., & Froelich, D. (1987). Influence of molecular weight distribution on viscoelastic constants of polymer melts in the terminal zone. New blending law and comparison with experimental data. Polymer, 28(9), 1577–1582. https://doi.org/10.1016/0032-3861(87)90362-4.

Zamora, M., Jefferson, D. T., Powell, J. W. (1993). Hole-Cleaning Study of Polymer-Based Drilling Fluid. SPE ATCE, Houston, TX. doi:10.2118/26329-MS.

Zhang, G., Li, M., Li, J., Yu, M., Qi, M., & Bai, Z. (2015). Wall Effects on Spheres Settling Through Non-Newtonian Fluid Media in Cylindrical Tubes. https://doi.org/10.1080/01932691.2014.966309

Appendix-A Assessment of Particle Setting Velocity in Viscoelastic Fluids – Sample Calculation

The Fluid #4; and the particle #1 were used in this sample calculations. ρs = 2700kg/m3, ρf = 1002kg/m3, k = 0.5676 Pa.sn, n = 0.29, d=1.2mm

1. Measured 600rev/min reading from API viscometry test of the fluid was 22 lbs/100ft^2.

2. Determine the apparent viscosity of the fluid.

$$AV = \frac{\theta 600}{2} = 11\ cp$$

3. The measured funnel viscosity (MFV) was 57s.

4. The field energy dissipation, E_{DF} can be determined using Eqs 5.2 and 5.3.

PFV = 2.67*AV+13.575 = 42.95 s

E_{DF} = 11.11*(MFV-PFV)/PFV+0.4817=11.11*(57-42.95)/ 42.95+0.4817 = 4.12 J/m^3

5. Determine settling velocity in shear-thinning visco-inelastic fluid having similar shear thinning characteristics as the test fluid#4, using Eqs 5.6, 5.10, 5.11, 5.12, 5.13, 5.15 and 5.17.

$$\bar{\tau} = \frac{dg\,(\rho_s - \rho_f)}{6} = \frac{0.0012*9.81\,(2700-1002)}{6} = 3.33\ Pa$$

$$\dot{\gamma} = \left(\frac{1}{k}\bar{\tau}\right)^{\frac{1}{n}} = (1/0.5676*3.33)^{1/0.2936} = 414.2\ 1/s$$

$$\mu = \frac{\bar{\tau}}{\dot{\gamma}} = \frac{3.33}{414.2} = 0.00804\ Pa.s$$

$$\sqrt{C_{D.}}Re_p = \sqrt{\frac{4(\rho_s - \rho_f)d^3 g\rho_f}{3\mu^2}}$$

$$= \sqrt{\frac{4(2700-1002)*0.0012^3*9.81*1002}{3*0.00804^2}} = 24.39$$

$$Re_p = 0.1147\left(\sqrt{\frac{4(\rho_s - \rho_f)d^3 g\rho_f}{3\mu^2}}\right)^{1.4901}$$

$$= 0.1147\left(\sqrt{\frac{4(2700-1002)0.0012^3*9.81*1002}{3*0.009423^2}}\right)^{1.4901}$$

$$= 13.38$$

$$V_{ti} = \frac{\mu Re_p}{\rho_f d} = \frac{0.00804*13.38}{1002*0.0012} = 0.0895 m/s$$

6. Determine true energy dissipation by using Eqs 5.18, 5.19 and 5.20.

$$V^* = \sqrt{\frac{dg\,(\rho_s - \rho_f)}{6\rho_f}} = \sqrt{\frac{0.0012*9.81*(2700-1002)}{6*1002}} = 0.0577\ m/s$$

$$Re^* = \frac{\rho_f V^* d}{\mu} = \frac{1002*0.0577*0.0012}{0.00804} = 8.623$$

$E_{DT}/E_{DF} = 1.2613*e^{-0.002Re^*} = 1.2613*e^{0.002*8.6323} = 1.283$

E_{DT} = 1.283*4.12 = 5.287

7. Finally, determine the true particle terminal settling velocity in the shear-thinning viscoelastic fluid by using Eq 5.21.

$V_{te} = V_{ti}\{1-[0.4752\ln(E_{DT})-0.0525]\}$

= 0.0895*{1-[0.4752ln(5.287)-0.0525]}

= 0.0234 m/s

The measured settling velocity for particle #1 settling in fluid #4 was 0.0231 m/s. The difference between predicted and measured settling velocity values is 0.0003m/s (~1.3% deviation).

Appendix-B Particle Settling Velocity Measurement

Fluid No.	Fluid density (Kg/m3)	n(-)	K (Pa.s^n)	Diameter (mm)	Density (kg/m3)	E_{DF} (J/m^3)	E_{DT} (J/m^3)	settling velocity (m/s)
1	1002	0.2808	0.569	1.2	3200	2.72	3.350	0.003643567
1	1002	0.2808	0.569	1.6	3200	2.72	3.240	0.008115223
1	1002	0.2808	0.569	2	3200	2.72	3.070	0.015416667
1	1002	0.2808	0.569	3	3200	2.72	2.320	0.042127813
1	1002	0.2808	0.569	4	3200	2.72	1.340	0.085290000

1	1002	0.2808	0.569	1.2	6000	2.72	2.560	0.014541110
1	1002	0.2808	0.569	1.6	6000	2.72	1.700	0.029393252
1	1002	0.2808	0.569	2	6000	2.72	0.854	0.050590000
1	1002	0.2808	0.569	3	6000	2.72	0.514	0.123392100
1	1002	0.2808	0.569	4	6000	2.72	0.029	0.222428333
1	1002	0.2808	0.569	1.2	2700	2.72	3.390	0.001766617
1	1002	0.2808	0.569	1.5	2700	2.72	3.360	0.004185911
1	1002	0.2808	0.569	2	2700	2.72	3.260	0.009153350
1	1002	0.2808	0.569	3	2700	2.72	2.870	0.060518877
1	1002	0.2808	0.569	4	2700	2.72	2.240	0.101368117
1	1002	0.2808	0.569	1	4500	2.72	3.420	0.004873767
1	1002	0.2808	0.569	2	4500	2.72	2.151	0.031726580
1	1002	0.2808	0.569	3	4500	2.72	0.683	0.083945533
1	1002	0.2808	0.569	4	4500	2.72	0.070	0.156714367
2	1002	0.2948	0.5435	1.2	3200	3.43	4.244	0.002860867
2	1002	0.2948	0.5435	1.6	3200	3.43	4.142	0.005583333
2	1002	0.2948	0.5435	2	3200	3.43	3.984	0.010957370

2	1002	0.2948	0.5435	3	3200	3.43	3.321	0.028711533
2	1002	0.2948	0.5435	4	3200	3.43	2.357	0.054381333
2	1002	0.2948	0.5435	1.2	6000	3.43	3.538	0.010445100
2	1002	0.2948	0.5435	1.6	6000	3.43	2.726	0.022061900
2	1002	0.2948	0.5435	2	6000	3.43	1.795	0.033431625
2	1002	0.2948	0.5435	3	6000	3.43	0.253	0.085522625
2	1002	0.2948	0.5435	4	6000	3.43	0.006	0.154508700
2	1002	0.2948	0.5435	1.2	2700	3.43	4.285	0.001544000
2	1002	0.2948	0.5435	1.5	2700	3.43	4.251	0.003310205
2	1002	0.2948	0.5435	2	2700	3.43	4.159	0.007080733
2	1002	0.2948	0.5435	3	2700	3.43	3.815	0.041652833
2	1002	0.2948	0.5435	4	2700	3.43	3.243	0.067689700
2	1002	0.2948	0.5435	1	4500	3.43	4.145	0.003595795
2	1002	0.2948	0.5435	2	4500	3.43	3.161	0.021382100
2	1002	0.2948	0.5435	3	4500	3.43	1.572	0.056014000
2	1002	0.2948	0.5435	4	4500	3.43	0.423	0.101983333
3	1002	0.2931	0.5641	1.2	3200	3.52	4.359	0.002402690

3	1002	0.2931	0.5641	1.6	3200	3.52	4.259	0.005129203
3	1002	0.2931	0.5641	2	3200	3.52	4.102	0.009317000
3	1002	0.2931	0.5641	3	3200	3.52	3.435	0.025124667
3	1002	0.2931	0.5641	4	3200	3.52	2.456	0.043662010
3	1002	0.2931	0.5641	1.2	6000	3.52	3.654	0.008337165
3	1002	0.2931	0.5641	1.6	6000	3.52	2.833	0.015353200
3	1002	0.2931	0.5641	2	6000	3.52	1.879	0.025691250
3	1002	0.2931	0.5641	3	6000	3.52	0.270	0.061576383
3	1002	0.2931	0.5641	4	6000	3.52	0.007	0.115638750
3	1002	0.2931	0.5641	1.2	2700	3.52	4.400	0.001352810
3	1002	0.2931	0.5641	1.5	2700	3.52	4.366	0.002733012
3	1002	0.2931	0.5641	2	2700	3.52	4.276	0.005950100
3	1002	0.2931	0.5641	3	2700	3.52	3.933	0.032436667
3	1002	0.2931	0.5641	4	2700	3.52	3.357	0.053464185
3	1002	0.2931	0.5641	1	4500	3.52	4.261	0.003182270
3	1002	0.2931	0.5641	2	4500	3.52	3.274	0.016842417
3	1002	0.2931	0.5641	3	4500	3.52	1.649	0.042762280

3	1002	0.2931	0.5641	4	4500	3.52	0.450	0.077360485
4	1002	0.2936	0.5676	1.2	3200	4.12	5.287	0.023104567
4	1002	0.2936	0.5676	1.6	3200	4.12	4.990	0.043532428
4	1002	0.2936	0.5676	2	3200	4.12	4.812	0.075495517
4	1002	0.2936	0.5676	3	3200	4.12	4.053	0.089195247
4	1002	0.2936	0.5676	4	3200	4.12	2.932	0.094209517
4	1002	0.2936	0.5676	1.2	6000	4.12	4.303	0.006835527
4	1002	0.2936	0.5676	1.6	6000	4.12	3.364	0.012291937
4	1002	0.2936	0.5676	2	6000	4.12	2.264	0.019444007
4	1002	0.2936	0.5676	3	6000	4.12	0.350	0.046436667
4	1002	0.2936	0.5676	4	6000	4.12	0.010	0.084520653
4	1002	0.2936	0.5676	1.2	2700	4.12	5.151	0.001211667
4	1002	0.2936	0.5676	1.5	2700	4.12	5.113	0.002460916
4	1002	0.2936	0.5676	2	2700	4.12	5.009	0.005185996
4	1002	0.2936	0.5676	3	2700	4.12	4.620	0.026621313
4	1002	0.2936	0.5676	4	2700	4.12	3.964	0.043125440
4	1002	0.2936	0.5676	1	4500	4.12	4.993	0.002818058

4	1002	0.2936	0.5676	2	4500	4.12	3.869	0.013382590
4	1002	0.2936	0.5676	3	4500	4.12	1.996	0.032752253
4	1002	0.2936	0.5676	4	4500	4.12	0.572	0.058712500
5	1002	0.2832	0.5689	1.2	3200	4.63	5.708	0.002004500
5	1002	0.2832	0.5689	1.6	3200	4.63	5.535	0.004249314
5	1002	0.2832	0.5689	2	3200	4.63	5.259	0.007058547
5	1002	0.2832	0.5689	3	3200	4.63	4.088	0.017748237
5	1002	0.2832	0.5689	4	3200	4.63	2.490	0.030720017
5	1002	0.2832	0.5689	1.2	6000	4.63	4.468	0.006377862
5	1002	0.2832	0.5689	1.6	6000	4.63	3.081	0.011254387
5	1002	0.2832	0.5689	2	6000	4.63	1.661	0.017715178
5	1002	0.2832	0.5689	3	6000	4.63	0.080	0.041900055
5	1002	0.2832	0.5689	4	6000	4.63	0.010	0.070494778
5	1002	0.2832	0.5689	1.2	2700	4.63	5.777	0.001154000
5	1002	0.2832	0.5689	1.5	2700	4.63	5.721	0.002328829
5	1002	0.2832	0.5689	2	2700	4.63	5.565	0.004792164
5	1002	0.2832	0.5689	3	2700	4.63	4.959	0.022400000

5	1002	0.2832	0.5689	4	2700	4.63	3.953	0.037656443
5	1002	0.2832	0.5689	1	4500	4.63	5.540	0.002695137
5	1002	0.2832	0.5689	2	4500	4.63	3.811	0.011728442
5	1002	0.2832	0.5689	3	4500	4.63	1.361	0.028529080
5	1002	0.2832	0.5689	4	4500	4.63	0.179	0.047832550
6	1002	0.2964	0.3589	1.2	3200	0.73	0.877	0.007567000
6	1002	0.2964	0.3589	1.6	3200	0.73	0.824	0.015473000
6	1002	0.2964	0.3589	2	3200	0.73	0.747	0.028086000
6	1002	0.2964	0.3589	3	3200	0.73	0.471	0.069225000
6	1002	0.2964	0.3589	4	3200	0.73	0.199	0.125696000
6	1002	0.2964	0.3589	1.2	6000	0.73	0.553	0.025313000
6	1002	0.2964	0.3589	1.6	6000	0.73	0.287	0.050950000
6	1002	0.2964	0.3589	2	6000	0.73	0.101	0.078862000
6	1002	0.2964	0.3589	3	6000	0.73	0.056	0.183620000
6	1002	0.2964	0.3589	4	6000	0.73	0.002	0.321273000
6	1002	0.2964	0.3589	1.2	2700	0.73	0.899	0.004686000
6	1002	0.2964	0.3589	1.5	2700	0.73	0.881	0.008793000

6	1002	0.2964	0.3589	2	2700	0.73	0.833	0.018622000
6	1002	0.2964	0.3589	3	2700	0.73	0.669	0.096691000
6	1002	0.2964	0.3589	4	2700	0.73	0.444	0.154144000
6	1002	0.2964	0.3589	1	4500	0.73	0.826	0.009426000
6	1002	0.2964	0.3589	2	4500	0.73	0.416	0.051196000
6	1002	0.2964	0.3589	3	4500	0.73	0.072	0.132152000
6	1002	0.2964	0.3589	4	4500	0.73	0.003	0.232522000
7	1002	0.3028	0.3698	1.2	3200	1.08	1.311	0.006702000
7	1002	0.3028	0.3698	1.6	3200	1.08	1.251	0.013429000
7	1002	0.3028	0.3698	2	3200	1.08	1.163	0.023823000
7	1002	0.3028	0.3698	3	3200	1.08	0.834	0.058222000
7	1002	0.3028	0.3698	4	3200	1.08	0.454	0.104472000
7	1002	0.3028	0.3698	1.2	6000	1.08	0.935	0.020484000
7	1002	0.3028	0.3698	1.6	6000	1.08	0.587	0.038537000
7	1002	0.3028	0.3698	2	6000	1.08	0.282	0.064227000
7	1002	0.3028	0.3698	3	6000	1.08	0.010	0.153476000
7	1002	0.3028	0.3698	4	6000	1.08	0.000	0.250210000

7	1002	0.3028	0.3698	1.2	2700	1.08	1.337	0.004150000
7	1002	0.3028	0.3698	1.5	2700	1.08	1.316	0.007823000
7	1002	0.3028	0.3698	2	2700	1.08	1.261	0.016098000
7	1002	0.3028	0.3698	3	2700	1.08	1.073	0.081402000
7	1002	0.3028	0.3698	4	2700	1.08	0.799	0.131000000
7	1002	0.3028	0.3698	1	4500	1.08	1.253	0.008541000
7	1002	0.3028	0.3698	2	4500	1.08	0.763	0.039483000
7	1002	0.3028	0.3698	3	4500	1.08	0.225	0.111918000
7	1002	0.3028	0.3698	4	4500	1.08	0.024	0.187291000
8	1002	0.3047	0.3586	1.2	3200	1.27	1.541	0.006413000
8	1002	0.3047	0.3586	1.6	3200	1.27	1.470	0.012465000
8	1002	0.3047	0.3586	2	3200	1.27	1.366	0.020145000
8	1002	0.3047	0.3586	3	3200	1.27	0.980	0.051230000
8	1002	0.3047	0.3586	4	3200	1.27	0.537	0.090756000
8	1002	0.3047	0.3586	1.2	6000	1.27	1.098	0.018364000
8	1002	0.3047	0.3586	1.6	6000	1.27	0.692	0.031245000
8	1002	0.3047	0.3586	2	6000	1.27	0.336	0.053412000

8	1002	0.3047	0.3586	3	6000	1.27	0.013	0.126540000
8	1002	0.3047	0.3586	4	6000	1.27	0.000	0.214680000
8	1002	0.3047	0.3586	1.2	2700	1.27	1.571	0.003864500
8	1002	0.3047	0.3586	1.5	2700	1.27	1.546	0.007631000
8	1002	0.3047	0.3586	2	2700	1.27	1.482	0.014879000
8	1002	0.3047	0.3586	3	2700	1.27	1.260	0.070648000
8	1002	0.3047	0.3586	4	2700	1.27	0.940	0.116450000
8	1002	0.3047	0.3586	1	4500	1.27	1.472	0.007695400
8	1002	0.3047	0.3586	2	4500	1.27	0.898	0.035426000
8	1002	0.3047	0.3586	3	4500	1.27	0.268	0.089451000
8	1002	0.3047	0.3586	4	4500	1.27	0.030	0.162378000
9	1002	0.3013	0.3524	1.2	3200	1.6	1.930	0.005766000
9	1002	0.3013	0.3524	1.6	3200	1.6	1.828	0.011208000
9	1002	0.3013	0.3524	2	3200	1.6	1.677	0.018651000
9	1002	0.3013	0.3524	3	3200	1.6	1.130	0.045647000
9	1002	0.3013	0.3524	4	3200	1.6	0.548	0.082106000
9	1002	0.3013	0.3524	1.2	6000	1.6	1.294	0.016392000

9	1002	0.3013	0.3524	1.6	6000	1.6	0.744	0.028974000
9	1002	0.3013	0.3524	2	6000	1.6	0.310	0.047411000
9	1002	0.3013	0.3524	3	6000	1.6	0.124	0.109694000
9	1002	0.3013	0.3524	4	6000	1.6	0.059	0.200382000
9	1002	0.3013	0.3524	1.2	2700	1.6	1.975	0.003630000
9	1002	0.3013	0.3524	1.5	2700	1.6	1.938	0.007056000
9	1002	0.3013	0.3524	2	2700	1.6	1.845	0.013417000
9	1002	0.3013	0.3524	3	2700	1.6	1.524	0.060704000
9	1002	0.3013	0.3524	4	2700	1.6	1.074	0.103239000
9	1002	0.3013	0.3524	1	4500	1.6	1.830	0.006985000
9	1002	0.3013	0.3524	2	4500	1.6	1.017	0.031363000
9	1002	0.3013	0.3524	3	4500	1.6	0.236	0.077340000
9	1002	0.3013	0.3524	4	4500	1.6	0.016	0.141609000
10	1002	0.2907	0.3645	1.2	3200	1.77	2.113	0.004322000
10	1002	0.2907	0.3645	1.6	3200	1.77	1.965	0.008576000
10	1002	0.2907	0.3645	2	3200	1.77	1.746	0.013554000
10	1002	0.2907	0.3645	3	3200	1.77	0.995	0.032691000

10	1002	0.2907	0.3645	4	3200	1.77	0.340	0.060690000
10	1002	0.2907	0.3645	1.2	6000	1.77	1.211	0.012210000
10	1002	0.2907	0.3645	1.6	6000	1.77	0.538	0.020363000
10	1002	0.2907	0.3645	2	6000	1.77	0.144	0.032902000
10	1002	0.2907	0.3645	3	6000	1.77	0.058	0.072798000
10	1002	0.2907	0.3645	4	6000	1.77	0.024	0.138313000
10	1002	0.2907	0.3645	1.2	2700	1.77	2.175	0.002516000
10	1002	0.2907	0.3645	1.5	2700	1.77	2.124	0.005480000
10	1002	0.2907	0.3645	2	2700	1.77	1.989	0.010803000
10	1002	0.2907	0.3645	3	2700	1.77	1.529	0.046512000
10	1002	0.2907	0.3645	4	2700	1.77	0.925	0.082835000
10	1002	0.2907	0.3645	1	4500	1.77	1.969	0.004711000
10	1002	0.2907	0.3645	2	4500	1.77	0.854	0.019431000
10	1002	0.2907	0.3645	3	4500	1.77	0.094	0.045358000
10	1002	0.2907	0.3645	4	4500	1.77	0.012	0.106400000

CHAPTER 6 Dynamic Filtration Loss Control Through Optimization of Drilling Fluid Rheological Properties: A Comparative Study of the Fluid Viscoelasticity versus Shear Viscosity Effects

6.1 Abstract

Formation damage following the invasion of reservoir rock by drilling, completion, and fracturing fluids is known to be one of the major causes of productivity reduction. Despite all the efforts, questions remain regarding the formulation of optimum fluid composition to minimize, if not eliminate, productivity impairment due to formation damage. There is a need for a better understanding of the quantitative relationship between various fluid rheological properties and the degree of productivity impairment. Fluid shear viscosity and elasticity have been identified as influential factors controlling filtration loss. However, past studies were mostly inconclusive regarding the individual effects of fluid shear viscosity vs elasticity, as it was very difficult to measure their effect independently. Therefore, we propose to investigate the relative contributions of fluid shear viscosity and elasticity on the volume of dynamic fluid loss and the associated formation damage. The main objectives of this study were: i) Demonstrate the sole effect of shear viscosity and viscoelasticity on filtration loss characteristics. ii) Investigate the dominant variable that controls filtration loss volume between shear viscosity and viscoelasticity.

24 water-based drilling fluids were prepared using various blends of three different molecular weight PHPA polymers. By using a special technique, we developed in our previous work, we have formulated two groups of fluids; one group having the same shear viscosity and variable elasticity and the other group having the same elasticity and variable shear viscosities.

We were, therefore, able to investigate the individual effects of both shear viscosity and the elasticity on the static, and dynamic filtration loss as well as on the formation damage. Additionally, 3 Xanthan Gum fluids (simulating typical drill-in fluids) were prepared to verify the generosity of the theory.

Detailed rheological characterizations of these fluids were carried out by conducting amplitude sweep test and controlled shear rate test, using an advanced rheometer with cone and plate geometry. The viscoelastic properties of the fluids were quantified in terms of energy dissipation, which physically signifies the amount of energy required per unit volume to cause an irreversible deformation in the fluid's internal structure. Static filtration tests and core flooding experiments were also conducted to measure the static filtration rate, pressure drop across the core at different flow rates, and formation damage induced by each fluid.

By investigating the independent effects of viscoelasticity and shear viscosity on the fluid filtration loss characteristics, we have observed that: 1-) The static filtration rate can be more effectively controlled by altering fluid viscoelasticity as compared to the fluid shear viscosity. 2-) Both shear viscosity and viscoelasticity have a proportional relationship to the pressure drop associated with the core flow. However, the effect of viscoelasticity on the pressure drop is more pronounced. 3-) Increasing fluid viscoelasticity does not cause the formation damage as much as the shear viscosity. 4-)The viscoelasticity has been found to be the predominant rheological property that controls the solid-free drill-in fluids' filtration loss characteristics.

The study introduces an innovative approach to investigate fluid loss and formation damage characteristics of viscoelastic, solid-free drill-in fluids. For the first time in literature, the sole effects of shear viscosity and viscoelasticity on filtration loss characteristics were investigated

and compared. The results have suggested that viscoelasticity can help develop non-invasive fluids by reducing static filtration rate, increasing pressure drop (effectively building internal cake), and minimizing formation damage. Understanding the mechanisms of internal cake formation and their quantitative relation to fluid viscous and elastic properties will help the design of optimum drill-in, completion, and fracturing fluid composition and hence, to minimize the productivity reduction associated with the application of these fluids in oil and gas wells.

Keywords: Drill-in fluid, viscoelasticity, shear viscosity, energy dissipation, filtration loss properties

6.2 Introduction

Strict control of drilling fluid filtration loss characteristics is required to limit borehole instability, excessive torque, and drag, differential pipe stuck, and formation damage (Cobianco et al., 2001). The problem becomes more critical when drilling/completing horizontal wells with water-based fluids where the fluid remains in contact with the pay zone for an extended period of time. Controlling filtration loss characteristics is, therefore, considered as one of the most critical tasks when designing optimum drilling fluid formulations for best drilling performance while preserving the original reservoir rock properties (Chesser et al. 1994; Lomba et al. 2002; Anyanwu and Momoh, 2016; Fink, 2021).

Despite the fact that the significance of fluid loss prevention has been well recognized and appreciable research effort has been spent towards the plight, the current strategy of minimizing invasion has some underlying deficiencies. The traditional solution to minimize the fluid loss into the reservoir generally includes two techniques, enhancing the mud cake functionalities with

innovative fluid loss additives (Salehi et al., 2015; Zamir and Siddiqui, 2017; Ikram et al., 2021) and increasing the shear viscosity of drilling fluid (Sassen et al., 1990; Zamora et al., 2000; Khan et al., 2007). The presence of mud cake can lead to a severe outcome of the borehole, such as reducing the borehole diameter and causing differential sticking of pipe and tubular; also, this strategy usually requires the implementation of additional processes to clean the wellbore filtercake post drilling activities. Increasing the drilling fluid's shear viscosity to improve filtration loss characteristics may not be desirable all the time due to the fact that additional shear viscosity can induce high annular pressure losses when drilling long horizontal and extended reach wells (Dehghanpour and Kuru, 2011).

To address these problems, the solid-free viscoelastic drill-in fluids will be analyzed in this study to develop a more comprehensive solution for better prevention of fluid loss into the reservoir. The solid-free feature will avert the problem induced by mud cake; it also mitigates the chip-hold down effect during drilling operation since it will make drilling fluid penetrate beneath the chip easily with less interference of the solid content from drilling fluid.

Although solid-free drill-in fluid has many merits compared with traditional drilling fluid, maintaining the flow resistance from the wellbore to formation can be a significant challenge without solids or a filtercake to prevent fluid invasion. Purely increasing the shear viscosity for increasing the pressure loss across the wellbore will likely cause undesirable outcomes, as mentioned previously. Instead of exclusively relying on the shear viscosity of drilling fluid to amplify the flow resistance, the viscoelastic fluid is utilized to ameliorate the performance of drill-in fluid in this study. Previous studies have indicated that viscoelastic fluids have a very practical appeal in many petroleum engineering applications such as controlling ECD, improving particle

suspension ability of drilling fluids (Chen et al, 2011) as well as potentially reducing the damage due to the drilling fluid invasion into the reservoir rock (Dehghanpour and Kuru, 2011). Studies as early as Durst et al. (1987), for example, reported that as much as 75% of the pressure losses in the formation may result from extensional viscosity, which is generally considered as the elasticity indicator.

Albeit viscoelasticity has been proven to be beneficial in preventing fluid loss (Gupta and Sridhar 1985; Saasen et al., 1990; Khan et al. 2004; Khan et al., 2007), there has not been adequate research conducted towards determining the independent effect of shear viscosity and viscoelasticity on filtration loss characteristics, including static filtration rate, pressure drop, and formation damage, mainly because of the difficulty of differentiating two properties. In this study, by using the concepts of average molecular weight and polydispersity index of polymer blends (Arnipally and Kuru 2018; Okesanya et al. 2020), the fluids are prepared in an ideal condition to demonstrate the sole contribution of two rheological properties (i.e. shear viscosity and elasticity) towards filtration loss characteristics of the fluids.

Furthermore, there is still extant confusion about the dominant role of both rheological properties in controlling filtration loss properties; such confusion is not a trivial problem; possessing an excess of either rheological property can potentially cause undesired issues that will have a tremendous negative impact on the subsequent operations post drilling activities, leading to enormous economic and time expense. Therefore, determining the prominent role that fluid shear viscosity and elasticity in controlling filtration loss characteristics becomes the primary objective in this study. The study presented here has two objectives: 1)Determining the sole contribution of shear viscosity and viscoelasticity to solid-free drill-in fluid's filtration loss

characteristics, including static filtration rate, pressure drop, and formation damage; 2) Investigate the dominant fluid properties that control filtration loss characteristics between shear viscosity and viscoelasticity..

6.2.1 Characterization of Fluid Viscoelasticity

Viscoelastic characteristics of a fluid can be determined by using amplitude sweep test data obtained from oscillatory rheometer tests. Examples of amplitude test results and some of the important information obtained from these test results are shown in Fig 6.1. Each set of amplitude sweep test results entails the recording of how the Elastic Modulus (G') and the Viscous Modulus (G") vary as a function of Oscillation stress (Fig 6.1a) and/or Oscillation Strain (Fig 6.1b).

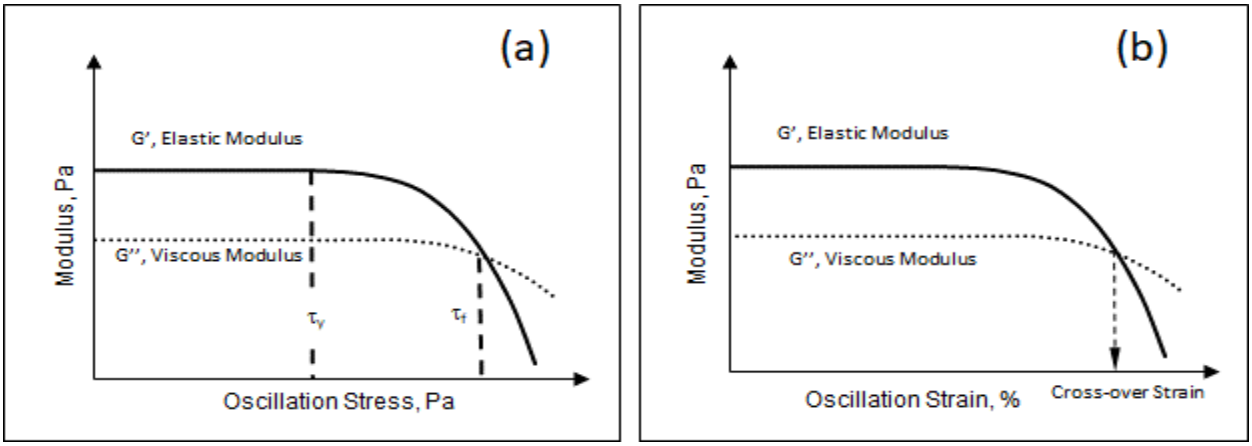

Figure 6.1 Amplitude Sweep Test Results Recorded as a Function of : a-) Oscillation Stress b-) Oscillation Strain

Typically, an initial constant interval of G' is observed (i.e., Linear Viscoelastic Region, G'-LVE) followed by a decreasing trend starting at a critical stress/strain level. The deformation of the fluid structure under stress is reversible in the linear viscoelastic region (LVE) and the fluid can fully recover from the deformation once the stress is released. This initial G'-LVE value is

also known as the “rigidity” of the fluid under investigation. The stress value where deviation from the LVE region is observed is known as true yield stress (τ_y) of the fluid. Another important information obtained from an amplitude sweep test results is the point where G’ and G” values intersect. This cross-over point (also called Gel Point) is identified either as Flow Point Stress (τ_f) or Cross-Over Strain. From a physical point of view, Gel Point defines maximum stress (or strain) that can be applied before the viscous modulus (G”) surpasses the elastic modulus (G’). After the cross-over point, the viscous behavior dominates over the elastic behavior and the fluid would experience permanent deformation under stress.

Several different parameters have been used for quantifying fluid’s viscoelasticity, including elastic modulus in the linear viscoelastic region (G’-LVE, also called rigidity), stretchiness (elastic modulus-viscous modulus cross-over strain), longest relaxation time, extensional viscosity, Deborah number, and Weissenberg number. (Urbissinova et al., 2010; Veerabhadrappa et al., 2013; Poole, 2012 and Ofei et al., 2020). These elasticity indicators have been utilized frequently in engineering research; however, some demerits need to be cogitated depending on the specific trait of versatile engineering processes. The fluid viscoelasticity is very often quantified either by using the fluid rigidity (i.e., G’ in the LVE region) or stretchiness (i.e., strain value at the crossover of G’ and G”) values, and both parameters can be obtained from an Amplitude Sweep Test result (Fig 6.1). Both the rigidity and stretchiness parameters can serve as the indicator of the strength of the viscoelasticity to some extent; however, from the practical point of view, neither the rigidity nor the stretchiness can fully demonstrate the level of fluid elasticity. Two viscoelastic fluids with the same rigidity (G’) values but with different stretchiness do not

necessarily have identical performance under the same deformation process. Therefore, a more comprehensive approach is needed for a more realistic assessment of fluid elasticity.

Maxey(2010) proposed quantifying the viscoelastic behavior using the energy dissipation theory. The energy dissipation concept assesses the level of viscoelasticity by computing the maximum energy the fluid can absorb per unit volume before getting permanently deformed. In other words, the fluid exhibits elastic behavior rather than viscous behavior below this threshold energy level. Higher the energy dissipation, more energy can be adsorbed by viscoelastic fluid without breaking its internal structure, representing a more robust structure and more significant viscoelastic behavior. Theoretically, the energy dissipation can be determined by integrating (Eq 6.1) the oscillation stress (Fig 6.1a) as a function of oscillation strain (Fig 6.1b) until the gel point, where elastic modulus and viscous modulus crossover in an amplitude sweep test.

$$E_D = \int \tau \, d\gamma \qquad 6.1$$

Where:

E_D = energy dissipation per unit volume, J/m^3

τ = oscillation stress, Pa

γ = oscillation strain, Fraction

Practically, energy dissipation can be determined using a simple two-step method, first plot the oscillation stress versus oscillation strain until gel point using amplitude sweep test results (Fig 6.2), then calculate the area under the plotted curve, which is the integral of the oscillation stress over the oscillation strain and the produced value is the energy dissipation. The gel point defines

the maximum stress (or strain) that the fluid is able to stand before it starts deforming irreversibly (i.e., beyond its elastic limit).

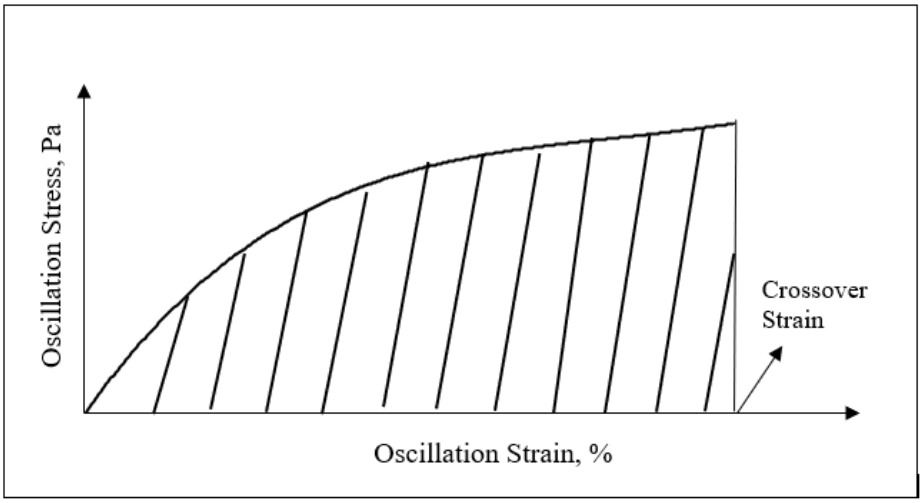

Figure 6.2 Oscillation Stress versus Oscillation Strain until Gel Point

Considering the practicality of field operations, including drilling, completion, and stimulation activities, the characterization of drilling fluid's viscoelasticity needs to be accomplished in a timely-urgent and field-accessible manner to fit into the nature of these operations. In such a case, the longest relaxation time, extensional viscosity, Deborah number, and Weissenberg number may not be the preferred choice to assess the fluid viscoelasticity since these parameters generally require advanced rheometer measurements and are mainly subject to characterizing the viscoelasticity of the small-scale deformation process.

Recently, Chen et al., (2021) presented a methodology to determine the fluid energy dissipation by using conventional field-testing equipment, including funnel viscometer and Fann viscometer, providing convenience for both industry professionals and researchers. In this study,

we will use Chen et al., (2021)'s method to assess the viscoelastic behavior with energy dissipation to address the plight.

6.2.2 Weighted Average Molecular Weight and Polydispersity Index of Polymer Blends

In order to determine individual effects of the drilling fluid shear viscosity and the elasticity on the filtration loss and associated formation damage, we have used fluids having similar shear viscosity and variable elasticity. It has been shown that polymer blends of the same weighted average molecular weight (Eq 6.2) and different polydispersity index (Eq 6.3) values can be used to formulate fluids with similar shear viscosity and variable elasticity (Zhang et al., 1987; Dehghanpour and Kuru, 2011; Veerabhadrappa et al., 2013). Generally, polymer blends with the same average molecular weight (Eq 6.2) can be used to formulate fluids with similar shear viscosity (Zhang et al., 1987; Dehghanpour and Kuru, 2011; Veerabhadrappa et al., 2013). The polydispersity index (Eq 6.3) is a relative measure of the molecular weight distribution of the individual polymers in a polymer blend (Zhang et al., 1987; Dehghanpour and Kuru, 2011; Veerabhadrappa et al., 2013). As the polydispersity index value increases, the heterogeneity in cross-linking, network formation, chain length, branching, hyper branching will also increase with the more random arrangement, which is all expected to contribute to the fluid elasticity. Therefore, the polydispersity index (PI) can be used as a relative measure of the degree of fluid elasticity for initial fluid formulation and screening purposes of the different polymer blends.

$$M_w = \prod_{i=1}^{n} M_{w,i}^{\Omega,i} \qquad 6.2$$

$$I = \left(\sum_{i=1}^{n} \Omega_i M_{w,i} \right) \times \left(\sum_{i=1}^{n} \frac{\Omega_i}{M_{w,i}} \right) \quad 6.3$$

Where:

M_w = average molecular weight of polymer blend, g/g mol

I = polydispersity index

Ω = weight fraction, fraction

6.3 Materials and Method

A total of 24 fluids in 6 groups were prepared in this study; in each group, the fluid possesses similar average molecular weight and different polydispersity, which enables direct observation of the effect of viscoelasticity and shear viscosity on the filtration loss characteristics. Two standard rheological measurements, including controlled shear rate and amplitude sweep tests, were conducted for each prepared fluid to determine the corresponding shear-thinning characteristic and viscoelastic behavior. The static filtration tests were implemented to determine the experimental fluids' static filtration rate; the core flooding experiments were conducted to compare the effect of two rheological properties on pressure drop and formation damage.

6.3.1 Experimental Fluids

A synthetic polymer commonly used for fluid formulation in oil and gas drilling activities, called PHPA, is utilized for preparing fluids in this study, also referred to as partially hydrolyzed polyacrylamide; it is formed from the monomers of acrylic acid and acrylamide.

The rheological behavior of PHPA is mainly dependent on the average molecular weight and degree of hydrolysis. Various blends of three types of PHPA polymers (Table 6-1) with different molecular weights were used in this study to formulate fluids with different viscoelastic properties**.**

Table 6-1 Average Molecular Weight of Three PHPA Polymers Used in this Study

Viscosifier	Average molecular weight (10^6 g/g mol)
PHPA-1	20
PHPA-2	8
PHPA-3	0.5

Polymer blend composition, average molecular weight, and polydispersity index of test fluids are summarized in Table 6-2.

Table 6-2 Polymer Blend Composition; Average Molecular Weight, and Polydispersity Index of all Test Fluids

Group No.	Fluid No.	Wt. % of polymer blend in solution	Wt.% of Polymer in each blend (%)			Average MW of the polymer blend (g/g mol)	Polydispersity Index
			PHPA-1	PHPA-2	PHPA-3		
1	1	0.25	0	100	0	$8*10^6$	1
	2	0.25	29.1	61.4	9.5	$8*10^6$	3
	3	0.25	49.1	34.6	16.3	$8*10^6$	5
	4	0.25	66.9	11.2	21.9	$8*10^6$	7
2	5	0.27	0	100	0	$8*10^6$	1

	6	0.27	29.1	61.4	9.5	$8*10^6$	3
	7	0.27	49.1	34.6	16.3	$8*10^6$	5
	8	0.27	66.9	11.2	21.9	$8*10^6$	7
3	9	0.3	0	100	0	$8*10^6$	1
	10	0.3	29.1	61.4	9.5	$8*10^6$	3
	11	0.3	49.1	34.6	16.3	$8*10^6$	5
	12	0.3	66.9	11.2	21.9	$8*10^6$	7
4	13	0.335	0	100	0	$8*10^6$	1
	14	0.335	29.1	61.4	9.5	$8*10^6$	3
	15	0.335	49.1	34.6	16.3	$8*10^6$	5
	16	0.335	66.9	11.2	21.9	$8*10^6$	7
5	17	0.35	0	100	0	$8*10^6$	1
	18	0.35	29.1	61.4	9.5	$8*10^6$	3
	19	0.35	49.1	34.6	16.3	$8*10^6$	5
	20	0.35	66.9	11.2	21.9	$8*10^6$	7
6	21	0.4	0	100	0	$8*10^6$	1
	22	0.4	29.1	61.4	9.5	$8*10^6$	3
	23	0.4	49.1	34.6	16.3	$8*10^6$	5
	24	0.4	66.9	11.2	21.9	$8*10^6$	7

6.3.2 Mixing Procedure

The mixing procedure of the experimental fluids was similar to the methodology recommended by Foshee et al., (1976), the de-ionized water was used as the base fluid, the liquid had the majority of the mineral ions removed, therefore mitigating the possibility of potential chemical reaction, that might ruin the result of measurements. The detailed mixing procedure involves the following three steps:

1. Measure the appropriate amount of each polymer and de-ionized water, pre-shear the base solution with a magnetic mixer at 300 RPM.

2. Slowly pour the polymer blend through the vortex edge to prevent forming dissolvable chunks. After adding the viscosifier, change the mixing speed to 150 RPM and continuously mix for 2 hours; a lower mixing speed is selected to avoid mechanical degradation of the polymers, which can severely damage the internal structure of the prepared fluid.

3. After mixing for 2 hours, if the solution is transparent with no visible polymer powder, it will be sealed and allowed to stay quiescent for 24 hours; the reason for doing this is to release the bubbles entrapped in the solution and allow it to reach a homogeneous state.

6.3.3 Laboratory Characterization of Rheological Properties

Controlled shear rate and amplitude sweep tests were conducted to characterize shear-thinning characteristics and viscoelastic behavior of the test fluids, respectively. Both tests were conducted using Anton Parr MCR 102e rheometer coupled with evaporation prevention system and cone and plate geometry, which has a dimension of 50mm diameter and angle of 1 degree.

6.3.3.1 Controlled Shear Rate Tests

The controlled shear rate test was conducted for each test fluid with a shear rate range of 0.1 1/s to 1200 1/s; a sample rheogram for sample No. 1 is shown in Fig 6.3. All fluids exhibited power-law (shear-thinning) behavior, which can be commonly described by Eq 6.4.

$$\tau = k\dot{\gamma}^n \qquad 6.4$$

Furthermore, the fluids in each group showed identical shear-thinning characteristic. Rheograms of four fluids with different polydispersity indices in group one are shown in Fig 6.4. As shown in Fig 6.4, all four fluids have almost identical shear stress vs shear rate relationships.

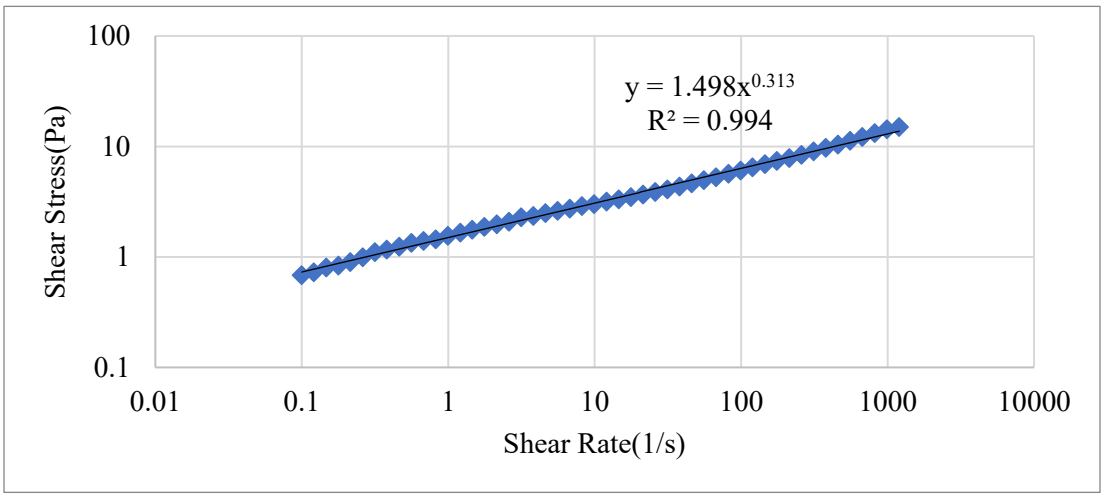

Figure 6.3 Controlled Shear Rate Test Result of No. 1 Fluid in Group 1

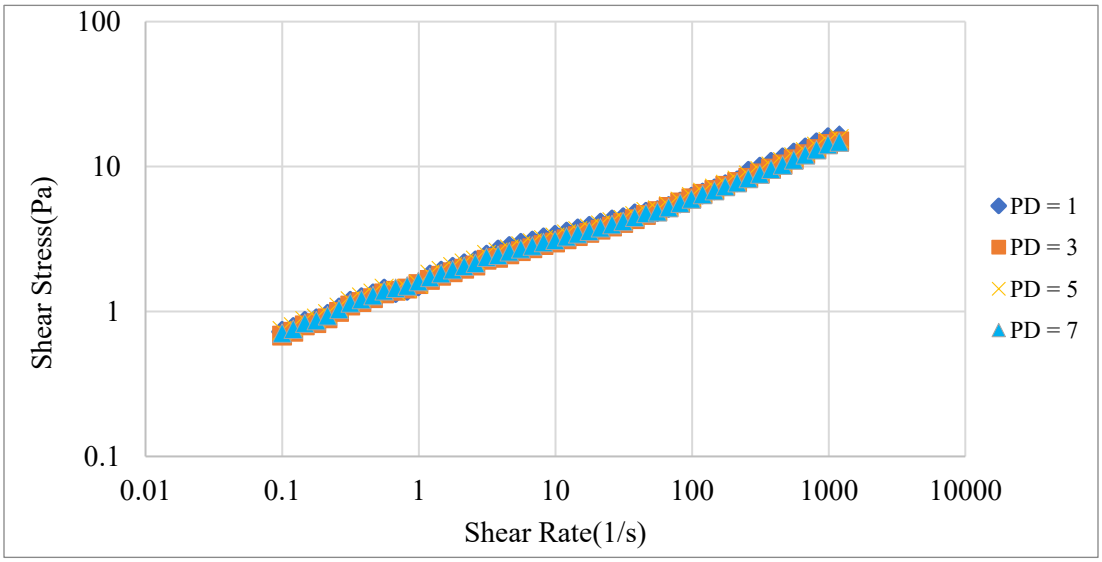

Figure 6.4 Controlled Shear Rate Test Results for Fluids in Group One

Summary of the controlled shear rate test results, including flow behavior indices and consistency indices, are given in Table 6-3. The results confirm that the fluids in each group have almost identical shear-thinning characteristics.

Table 6-3 Controlled Shear Rate Test Results of Test Fluids

Group No.	Fluid No.	Flow behavior index (Pa.s^n)	Flow consistency index (-)
1	1	1.498	0.313
	2	1.487	0.315
	3	1.493	0.308
	4	1.484	0.307
2	5	1.763	0.296
	6	1.751	0.301
	7	1.776	0.298
	8	1.781	0.294
3	9	1.902	0.306
	10	1.861	0.303
	11	1.903	0.285
	12	1.902	0.298
4	13	2.451	0.294
	14	2.483	0.289
	15	2.503	0.293
	16	2.476	0.286
5	17	2.633	0.279
	18	2.659	0.276

	19	2.701	0.271
	20	2.689	0.275
6	21	3.174	0.273
	22	3.186	0.277
	23	3.169	0.269
	24	3.176	0.274

6.3.3.2 Amplitude Sweep Test

The amplitude sweep tests were utilized to assess the viscoelastic properties of the test fluids. The test applies a sinusoidal deformation to test fluid and measures the resulting mechanical response as a function of the oscillation frequency. The amplitude sweep test was conducted for each test fluid with an oscillation strain range up to 600 %, and an angular frequency of 10 rad/s. Examples of an amplitude sweep test results for sample No. 1 are shown in Figs 6.1a and 6.1b. By plotting the oscillation strain versus oscillations stress, (Fig 6.2) which is the corresponding stress for inducing the deformation strain, the energy dissipation can be computed by determining the area under the curve which is the integral of oscillation stress over oscillation strain until gel point. (Eq 6.1) A summary of the amplitude sweep test results is shown in Table 6-4. It can be seen that the energy dissipation for fluids in each group has a direct proportional relationship with the polydispersity index.

Table 6-4 Amplitude Sweep Test Results of Experimental Fluids

Group No.	Fluid No.	Polymer Concentration (%)	Polydispersity	Energy dissipation (J/m^3)
1	1	0.25	1	13.8
	2	0.25	3	15.5

	3	0.25	5	20.1
	4	0.25	7	24.7
2	5	0.27	1	14.2
	6	0.27	3	15.9
	7	0.27	5	22.4
	8	0.27	7	27.3
3	9	0.3	1	15.7
	10	0.3	3	21.1
	11	0.3	5	27.2
	12	0.3	7	33.4
4	13	0.335	1	17.6
	14	0.335	3	27.1
	15	0.335	5	35.8
	16	0.335	7	39.7
5	17	0.35	1	18.6
	18	0.35	3	29.7
	19	0.35	5	37.8
	20	0.35	7	42.3
6	21	0.4	1	27.7
	22	0.4	3	34.2
	23	0.4	5	41.7
	24	0.4	7	47.2

6.3.4 Assessment of Formation Damage Potential of Test Fluids

Static filtration and dynamic core flooding tests were conducted to determine formation damage characteristics of the test fluids. Static filtration loss volume, pressure drop across the core, and permeability reduction after polymer flooding were measured.

6.3.4.1 Static Filtration Tests

A total of 24 static filtration tests were conducted using the test fluids. API standard procedure (API 13B-1, 2019) was followed in this case. Filtration tests were conducted at 100 psia and atmospheric pressure conditions. We have used non-standard, low permeability filter papers (Advantec GA5590 Grade Glass fiber filters with 0.6-micron pore size) in these experiments. Filtration loss volumes of all fluids collected in 30 minutes are presented in Table 6-5. Since fluids contained no solids, there was no mud cake observed.

Table 6-5 Static Filtration Test Results

Group No.	Fluid No.	Temperature (°C)	Static Filtration Rate (ml/30min)
1	1	21	55
	2	21	42
	3	21	31
	4	21	25
2	5	21	48
	6	21	41
	7	21	27
	8	21	22

3	9	21	40
	10	21	29
	11	21	21
	12	21	15
4	13	21	35
	14	21	20
	15	21	11
	16	21	8
5	17	21	32
	18	21	18
	19	21	10
	20	21	6
6	21	21	19
	22	21	12
	23	21	6
	24	21	4

6.3.4.2 Core Flooding Experiments

A total of 7 core flooding experiments were conducted using fluids No. 8, No.11, No. 21, and four fluids in group 4(#13-16). Fluids # 8, 11, and 21 were selected to demonstrate the effect of the shear viscosity of the fluids on the pressure drop and formation damage because these fluids possess similar energy dissipation and different shear viscosity values. Four fluids in group 4 were selected to compare the effect of viscoelasticity on pressure drop and formation damage, since they

have similar shear thinning characteristics and different energy dissipation (i.e., viscoelasticity) values.

A schematic view of the experimental set-up used for conducting the core flooding test is shown in Fig 6.5. A syringe pump with a pressure capacity of up to 7500 psi is used to inject the polymer fluid through the core. The controlled flow rate model was used to ensure the accuracy of flow rate measurement. A pressure transducer with a sampling rate of 10 samples per second, is connected to the inlet of the core holder for computing the pressure drop across the core, the outlet of the cell is open to atmospheric pressure. A confining pressure control system is installed to make sure the fluid flows through the core's permeable media instead of slipping through by the side of the core. Berea Sandstone core samples with 1 inch diameter and 1 inch length were used for core flooding experiments. Berea sandstone was selected because the sandstone formation is generally more susceptible to fluid loss problems because of their high permeability, also high permeability sample will make the results have a noticeable difference, making it more suitable for observing the effects of two rheological properties on the filtration loss properties.

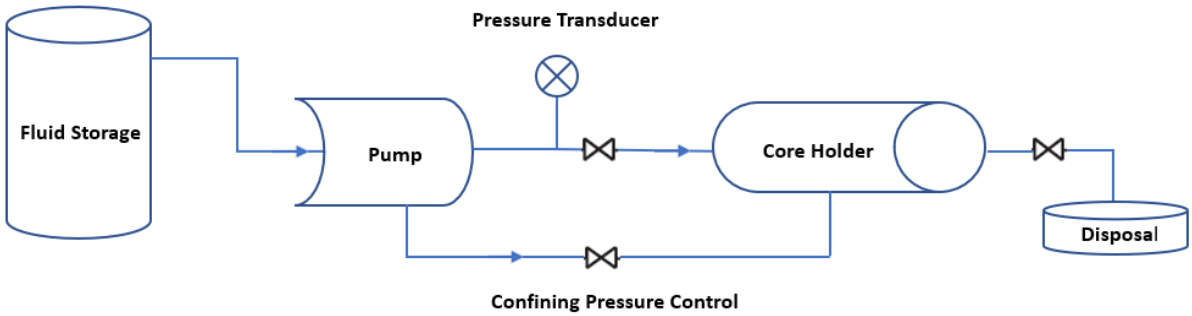

Figure 6.5 Core Flooding Experimental Apparatus

6.3.4.2.1 Experimental Procedure

Before starting the test, the Berea sandstone was placed in the core holder, and the confining pressure of 450 psi was applied to make sure the fluid only went through the porous media of the core. Each experiment starts with a new sample core (ensuring an original clean rock condition with no polymer residue). All measurements were taken at the steady-state condition when the inlet pressure stabilized and did not change for at least 15 minutes. The experimental procedure includes the following steps:

Step-1: The de-ionized water is injected into the core holder at five different flow rates to compute the absolute (original) permeability of Berea sandstone. The permeability of the rock was determined by using the measured injection pressure, flow rate, water viscosity, density values, and classical theory of Darcy law (Eq 6.5). If no significant difference was observed in the calculated permeability values at five different flow rates, the average of five values will be used as the absolute permeability.

Step-2: The selected polymer solution was pumped through the core holder at five different flow rates; the pressure drop at each flow rate was recorded.

Step-3: The polymer flooded core is flushed with de-ionized water for 24 hours to remove the polymer residue inside the core. Another permeability measurement was taken to determine the altered permeability due to polymer flooding (i.e., permeability reduction due to mainly because of the polymer retention on the rock surface).

6.3.4.2.2 Experimental Measurements

Polymer flooding experiments were conducted at 5 different steady-state flow rates. The resultant pressure drops were recorded as the difference between the inlet and outlet pressure of the core holder once the flow reaches the steady-state condition. The fluid flow was considered in steady-state condition when the inlet pressure measurement stopped fluctuating and stayed consistent for at least 15 minutes. The results of pressure drop measurements are presented in Table 6-6.

Table 6-6 Pressure Drop Data Results from Core Flooding Experiment

Fluid No.	Pressure drop (psi) at different flow rate				
	20 ml/hr	60 ml/hr	100 ml/hr	150 ml/hr	210 ml/hr
8	18.1	56.8	106.5	150.8	172.6
11	19.6	62.4	112.9	159.4	181.5
13	15.6	48.9	89.2	130.8	152.9
14	20.9	67.9	118.6	168.7	192.3
15	26.8	90.2	155.4	214.3	240.2
16	34.6	120.7	195.6	257.2	293.4
21	21.4	73.6	127.2	177.2	205.1

Permeability measurements of Berea sandstone core samples were conducted using de-ionized water before and after polymer fluid flooding tests to observe the permeability reduction caused by polymer fluid flooding. The pressure drop versus water flow rate data collected under steady-state conditions was used together with Darcy's law (Eq 6.5) to determine the permeability of the Berea sandstone cores before and after polymer flooding experiments. Examples of such

data obtained from water flooding tests conducted by de-ionized water are shown in Fig 6.6. The summary of the permeability measurements is presented in Table 6-7.

$$Q = -\frac{kA}{\mu}\frac{\Delta P}{L} \qquad 6.5$$

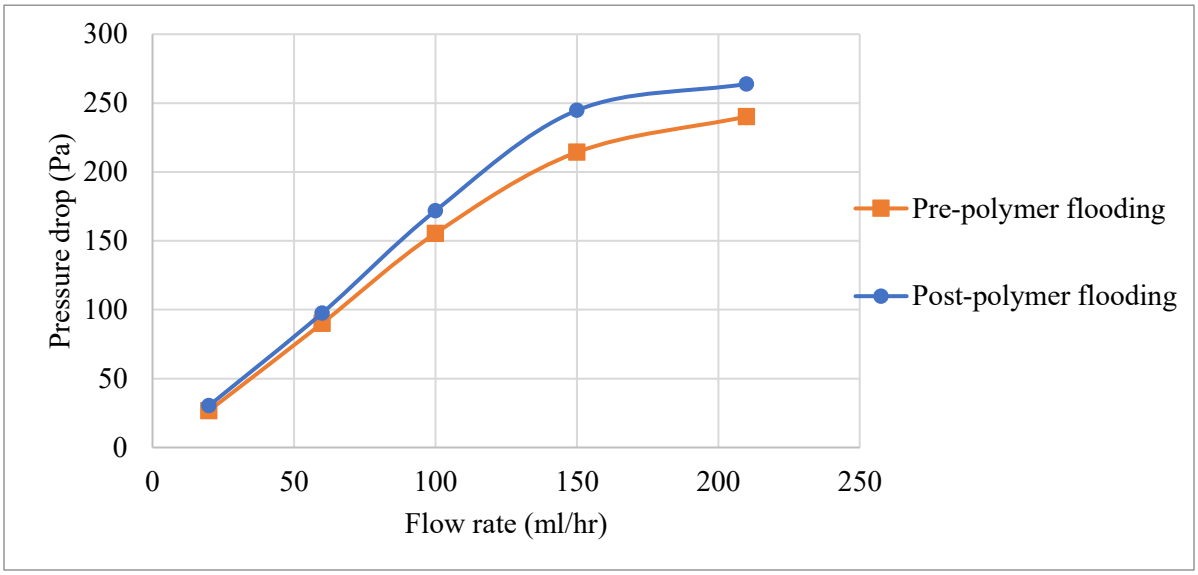

Figure 6.6 Pressure Drop versus Flow Rate Plot for Sample No.15 and after Polymer Flooding

Table 6-7 Permeability of Berea Sandstone Cores Measured Before and After Polymer Fluid Flooding Experiment

Fluid No.	Absolute permeability measurement (md)		Permeability reduction (%)
	Before polymer flooding	Post polymer flooding	
8	178.8	171.1	4.3
11	183.4	170.7	6.9
13	179.1	162.8	9.1
14	178.6	161.3	9.7
15	182.7	163.7	10.4

16	180.2	159.7	11.4
21	178.4	151.8	14.9

6.4 Discussion of the Experimental Results

In order to investigate the effect of individual effects of shear viscosity and elasticity on the formation damage potential of polymer fluids, we have prepared 6 different sets of fluids whose shear viscosity and elasticity properties are summarized in Tables 6-3 and 6-4, respectively. Ultimately, the main objective was to compare the effects of fluid shear viscosity and elasticity properties and determine the dominant fluid property between the two that control static filtration rate, pressure drop, and formation damage.

6.4.1 Effect of Viscoelasticity and Shear Viscosity on Static Filtration Rate

Table 6-8 summarizes the static filtration rate measurements of four fluids in group 6, which have similar shear viscosity (k and n) and different viscoelasticity (Energy dissipation). A 70% increase in energy dissipation (between Fluids #21 and 24) caused a 78.9% reduction in the static filtration rate. Results confirm that increasing energy dissipation can lead to a dramatic reduction in static filtration rate.

Table 6-8 Static Filtration Measurements of Experimental Fluids in Group 1

Fluid No.	k ($Pa.s^n$)	n	E_D (J/m^3)	Static Filtration Rate (ml/30min)	Change in Percentage(%)
21	3.174	0.273	27.7	19	0
22	3.186	0.277	34.2	12	36.8
23	3.169	0.269	41.7	6	68.4

24	3.176	0.274	47.2	4	78.9

Table 6-9 summarizes the static filtration rate test results of four fluids that have similar viscoelasticity and different shear viscosity values. A 78% increase in consistency index, reduced the static filtration rate only by 13.6%. Clearly, a significant increase in fluid shear viscosity did not influence the static filtration rate much in this case.

Table 6-9 Static Filtration Measurements of Fluids #8, 11, 14, and 21

Fluid No.	k ($Pa.s^n$)	n	E_D (J/m^3)	Static Filtration Rate (ml/30min)	Change in Percentage(%)
8	1.781	0.294	27.3	22	0
11	1.903	0.285	27.2	21	4.5
14	2.483	0.289	27.1	20	9.1
21	3.174	0.273	27.7	19	13.6

Moreover, when we compare the performance of Fluids #24 and 21, which have almost identical shear viscosity characteristics (very similar n & k values) and significantly different elasticity (E_D) values (47.2 J/m^3 vs. 27.7 J/m^3, for fluids #4 and 21, respectively), we can see that static filtration rates recorded for fluids #24 and 21 are 4 ml and 19 ml, respectively. Considering that both fluids have the similar shear viscosity characteristics, we can say that the dramatic 78.9% reduction of fluid loss obtained by using Fluid # 24 was mainly due to the higher elasticity value of this fluid.

Comparison of the results shown in Tables 6-8 and 6-9, indicates that both shear viscosity and elasticity properties can mitigate the static filtration rate. However, increasing the viscoelasticity seems to be the more efficient choice since the increasing viscoelasticity has a more substantial impact than that of the shear viscosity on the static filtration rate.

6.4.2 Effect of Viscoelasticity and Shear Viscosity on Pressure Drop and Formation Damage

Solids-free, drill-in, fluids are typically used to drill through reservoir (i.e., pay zone) sections in order to minimize pore plugging and its associated formation damage and, thereby, eliminate the need for costly stimulating operations. Since the drill-in fluids are solids-free, there will be no external filter cake to control the filtration loss in this case. Very often, building an internal filter cake (i.e., increasing the resistance for flow through the porous media manifested as increasing pressure drop) is the only option available in this case to minimize the volume of fluid loss into the reservoir and, therefore, effective way to reduce formation damage. Therefore, we have compared the effect of shear viscosity and the elasticity on the fluids' capacity of building the internal cake, which has been measured in terms of pressure drop in core flooding experiments.

Table 6-10 presents the pressure drop measurement results of four fluids in group 4, which have similar shear thinning characteristics and different viscoelasticity.

Table 6-10 Pressure Drop versus Flow Rate Data for the Flow of Fluids with Similar Shear Viscosity and Variable Elasticity (Group#4) through Berea Sandstone cores

Fluid No.	E_D (J/m3)	k (pa.s^n)	n	Pressure drop (psi) at different flow rate				
				20 ml/hr	60 ml/hr	100 ml/hr	150 ml/hr	210 ml/hr
13	17.6	2.452	0.294	15.6	48.9	89.2	130.8	152.9

14	27.1	2.484	0.289	20.9	67.9	118.6	168.7	192.3
15	35.8	2.503	0.293	26.8	90.2	155.4	214.3	240.2
16	39.7	2.476	0.286	34.6	120.7	195.6	257.2	293.4

The flow rate versus pressure drop data was also plotted in Fig 6.7. Results clearly indicated that the pressure drop (i.e., resistance to flow of fluid through the porous media) significantly increased with the increasing viscoelasticity (i.e., energy dissipation). It was also noticed that the effect of viscoelasticity on the pressure drop was amplified at higher fluid injection rates.

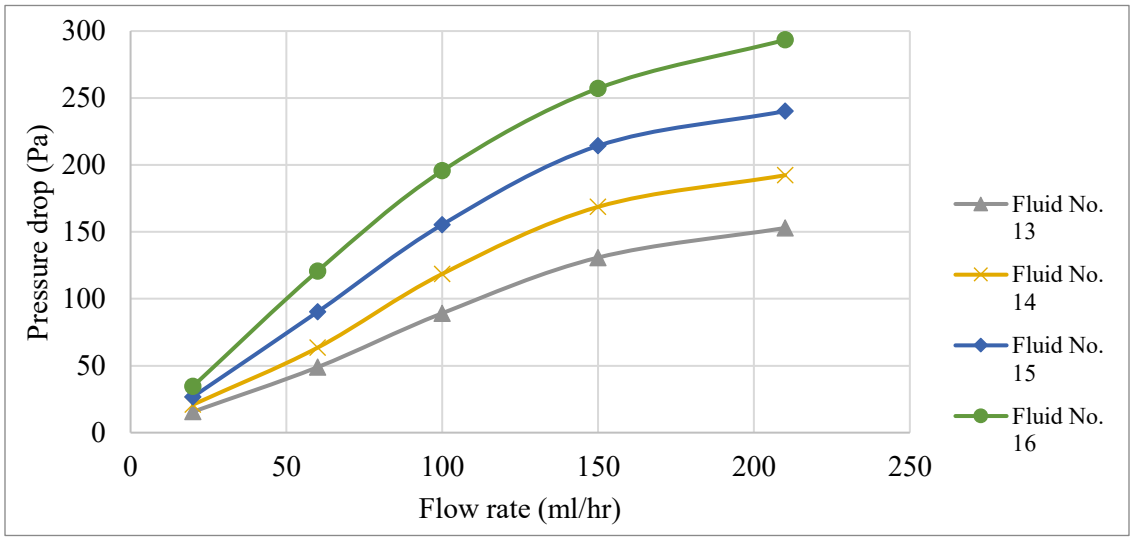

Figure 6.7 Pressure Drop versus Flow Rate Data for the Flow of Fluids with Similar Shear Viscosity and Variable Elasticity (Group#4) through Berea Sandstone Cores

Table 6-11 summarizes the pressure drop across the core for the flow of fluids # 8, 11, 14, and 21, which have similar viscoelasticity and different shear viscosity. The flow rate versus pressure drop was also plotted in Fig 6.8. Results have shown that the increasing shear viscosity did not influence the pressure drop as significantly as by increasing the viscoelasticity.

We will show the difference between the effect of changing shear viscosity vs changing elasticity on the pressure drop using an example. We will use the pressure drop obtained for the flow of Fluid # 14 (Table 6-11) as the benchmark in this example. If we compare the pressure drop obtained for the flow of Fluid # 16, which has a similar shear-viscosity characteristic as Fluid No.14; we can see that increasing the energy dissipation by 46% resulted in a 52% increase in pressure drop at 210 ml/hr flow rate. However, if we compare the pressure drop for the flow of fluid # 14 with Fluid #21, (both fluids have similar viscoelasticity), an increase of flow consistency index by 28% only causes a 6.6% increase in pressure drop at 210 ml/hr flow rate.

Moreover, increasing the shear viscosity would require using higher polymer concentration(i.e., decreasing the cost-effectiveness of the method, as well as increasing potential of formation damage due to polymer deposition on the rock surface), whereas viscoelasticity increase can be achieved by changing the molecular weight distribution (i.e., by varying the molecular weight distribution of the polymers in the polymer blend) while keeping the polymer concentration constant. These results also suggest that fluid filtration loss into the formation can be more effectively mitigated (i.e., increasing resistance to the flow of fluid into the rock and building a more effective internal filter cake) by increasing the fluid viscoelasticity rather than the shear viscosity.

Table 6-11 Pressure Drop Data for Fluids with Similar Viscoelasticity and Different Shear Viscosity (Fluid# No.8, No.11, No.14 and No.21)

Fluid No.	E_D (J/m3)	k (pa.s^n)	n	Pressure drop (psi) at different flow rate				
				20 ml/hr	60 ml/hr	100 ml/hr	150 ml/hr	210 ml/hr
8	27.3	1.781	0.294	18.1	56.8	106.5	150.8	172.6

11	27.2	1.903	0.285	19.6	62.4	112.9	159.4	181.5
14	27.1	2.483	0.289	20.9	67.9	118.6	168.7	192.3
21	27.7	3.174	0.273	21.4	73.6	127.2	177.2	205.1

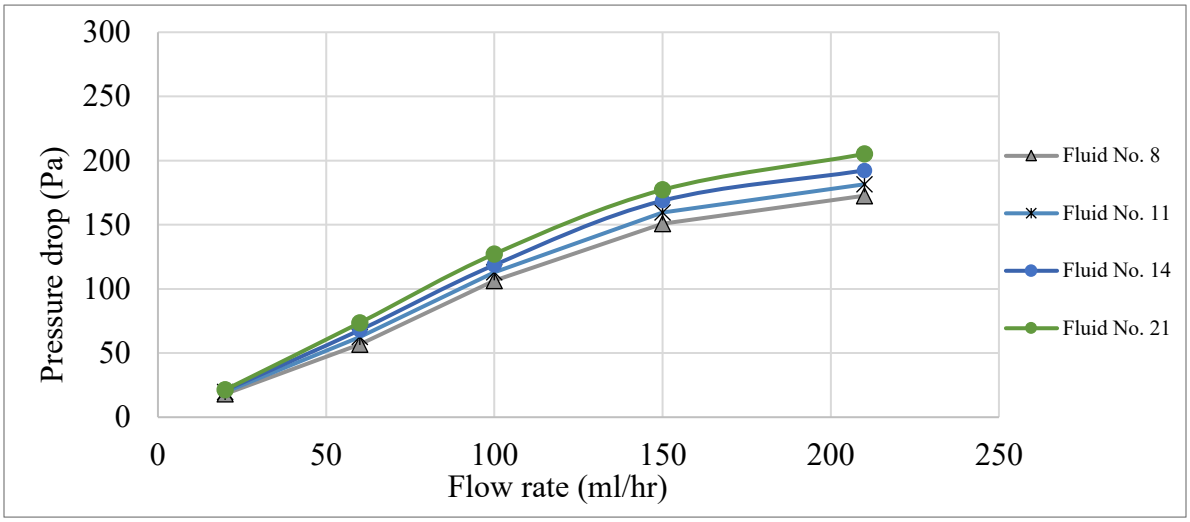

Figure 6.8 Pressure Drop versus Flow Rate for Fluids with Similar Viscoelasticity and Different Shear Viscosity (Fluids # No.8, No.11, No.14 and No.21)

Furthermore, a comparison of the pressure drop trends in Figs 6.7 and 6.8 indicate that the effect of increasing viscoelasticity on the pressure drop is more augmented at the higher flow rates while the increasing flow rate of high shear viscosity fluids did not show any significant impact on the pressure drop (i.e., resistance to flow of fluid into the rock). Such behavior of shear-thinning fluid under a high shear rate is rather expected as the shear rate is increased; apparent fluid viscosity is reduced and finally levels off to a constant value as a result of the shear degradation.

Table 6-12 summarizes the results of the water permeability measurements conducted before and after polymer flooding tests (and hence the reduction of permeability due to polymer

flooding test) using four fluids in group 4. The Berea sandstone core permeability was measured before and after polymer flooding tests by using de-ionized water. The permeability reduction was assessed as an indication of the formation damage induced by the flow of a particular fluid. Apart from the interaction between water and some reactive clays that may exist in the reservoir rock, one of the main mechanisms of permeability reduction can be due to the polymer deposition in the pores of the rock (Khan et al., 2017).

Table 6-12 Permeability Measurements for Fluids with Similar Shear Viscosity and Variable Elasticity in Group 4

Fluid No.	E_D (J/m3)	k ($pa.s^n$)	n	Absolute permeability measurement (md)		Permeability reduction (%)
				Before polymer flooding	Post polymer flooding	
13	17.6	2.451	0.294	179.1	162.8	9.1
14	27.1	2.483	0.289	178.6	161.3	9.7
15	35.8	2.503	0.293	182.7	163.7	10.4
16	39.7	2.476	0.286	180.2	159.7	11.4

Table 6-13 summarizes the permeability measurement results for the flow of Fluids # 8, 11, 14, and 21, which have similar viscoelasticity and different shear viscosity values.

Table 6-13 Permeability Measurements for Fluids with Similar Viscoelasticity and Different Shear Viscosity (Fluids No.8, No.11, No.14 and No.21)

Fluid No.	E_D (J/m3)	k ($pa.s^n$)	n	Absolute permeability measurement (md)		Permeability reduction (%)
				Before polymer flooding	Post polymer flooding	

8	27.3	1.781	0.294	178.8	171.1	4.3
11	27.2	1.903	0.285	183.4	170.7	6.9
14	27.1	2.483	0.289	178.6	161.3	9.7
21	27.7	3.174	0.273	178.4	151.8	14.9

Comparison of the core flooding test results of Fluid # 14 and 16 (Table 6-12), indicates that the permeability reduction increased from 9.7% to 11.4% (roughly 18% increase) when the energy dissipation (i.e., viscoelasticity) increased by 46%.

Comparison of the core flooding test results of Fluid # 14 and 21 (Table 6-13), indicates that the permeability reduction increased from 9.7% to 14.9% (roughly 54% increase) when the fluid consistency index increased 28%.

Moreover, when we compared performances of fluids # 8 and 21 (Table 6-13), we could see that a 78% increase in the consistency index (formulated by increasing polymer concentration from 0.27% to 0.4% wt./wt.) caused the permeability reduction to increase from 4.3% to 14.9% (an increase of 247%).

6.4.3 Shear Viscosity vs. Elasticity-Overall Performance Comparison

To make a more direct comparison of the individual effect of shear viscosity and viscoelasticity on the filtration loss volume, building internal cake (frictional pressure drop due to flow through reservoir rock) and formation damage, we summarized the static filtration loss volume, pressure loss and formation damage measurement results of the Fluid No. 8, 21 and 24's (Table 6-14).

Fluids No.8 and 21 have similar elasticity and significantly different shear viscosity values. The results here show the individual effect of increasing shear viscosity on the filtration loss, pressure drop and the formation damage. Increasing the consistency index from 1.781 pa.s^n to 3.174 pa.s^n (78% increase) caused a decrease in static filtration loss volume from 22ml to 19 ml (reduction of 13.6%) and a significant increase in formation damage from 4.3% to 14.9 % (246.5% increase).

Fluids No.21 and 24 have similar shear viscosity and significantly different elasticity values. The results here show the individual effect of increasing elasticity on the filtration loss, pressure drop and the formation damage. Increasing the energy dissipation (fluid elasticity) from 27.7 J/m^3 to 47.3 J/m^3 (70.4% increase) caused a decrease in static filtration loss volume from 19 ml to 4 ml (reduction of 79%) and a small increase in formation damage from 14.9% to 16.6 % (11.4 % increase).

Table 6-14 Static Filtration Rate, Pressure Drop, and Formation Damage Measurements of Fluids #8, 21 and 24

Fluid No.	E_D (J/m^3)	k (pa.s^n)	n	Static Filtration Rate (ml/30min)	Pressure drop (psi) at different flow rate					Formation Damage (%)
					20	60	100	150	210	
8	27.3	1.781	0.294	22	18.1	56.8	106.5	150.8	172.6	4.3
21	27.7	3.174	0.273	19	21.4	73.6	127.2	177.2	205.1	14.9
24	47.2	3.176	0.274	4	46.9	163.4	238.8	305.9	352.4	16.6

A summary of frictional pressure drop versus flow rate measurements for Fluid No. 8, No. 21 and No. 24 is shown in Fig 6.9. These results have indicated that increasing shear viscosity (Fluid #8 vs #21) did not yield a significant impact on the pressure drop (i.e., ineffective for

internal cake building), whereas increasing fluid elasticity (Fluid #21 vs #24) did cause a significant increase in pressure drop (i.e., effective for internal cake building).

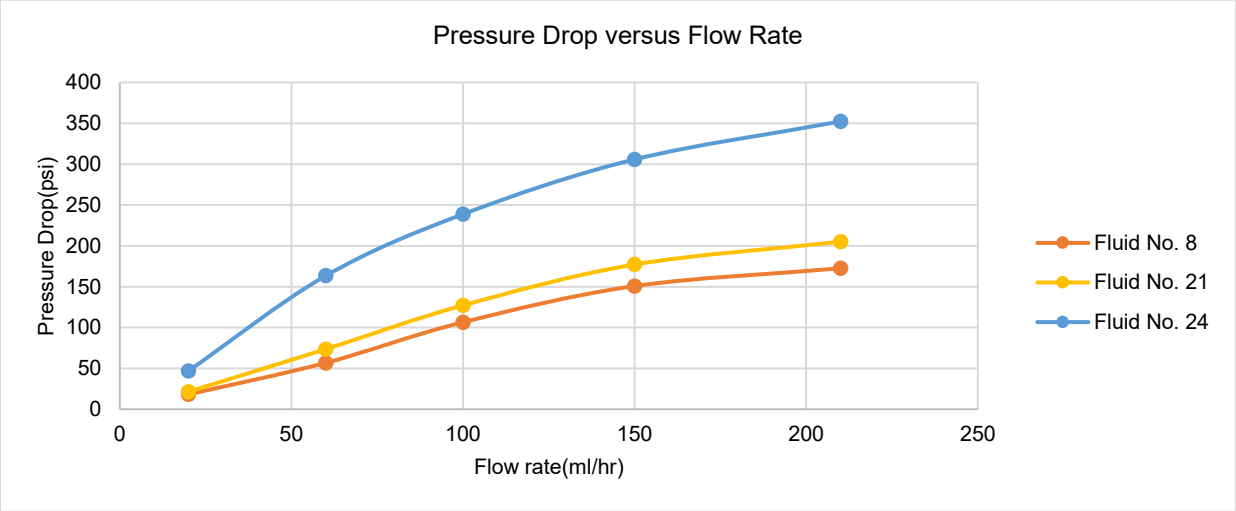

Figure 6.9 Pressure Drop versus Flow Rate for Fluids #8, 21 and 24

6.4.4 Comparison of the Formation Damage Potential of Viscoelastic vs. Visco-Inelastic Drill-in Fluids

Xanthan Gum (XG) is commonly used for formulating drilling fluids. Its use is sometimes avoided in drill-in fluids due its resiliency to enzymes, oxidizers, and acids, which make it difficult to remove or breakdown prior to completions. However, it is the most popular viscosifying polymer and it provides an alternative to PHPA, which can be formulated and blended for low E_D values while retaining similar apparent viscosities for the purposes of this study. In this part of the study, we wanted to compare the formation damage potential of the typical XG-based fluids (typically showing low viscoelasticity) versus the high viscoelasticity fluids. Three fluids (Fluids # 25-27) were prepared by using high purity, high-performance Xanthan Gum. The concentrations

of the XG in fluids #25-27 were adjusted such that the fluids have a similar apparent viscosity (as per API definition, it is one-half of the 600 RPM measurement using API rotational viscometer) as the viscoelastic fluids, No. 8, 14 and 21. Rheograms of the XG-based fluids is shown in Fig 6.10.

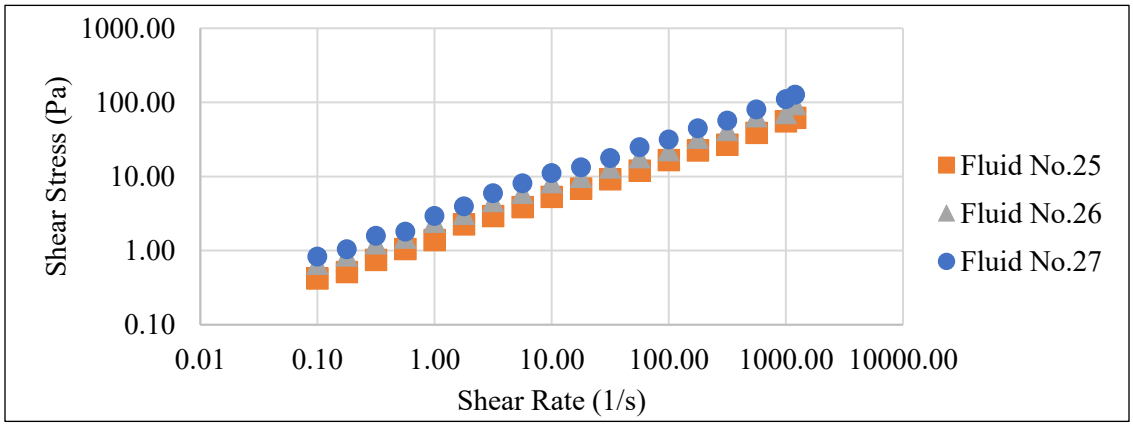

Figure 6.10 Rheograms of the XG-based Fluids (Fluids #25-27)

The static filtration test results together with fluid rheological properties (AV, n, k, and E_D) of XG-based fluids (#25-27) and viscoelastic fluids (#,8,14, and 21) were presented in Tables 6-15 and 6-16, respectively.

Table 6-15 Static Filtration Test Results of XG-Based Fluids (Fluids No. 25, 26 and 27)

Fluid No.	Additive	Concentration (%)	Apparent Viscosity (cp)	k (Pa.s^n)	n (-)	E_D (J/m^3)	Static Filtration Rate (ml/30min)
25	Flowzan	0.24	16	1.456	0.528	0.25	156
26	Flowzan	0.35	24.75	2.266	0.517	0.37	138
27	Flowzan	0.5	34	2.866	0.532	0.62	122

Table 6-16 Static Filtration Test Results of Viscoelastic Fluids (Fluids No. 8, No.14, and No. 21)

Fluid No.	Apparent Viscosity (cp)	k ($Pa.s^n$)	n (-)	E_D (J/m^3)	Static Filtration Rate (ml/30min)
8	15.5	1.781	0.294	27.3	22
14	24	2.483	0.289	27.1	20
21	34.5	3.174	0.273	27.7	19

Fluids # 25 and 8; 26 and 14, 27 and 21 have comparable AV values. Very low E_D values of Fluids #25-27 indicate that XG-based fluids can be considered visco-inelastic.

Static filtration test results show that XG-based fluids have fluid loss volumes order of magnitude higher than that of viscoelastic fluids. Such high static filtration rates can cause excessive fluid invasion into the reservoir and, as a result, induce very high formation damage due to phase trapping clay swelling, scaling, etc. effects.

XG-based fluids were also used to conduct core flooding experiments. Results of the pressure drop measurements conducted at five different flow rates and water permeability measurements conducted before and after polymer flooding experiments are summarized in Tables 6-17 and 6-18, respectively.

We have then compared these results with pressure loss (Table 6-19) and permeability measurements (Table 6-20) from viscoelastic fluids (#8, 14, and 21) tests.

Table 6-17 Pressure Drop Data for XG-Based Fluids (No.25, 26 and 27)

Fluid No.	Additive	Concentration (%)	Apparent viscosity (cp)	k (Pa.s^n)	n (-)	E_D (J/m3)	Pressure drop (psi) at different flow rate				
							20 ml/hr	60 ml/hr	100 ml/hr	150 ml/hr	210 ml/hr
25	Flowzan	0.24	16	1.456	0.528	0.25	5.3	16.9	28.6	35.7	40.4
26	Flowzan	0.35	24.75	2.266	0.517	0.37	5.7	18.6	30.8	38.2	43.2
27	Flowzan	0.5	34	2.866	0.532	0.62	6.5	20.5	32.5	39.9	45.7

Table 6-18 Permeability Measurements for XG-Based Viscoinelastic Fluid (No. 25, 26, 27)

Fluid No.	Additive	Concentration (%)	Apparent Viscosity (cp)	k (Pa.s^n)	n (-)	E_D (J/m3)	Absolute permeability measurement (md)		Permeability reduction (%)
							Before polymer flooding	Post polymer flooding	
25	Flowzan	0.24	16	1.456	0.528	0.25	179.5	173.4	3.4
26	Flowzan	0.35	24.75	2.266	0.517	0.37	181.9	165.7	8.9
27	Flowzan	0.5	34	2.866	0.532	0.62	181.7	157.2	13.5

Table 6-19 Pressure Drop Data for Viscoelastic Fluids (No.8, 14 and 21)

Fluid No.	Apparent Viscosity (cp)	k (Pa.s^n)	n (-)	E_D (J/m3)	Pressure drop (psi) at different flow rate				
					20 ml/hr	60 ml/hr	100 ml/hr	150 ml/hr	210 ml/hr
8	15.5	1.781	0.294	27.3	18.1	56.8	106.5	150.8	172.6
14	24	2.483	0.289	27.1	20.9	67.9	118.6	168.7	192.3
21	34.5	3.174	0.273	27.7	21.4	73.6	127.2	177.2	205.1

Table 6-20 Permeability Measurements for Viscoelastic Fluid (No. 8, 14 and 21)

Fluid No.	Apparent Viscosity (cp)	k ($Pa.s^n$)	n (-)	E_D (J/m3)	Absolute permeability measurement (md)		Permeability reduction (%)
					Before polymer flooding	Post polymer flooding	
8	15.5	1.781	0.294	27.3	178.8	171.1	4.3
14	24	2.483	0.289	27.1	178.6	161.3	9.7
21	34.5	3.174	0.273	27.7	178.4	151.8	14.9

Pressure drop versus flow rate data for XG-based viscoinelastic fluids (Fluids # 25, 26, and 27) are also plotted in Fig 6.11. A 122.5% increase in apparent viscosity caused only a 16.4% increase in the pressure drop on average. Results confirm that increasing in apparent viscosity of XG-based viscoinelastic fluids did not have a significant impact on the pressure drop.

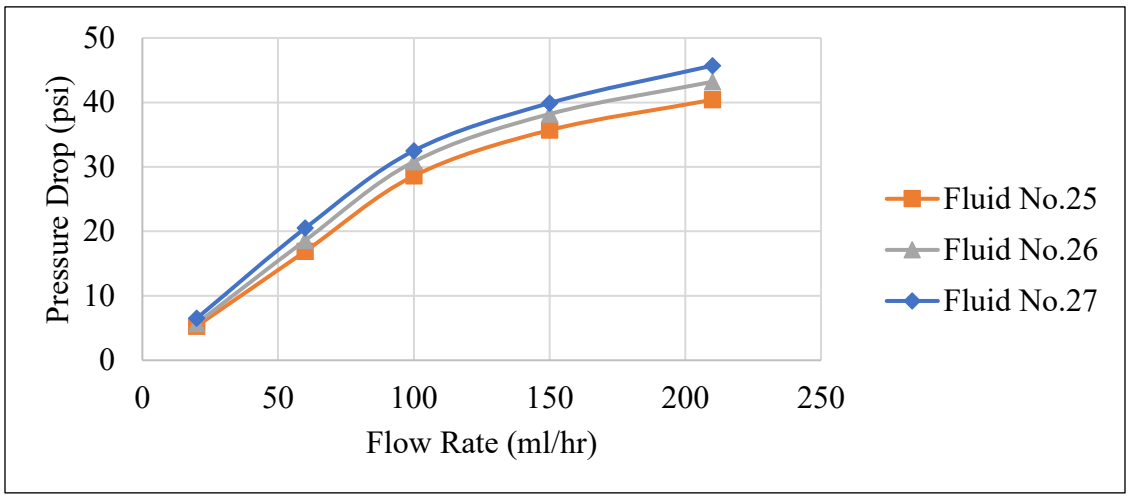

Figure 6.11 Pressure Drop versus Flow Rate Data for XG-Based Fluids (No. 25, 26, and 27)

By comparing the pressure drop results of XG-based viscoinelastic fluids (Table 6-17) versus viscoelastic fluids (Table 6-19), which have the same apparent viscosity, we see that viscoelastic fluids can induce 240-350% more pressure drop than that of XG-based viscoinelastic

fluids at the same flow rates, confirming that viscoelastic fluids can build internal cake more effectively than the viscoinelastic fluids.

Permeability test results of XG-based viscoinelastic fluids (Table 6-18) indicate that a 122.5% increase in apparent viscosity of these fluids (corresponding to polymer concentration increase from 0.24% to 0.5% for fluids# 25 and 27, respectively) caused the increase of permeability reduction to 297.1% (an increase from 3.4% to 13.5%, for fluids# 25 and 27, respectively), most likely due to polymer deposition. The order of magnitude of the permeability reduction (varying from 4.3% to 14.9%, Table 6-20) due to the viscoelastic fluid invasion was more or less the same as the viscoinelastic fluids. The most likely cause of the permeability reduction in both cases would be polymer deposition (and the resultant reduction of pore size) on the rock pores. Considering the volume of XG-based viscoinelastic fluids invasion is the order of magnitude higher than viscoelastic fluids, it would be reasonable to expect significantly higher formation damage with the former fluids if there are other factors contributing to the damage (e.g., presence of reactive clays, aqueous trapping, scaling, etc.) are present.

6.5 Summary of Key Findings from this Study

In summary, by conducting the static filtration rate tests and core flooding experiments to measure, pressure drop, and permeability of the rock samples, we have investigated the individual effect of varying fluid shear viscosity and elasticity on these variables.

Results have shown that increasing fluid viscoelasticity suppresses the static filtration rate more effectively than that of increasing the shear viscosity. Both the shear viscosity and the viscoelasticity directly affect the pressure drop (i.e. building internal cake). However, increasing

viscoelasticity seems to be the more effective way of building internal cake and, thereby, reducing the volume of fluid loss into the formation.

One of the key findings from these observations is that the formation damage can be severely exacerbated by the increasing polymer concentration (i.e. increasing shear viscosity). While on the other hand; the elevated energy dissipation (or increasing viscoelasticity, which does not require increasing polymer concentration) did not cause a significant reduction in permeability (as much as caused by increasing the shear viscosity).

Based on these analyses, we can conclude that drill-in fluid properties may be more effectively optimized for mitigating formation damage by adjusting viscoelasticity rather than the shear viscosity of the fluids.

6.6 Recommendations

One of the main conclusions of this study is that fluid viscoelasticity plays a dominant role in controlling filtration loss characteristics of drilling fluid. However, having too high viscoelasticity may also lead to potential problems such as forming micelles and plugging up the pores in the near wellbore zone permanently. Further research is needed to determine the optimum level of viscoelasticity considering the formation type and ultimately come up with a method that can find a balanced mix between the shear viscosity and viscoelasticity and provide an optimized fluid rheology solution for handling fluid loss problems.

Furthermore, the core flooding experiments conducted in this study only considered the physical interaction (i.e., the effect of polymer deposition on the rock surface). Most of the time, however, optimum fluid formulation requires careful assessment of the potential chemical

interaction between the fluid and the rock. In such cases, the fluid composition needs to be designed on a case-by-case basis to ensure that the potential chemical reaction between drilling fluid and rock, drilling fluid and formation fluid will not induce additional damage.

A final note to be made is this study focused primarily on various blends of PHPA, since prior research had been able to alter the elasticity without meaningfully increasing the fluid's viscosity. However, in practice PHPA struggles to maintain it's properties while drilling after continuously being exposed to high shear conditions typical of a drilling fluid circulation system (mud pumps, tank agitators, pipe turbulence, mud motors, bit nozzles, decanter centrifuge, etc.). Future work may use or investigate the potential of other polymers that are capable of increasing E_D without increasing viscosity, which are able to better maintain rheological properties.

6.7 Conclusion

The following conclusions can be offered based on the results obtained from this study:

1. The static filtration rate can be more effectively controlled by altering fluid viscoelasticity rather than the fluid shear viscosity.

2. Both shear viscosity and viscoelasticity have a proportional relationship with the pressure drop across the core. However, the effect of viscoelasticity on the pressure drop (i.e., development of internal cake) is more pronounced.

3. The effect of the fluid shear viscosity on the pressure drop is undermined when the flow rate increases due to its unique shear thinning behavior.

4. Increase in viscoelasticity does not exacerbate the formation damage problem as significant as increasing shear viscosity.

5. The viscoelastic property has been found to be the predominant rheological property that controls the solid-free drill-in fluids' filtration loss characteristics considering three attributes including, static filtration rate, pressure drop, and formation damage.

Based on what we have learned from the results of this study, it is reasonable to say that the fluid loss problem may not be effectively handled by solely depending on changing the shear viscosity of the drilling fluids. The viscoelasticity of the fluid can be effectively used as an additional rheology modifier to optimize the filtration loss characteristics. Alternatively, additional viscoelasticity can be utilized to compensate for the functionality of the shear viscosity, which would lower the concentration of viscosifier needed and, therefore, reduce the cost of drilling fluid. With this in mind, the industry professionals can ultimately solve the complications associated with extreme fluid loss to the greatest extent, by designing drilling fluid formulation with a versatile level of viscoelasticity.

6.8 Nomenclature

G'	elastic modulus (Pa)
G''	viscous modulus (Pa)
E_D	energy dissipation (J/m^3)
τ	oscillation/shear stress (Pa)

γ	oscillation/shear strain (%)
M_w	molecular weight (g/g mol)
I	polydispersity index (-)
Ω	weight fraction (-)
k	power-law consistency index ($Pa.s^n$)
n	power-law flow behavior index (-)
$\dot{\gamma}$	shear rate (1/s)
Q	volumetric flow rate (cm^3/s)
k	permeability (Darcy)
A	cross-sectional area of flow (cm^2)
μ	viscosity (cp for Eq 6.5 / Pa.s for Eq 6.6)
ΔP	pressure drop across the core (atm)
L	length of the core (cm)
Re	Reynolds number (-)
ρ	density (kg/m^3)
V	flow velocity (m/s)

D characteristic linear dimension (m)

6.9 Acknowledgements

This project is financially supported through the funds provided by the Natural Sciences and Engineering Research Council of Canada (NSERC RGPIN-2016-04647 Kuru, NSERC EGP 543455-19 Kuru).

6.10 References

API RP 13B-1, Recommended Practice for Field Testing Water-based Drilling Fluids. (2019). Washington, DC United States: API.

Anyanwu, C., and Momoh, U. "Experimental Evaluation of Particle Sizing in Drilling Fluid to Minimize Filtrate Losses and Formation Damage." Paper presented at the SPE Nigeria Annual International Conference and Exhibition, Lagos, Nigeria, August 2016. doi: https://doi.org/10.2118/184303-MS

Arnipally, S. K., & Kuru, E. (2018). Settling Velocity of Particles in Viscoelastic Fluids: A Comparison of the Shear-Viscosity and Elasticity Effects. *SPE Journal*, *23*(05), 1689–1705. https://doi.org/10.2118/187255-PA

Chen, H., Okesanya, T., Kuru, E., Heath, G., & Hadley, D. (2021). A Generalized Model for the Field Assessment of Drilling Fluid Viscoelasticity. *Proceedings - SPE Annual Technical Conference and Exhibition*, *2021-September*, 205953. https://doi.org/10.2118/205953-MS

Chesser, B. G., Clark, D. E., and W. V. Wise. "Dynamic and Static Filtrate-Loss Techniques for Monitoring Filter-Cake Quality Improves Drilling-Fluid Performance." *SPE Drill & Compl* 9 (1994): 189–192. doi: https://doi.org/10.2118/20439-PA

Cobianco, S., Bartosek, M., Lezzi, A., & Guarneri, A. (2001). How To Manage Drill-In Fluid Composition To Minimize Fluid Losses During Drilling Operations. *SPE Drilling & Completion*, *16*(03), 154–158. https://doi.org/10.2118/73567-PA

Dehghanpour, H., & Kuru, E. (2011). Effect of viscoelasticity on the filtration loss characteristics of aqueous polymer solutions. *Journal of Petroleum Science and Engineering*, *76*(1–2), 12–20. https://doi.org/10.1016/J.PETROL.2010.12.005

Durst, F., Haas, R., & Interthal, W. (1987). The nature of flows through porous media. *Journal of Non-Newtonian Fluid Mechanics*, *22*(2), 169–189. https://doi.org/10.1016/0377-0257(87)80034-4

Fink, J. (2021). Fluid loss additives. In *Petroleum Engineer's Guide to Oil Field Chemicals and Fluids*. Elsevier. https://doi.org/10.1016/B978-0-323-85438-2.00002-5

Foshee, W. C., Jennings, R. R., & West, T. J. (1976). Preparation and Testing of Partially Hydrolyzed Polyacrylamide Solutions. *Proceedings - SPE Annual Technical Conference and Exhibition*, *1976-Octob*. https://doi.org/10.2118/6202-MS

Gupta, R.K., Sridhar, T., 1985. Viscoelastic effects in non-Newtonian flows through porous media. Rheol. Acta 24, 148–151.

Ikram, R., Jan, B. M., Sidek, A., Kenanakis, G., Jan, M., Sidek, B. ;, Kulinich, S., Svetlichnyi, V. A., Kuchmizhak, A., & Honda, M. (2021). Utilization of Eco-Friendly Waste Generated Nanomaterials in Water-Based Drilling Fluids; State of the Art Review. *Materials 2021, Vol. 14, Page 4171*, *14*(15), 4171. https://doi.org/10.3390/MA14154171

Khan, R., Kuru, E., Tremblay, B., & Saasen, A. (2007). Extensional Viscosity of Polymer Based Fluids as a Possible Cause of Internal Cake Formation. *Http://Dx.Doi.Org/10.1080/00908310600626630*, *29*(16), 1521–1528. https://doi.org/10.1080/00908310600626630

Khan, R., Kuru, E., Tremblay, B., & Saasen, A. (2004). An Investigation of the Extensional Viscosity of Polymer Based Fluids as a Possible Mechanism of Internal Cake Formation. *Proceedings - SPE International Symposium on Formation Damage Control*, 375–389. https://doi.org/10.2118/86499-MS

Lomba, R. F. T., Martins, A. L., Soares, C. M., Brandao, E. M., Magalhaes, J. V. M., & Ferreira, M. V.D. (2002). Drill-In Fluids: Identifying Invasion Mechanisms. *Proceedings - SPE International Symposium on Formation Damage Control*, 131–142. https://doi.org/10.2118/73714-MS

Maxey, J. (2010). A Rheological Approach to Differentiating Muds by Gel Structure. *AADE Fluids Conference and Exhibition*

Okesanya, T., Kuru, E., & Sun, Y. (2020). A New Generalized Model for Predicting the Drag Coefficient and the Settling Velocity of Rigid Spheres in Viscoplastic Fluids. SPE Journal, 25(06), 3217–3235. https://doi.org/10.2118/196104-PA.

Ofei, T. N., Cheng, I., Lund, B., Saasen, A., & Sangesland, S. (2020). On the Stability of Oil-Based Drilling Fluid: Effect of Oil-Water Ratio. *Proceedings of the International Conference on Offshore Mechanics and Arctic Engineering - OMAE*, *11*. https://doi.org/10.1115/OMAE2020-19071

Poole, R., (2012), The Deborah and Weissenberg numbers. The British Society of Rheology, Rheology Bulletin. 53(2) pp 32-39

Salehi, S. (2015). *SPE-174273-MS Study of Filtrate and Mud Cake Characterization in HPHT: Implications for Formation Damage Control*. http://onepetro.org/SPEEFDC/proceedings-pdf/15EFDC/All-15EFDC/SPE-174273-MS/1438069/spe-174273-ms.pdf/1

Saasen, A., Tengbreg-Hansen, H., Marken C., and Stavland A.: "Influence of linear Viscoelastic Properties on Invasion of Drilling Fluid Filtrate into a Porous Formation", Oil Gas European Magazine, Vol.4, 1990.

Urbissinova, T. S., Trivedi, J., and Kuru, E. "Effect of Elasticity During Viscoelastic Polymer Flooding: A Possible Mechanism of Increasing the Sweep Efficiency." J Can Pet Technol 49 (2010): 49–56. doi: https://doi.org/10.2118/133471-PA.

Veerabhadrappa, S. K., Doda, A., Trivedi, J. J., & Kuru, E. (2013). On the Effect of Polymer Elasticity on Secondary and Tertiary Oil Recovery. *Industrial and Engineering Chemistry Research*, *52*(51), 18421–18428. https://doi.org/10.1021/IE4026456

Zamir, A., & Ahmad Siddiqui, N. (2017). *Investigating and Enhancing Mud Cake Reduction Using Smart Nano Clay Based WBM*. *8*, 1. https://doi.org/10.4172/2157-7463.1000315

Zamora, M., Broussard, P. N., & Stephens, M. P. (2000). The Top 10 Mud-Related Concerns in Deepwater Drilling Operations. *SPE International Petroleum Conference and Exhibition in Mexico, IPCEM*. https://doi.org/10.2118/59019-MS

Zang, Y. H., Muller, R., & Froelich, D. (1987). Influence of molecular weight distribution on viscoelastic constants of polymer melts in the terminal zone. New blending law and comparison with experimental data. Polymer, 28(9), 1577–1582. https://doi.org/10.1016/0032-3861(87)90362-4.

CHAPTER 7 Conclusions and Recommendations

This section provides the summary of major conclusions obtained through three experimental studies, which are presented in Chapters 4, 5 and 6. Recommendations for future studies are also provided.

7.1 Conclusions of the Experimental Studies

A summary of the work conducted, and specific conclusions are presented separately under the title of specific study.

A Generalized Model for the Field Assessment of Drilling Fluid Viscoelasticity**:**

A new methodology was developed to determine the viscoelasticity of the drilling fluids using funnel viscosity and apparent viscosity, which are commonly measured using conventional field-testing equipment (i.e., funnel viscometer and rotational viscometer).

The new method uses the energy dissipation concept to quantify the drilling fluid viscoelasticity and correlates it to the apparent viscosity and the funnel viscosity of drilling fluids. Statistical assessments confirm that the model for unweighted drilling fluids can predict the energy dissipation of the viscoelastic fluid with a RMSE of 0.167 J/m^3 and a MAPE of 4.67%. The model for weighted drilling fluids can predict the energy dissipation a RMSE of 0.547 J/m^3 and MAPE of 5.28%.

Study also provides results of investigations on how the change in oil-water ratio and the presence of clays/drilled solids would affect the elasticity of the drilling fluids.

Based on the results from this study following additional conclusions can be offered:

- Neither the rigidity modulus (G') nor the stretchiness (oscillation strain % at the crossover point of G' and G" curves) can solely characterize the viscoelastic property of the drilling fluid. More comprehensive assessment on the viscoelastic characteristics of the drilling fluid can be done using the "energy dissipation" concept.

- For the same concentration of a viscosifying additive and the type of base oil, the fluid's viscoelasticity shows to be inversely proportional to the oil-water ratio.

- Viscoelasticity oil-based drilling fluids show a reduction with additions of clays.

- Since the presence of clays influences the viscoelasticity, it is important to consider the effect of natural clay and drill solids as they intermix with the drilling fluid.

With the development of the new model, drilling fluid viscoelasticity can now be evaluated at the well site by using commonly measured apparent viscosity and funnel viscosity data. A better understanding of the drilling fluid viscoelastic properties would help field engineers to develop optimum drilling fluid formulations and hydraulic programs for effective hole cleaning operations, improved ECD management, and mitigating barite sag problems.

A Generalized Model For Field Assessment of Particle Settling Velocity In Viscoelastic Fluids:

A generalized model for determining particle terminal settling velocity in shear-thinning viscoelastic fluids has been developed. The model uses the concept of energy dissipation to

quantify fluid elasticity, which can be conveniently determined by using standard field measurements of apparent viscosity (AV) and funnel viscosity.

Based on the results from this study following additional conclusions can be offered:

- The viscoelasticity of the fluid media surrounding the settling particle is a shear rate dependent property. Higher the shear rate, less viscoelasticity in terms of energy dissipation is preserved.
- The results show that the fluid's viscoelasticity (energy dissipation) is a direct function of oscillation frequency; higher the frequency is lower the viscoelasticity will be.
- The local shear rate induced by settling particle on the fluid can be directly related to oscillation frequency as per Corx-Merz rules, which states that the shear rate is equivalent to frequency.

According to statistical evaluation of the proposed model, the model has a MAPE of 4.1 percent and RMSE of 0.0032 m/s indicating that the model predictions of particle settling velocity in viscoelastic fluids are sufficiently accurate for all practical purposes.

The new methodology provides a practical tool for determining particle terminal velocity in shear-thinning viscoelastic drilling fluids based on the standard field measurements of drilling fluid properties.

<u>Dynamic Filtration Loss Control Through Optimization of Drilling Fluid Rheological Properties: A Comparative Study of the Fluid Viscoelasticity versus Shear Viscosity Effects:</u>

This study investigated the relative contributions of fluid shear viscosity and elasticity on the volume of dynamic fluid loss and the associated formation damage. Based on the results of the study, it was possible to demonstrate the sole effect of shear viscosity and viscoelasticity on the filtration loss characteristics and also determine the dominant variable that controls filtration loss volume between shear viscosity and viscoelasticity.

The following conclusions can be offered based on the results obtained from this study:

- The static filtration rate can be more effectively controlled by altering fluid viscoelasticity rather than the fluid shear viscosity.
- Both shear viscosity and viscoelasticity have a direct relationship with the pressure drop across the reservoir rock. However, the effect of viscoelasticity on the pressure drop (i.e., development of internal cake) is more pronounced.
- The effect of the fluid shear viscosity on the pressure drop is undermined when the flow rate increases due to its unique shear thinning behavior.
- Increase in viscoelasticity does not exacerbate the formation damage problem as significant as increasing shear viscosity.
- The viscoelastic property has been found to be the predominant rheological property that controls the solid-free drill-in fluids' filtration loss characteristics considering three attributes including, static filtration rate, pressure drop, and formation damage.

With the conclusions made in this study, it is reasonable to say that the fluid loss problem can be better handled without solely depending on changing the shear viscosity of the drilling fluid. The viscoelasticity of the fluid can be adjusted to optimize the filtration loss characteristics.

Alternatively, additional viscoelasticity can be utilized to compensate for the functionality of shear viscosity, which would lower the concentration of viscosifier needed and, therefore, reduce the cost of drilling fluid. With this in mind, the industry professionals can ultimately solve the complications associated with extreme fluid loss to the greatest extent, by designing drilling fluid formulation with a versatile level of viscoelasticity.

7.2 Recommendations for Future Study

Following recommendations can be offered for future studies.

- The results in chapter 4 has shown that the presence of clay reduces the viscoelasticity of drilling fluids. However, more work can be conducted to develop a practical correlation, enabling drilling engineers in the field to quantify the effect of clay concentration or contamination on viscoelasticity. Future research efforts should also address the influence of oil-water ratio changes on energy dissipation while keeping the Viscosifier concentration constant.
- One of the main conclusions of this study is that fluid viscoelasticity plays a dominant role in controlling filtration loss characteristics of drilling fluid. However, having too high viscoelasticity may also lead to potential problems such as forming micelles and plugging up the pores in the near wellbore zone permanently. Further research is needed to determine the optimum level of viscoelasticity considering the formation type and ultimately come up with a method that can find a balanced mix between the shear viscosity and viscoelasticity and provide an optimized fluid rheology solution for handling fluid loss problems.

- Furthermore, the core flooding experiments conducted in this study only considered the physical interaction (i.e., the effect of polymer deposition on the rock surface). Most of the time, however, optimum fluid formulation requires careful assessment of the potential chemical interaction between the fluid and the rock. In such cases, the fluid composition needs to be designed on a case-by-case basis to ensure that the potential chemical reaction between drilling fluid and rock, drilling fluid and formation fluid will not induce additional damage.

References

Abdelgawad, K., Elzenary, M., Elkatatny, S. et al (2018). New approach to evaluate the equivalent circulating density (ECD) using artificial intelligence techniques. Journal of Petroleum Exploration and Production Technology. 9. 10.1007/s13202-018-0572-y.

AlBahrani, H., Alsheikh, M., Wagle, V., and Aqeel A. Designing Drilling Fluids Rheological Properties with a Numerical Geomechanics Model for the Purpose of Improving Wellbore Stability. Paper presented at the IADC/SPE International Drilling Conference and Exhibition, Galveston, Texas, USA, March 2022. doi: https://doi.org/10.2118/208753-MS

Allahvirdizadeh, P., & Kuru, E. (2015). A Comparative Study of Cuttings Transport Performance of Water versus Polymer-Based Fluids in Horizontal wells. https://www.researchgate.net/publication/276354306

Amighi, M. R. and Khalil S. "Effective Ways to Avoid Barite Sag and Technologies to Predict Sag in HPHT and Deviated Wells." Paper presented at the SPE Deep Gas Conference and Exhibition, Manama, Bahrain, January 2010. doi: https://doi.org/10.2118/132015-MS

API RP 13B-1, Recommended Practice for Field Testing Water-based Drilling Fluids. (2019). Washington, DC United States: API.

API RP 13B-2, Recommended Practice for Field Testing Oil-based Drilling fluids. (2014). Washington, DC United States: API.

Altindal, M C, E Ozbayoglu, S Miska, M Yu, and N Takach. (2017). Impact of Viscoelastic Characteristics of Oil-Based Muds / Synthetic Based Muds on Cuttings Settling Velocities.

OMAE2017-62129. ASME 2017 36th International Conference on Ocean, Offshore and Arctic Engineering. June 25–30, 2017. Trondheim, Norway.https://doi.org/10.1115/OMAE2017-62129.

Agwu, Okorie E., Julius U. Akpabio, Sunday B. Alabi, and Adewale Dosunmu. 2018. Settling Velocity of Drill Cuttings in Drilling Fluids: A Review of Experimental, Numerical Simulations, and Artificial Intelligence Studies. Powder Technology 339: 728–46. https://doi.org/10.1016/j.powtec.2018.08.064.

Anyanwu, C., and Momoh, U. "Experimental Evaluation of Particle Sizing in Drilling Fluid to Minimize Filtrate Losses and Formation Damage." Paper presented at the SPE Nigeria Annual International Conference and Exhibition, Lagos, Nigeria, August 2016. doi: https://doi.org/10.2118/184303-MS

Arabi, Ameneh S., Sean Sanders, R., 2016. Particle terminal settling velocities in non- Newtonian visco-plastic fluids. Can. J. Chem. Eng. 94 (6), 1092–1101. https://doi. org/10.1002/cjce.22496.

Arnipally, S. K., & Kuru, E. (2018). Settling Velocity of Particles in Viscoelastic Fluids: A Comparison of the Shear-Viscosity and Elasticity Effects. *SPE Journal*, *23*(05), 1689–1705. https://doi.org/10.2118/187255-PA

Baldino, S., R. E. Osgouei, E. Ozbayoglu, S. Miska, N. Takach, R. May, and D. Clapper. 2015. “Cuttings Settling and Slip Velocity Evaluation in Synthetic Drilling Fluids.” In Offshore Mediterranean Conference and Exhibition, OMC 2015.

Biheri, G., & Imqam, A. (2021). Settling of Spherical Particles in High Viscosity Friction Reducer Fracture Fluids. Energies 2021, Vol. 14, Page 2462, 14(9), 2462. https://doi.org/10.3390/EN14092462

Bizhani, M. and Kuru, E. (2018). Particle Removal From Sandbed Deposits in Horizontal Annuli Using Viscoelastic Fluids. SPE J. 23 (2018): 256–273. doi: https://doi.org/10.2118/189443-PA

Bui, B., Saasen, A., Maxey, J., Ozbayoglu, E., Miska, S., Yu, M. (2012). Viscoelastic properties of oil-based drilling fluids. Annual Trans Nordic Rheol Soc. 20. 33-47.

Chesser, B. G., Clark, D. E., and W. V. Wise. "Dynamic and Static Filtrate-Loss Techniques for Monitoring Filter-Cake Quality Improves Drilling-Fluid Performance." *SPE Drill & Compl* 9 (1994): 189–192. doi: https://doi.org/10.2118/20439-PA

Chen, H., Temi, O., Ergun, K., Garett, H., & Dylan, H. (2021). A Generalized Model for the Field Assessment of Drilling Fluid Viscoelasticity. *Proceedings - SPE Annual Technical Conference and Exhibition*, *2021-September*, 205953. https://doi.org/10.2118/205953-MS

Chevron Phillips Chemical. (2022). Flowzan Bio polymer. www.cpchem.com

Chhabra, R. P. (2006). Bubbles, Drops, and Particles in Non-Newtonian Fluids. Bubbles, Drops, and Particles in Non-Newtonian Fluids. https://doi.org/10.1201/9781420015386.

Chien, S. F. (1994). Settling velocity of irregularly shaped particles. Proceedings - SPE Annual Technical Conference and Exhibition, Delta, 9–22. https://doi.org/10.2118/26121-PA

Clift, R, J R Grace, and M E Weber. 1978. Bubbles, Drops, and Particles., 2005. Dover Publications Inc. Mineola, New York. ISBN:0-486-44580-1.

Cobianco, S., Bartosek, M., Lezzi, A., & Guarneri, A. (2001). How To Manage Drill-In Fluid Composition To Minimize Fluid Losses During Drilling Operations. *SPE Drilling & Completion*, *16*(03), 154–158. https://doi.org/10.2118/73567-PA

Dehghanpour, H., & Kuru, E. (2011). Effect of viscoelasticity on the filtration loss characteristics of aqueous polymer solutions. *Journal of Petroleum Science and Engineering*, *76*(1–2), 12–20. https://doi.org/10.1016/J.PETROL.2010.12.005

Durst, F., Haas, R., & Interthal, W. (1987). The nature of flows through porous media. *Journal of Non-Newtonian Fluid Mechanics*, *22*(2), 169–189. https://doi.org/10.1016/0377-0257(87)80034-4

Fink, J. (2021). Fluid loss additives. In *Petroleum Engineer's Guide to Oil Field Chemicals and Fluids*. Elsevier. https://doi.org/10.1016/B978-0-323-85438-2.00002-5

Foshee, W. C., Jennings, R. R., & West, T. J. (1976). Preparation and Testing of Partially Hydrolyzed Polyacrylamide Solutions. *Proceedings - SPE Annual Technical Conference and Exhibition*, *1976-Octob*. https://doi.org/10.2118/6202-MS

Gupta, R.K., Sridhar, T., 1985. Viscoelastic effects in non-Newtonian flows through porous media. Rheol. Acta 24, 148–151.

Hirpa, M.M. and Kuru, E. (2020). Hole Cleaning in Horizontal Wells Using Viscoelastic Fluids: An Experimental Study of Drilling-Fluid Properties on the Bed-Erosion Dynamics. SPE J. 25 (2020): 2178–2193. doi: https://doi.org/10.2118/199636-PA

Ikram, R., Jan, B. M., Sidek, A., Kenanakis, G., Jan, M., Sidek, B. ;, Kulinich, S., Svetlichnyi, V. A., Kuchmizhak, A., & Honda, M. (2021). Utilization of Eco-Friendly Waste Generated Nanomaterials in Water-Based Drilling Fluids; State of the Art Review. *Materials 2021, Vol. 14, Page 4171*, *14*(15), 4171. https://doi.org/10.3390/MA14154171

Kelessidis, V. C., and G. Mpandelis. 2004. "Measurements and Prediction of Terminal Velocity of Solid Spheres Falling through Stagnant Pseudoplastic Liquids." Powder Technology 147 (1–3): 117–25. https://doi.org/10.1016/j.powtec.2004.09.034.

Khan, R., Kuru, E., Tremblay, B., & Saasen, A. (2007). Extensional Viscosity of Polymer Based Fluids as a Possible Cause of Internal Cake Formation. *Http://Dx.Doi.Org/10.1080/00908310600626630*, *29*(16), 1521–1528. https://doi.org/10.1080/00908310600626630

Khan, R., Kuru, E., Tremblay, B., & Saasen, A. (2004). An Investigation of the Extensional Viscosity of Polymer Based Fluids as a Possible Mechanism of Internal Cake Formation. *Proceedings - SPE International Symposium on Formation Damage Control*, 375–389. https://doi.org/10.2118/86499-MS

Lomba, R. F. T., Martins, A. L., Soares, C. M., Brandao, E. M., Magalhaes, J. V. M., & Ferreira, M. V.D. (2002). Drill-In Fluids: Identifying Invasion Mechanisms. *Proceedings - SPE International Symposium on Formation Damage Control*, 131–142. https://doi.org/10.2118/73714-MS

Malhotra, Sahil, and Mukul M. Sharma. 2012. "Settling of Spherical Particles in Unbounded and Confined Surfactant-Based Shear Thinning Viscoelastic Fluids: An Experimental Study." Chemical Engineering Science 84 (January): 646–55. https://doi.org/10.1016/j.ces.2012.09.010.

Malhotra, S., Lehman, E. R., & Sharma, M. M. (2013). Proppant placement using Alternate-Slug fracturing. Society of Petroleum Engineers - SPE Hydraulic Fracturing Technology Conference 2013, 405–420. https://doi.org/10.2118/163851-MS

Maxey, J. (2010). A Rheological Approach to Differentiating Muds by Gel Structure. *AADE Fluids Conference and Exhibition*

May, R., C. (2013). Rheological Behavior and Processing of Unvulgarized Rubber. The Science and Technology of Rubber. 4th Edition. Academic Press. https://doi.org/10.1016/B978-0-12-394584- 6.00006-6.

Mezger, T. G. (2006). The rheology handbook: For users of rotational and oscillatory rheometers. 2nd Edition. Vincentz Network. Hannover, Germany. ISBN 978-3-86630-890-9

Miura, H., Takahashi, T., Ichikawa, J., Kawase, Y. (2001). Bed expansion in liquid-solid two-phase fluidized beds with Newtonian and non-Newtonian fluids over the wide range of Reynolds numbers. Powder Tech., 117(3), 239–246. https://doi.org/10.1016/S0032-5910(00)00375-2.

Morrison, Faith A., 2013. Data Correlation for Drag Coefficient for Spheres, vol. 10. Cambridge University Press, New York, pp. 1–2. November.

Okesanya, T., Kuru, E., & Sun, Y. (2020). A New Generalized Model for Predicting the Drag Coefficient and the Settling Velocity of Rigid Spheres in Viscoplastic Fluids. SPE Journal, 25(06), 3217–3235. https://doi.org/10.2118/196104-PA.

Ofei, T. N., Cheng, I., Lund, B., Saasen, A., & Sangesland, S. (2020). On the Stability of Oil-Based Drilling Fluid: Effect of Oil-Water Ratio. *Proceedings of the International Conference on Offshore Mechanics and Arctic Engineering - OMAE*, *11*. https://doi.org/10.1115/OMAE2020-19071

Pitt, M. J.. "The Marsh Funnel and Drilling Fluid Viscosity: A New Equation for Field Use." SPE Drill & Compl 15 (2000): 3–6. doi: https://doi.org/10.2118/62020-PA

Poole, R. (2012). The Deborah and Weissenberg numbers. The British Society of Rheology - Rheology Bulletin. 53. 32-39.

Powell, J. W., Parks, C. F., and Seheult, J. M. (1991). Xanthan and Welan: The Effects of Critical Polymer Concentration on Rheology and Fluid Performance. International Arctic Technology Conference. Society of Petroleum Engineers. https://doi.org/10.2118/22066-MS.

Rabenjafimanantsoa, H. A., Rune, W. T. and Saasen, A. (2005). Flow regimes over particle beds experimental studies of particle transport in horizontal pipes. Annual Transactions of the Nordic Rheology Society.

Rushd, S., Hassan, I., Sultan, R. A., Kelessidis, V. C., Rahman, A., Hasan, H. S., and Hasan, A. (2018). Terminal settling velocity of a single sphere in drilling fluid. Particulate Science and Technology. Taylor & Francis, 0(0), pp. 1–10. DOI: 10.1080/02726351.2018.1472162.

Salehi, S. (2015). *SPE-174273-MS Study of Filtrate and Mud Cake Characterization in HPHT: Implications for Formation Damage Control*. http://onepetro.org/SPEEFDC/proceedings-pdf/15EFDC/All-15EFDC/SPE-174273-MS/1438069/spe-174273-ms.pdf/1

Saasen, A., Tengbreg-Hansen, H., Marken C., and Stavland A.: "Influence of linear Viscoelastic Properties on Invasion of Drilling Fluid Filtrate into a Porous Formation", Oil Gas European Magazine, Vol.4, 1990.

Saasen, A. and Løklingholm, G. (2002). The Effect of Drilling Fluid Rheological Properties on Hole Cleaning. IADC/SPE Drilling Conference. Dallas, Texas, 26-28 February, SPE-74558-MS, DOI: 10.2118/74558-MS.

Sayindla, S., Lund, B., Ytrehus, J. D., & Saasen, A. (2017). Hole-cleaning performance comparison of oil-based and water-based drilling fluids. Journal of Petroleum Science and Engineering, 159, 49-57. https://doi.org/10.1016/j.petrol.2017.08.069.

Sedaghat, A. (2017). A novel and robust model for determining rheological properties of Newtonian and non-Newtonian fluids in a marsh funnel. Journal of Petroleum Science and Engineering, 156, 896–916. https://doi.org/10.1016/j.petrol.2017.06.057

Shah, Subhash N, Youness E El-Fadili, and R P Chhabra. 2007. "New Model for Single Spherical Particle Settling Velocity in Power Law (Visco-Inelastic) Fluids" 33: 51–66. https://doi.org/10.1016/j.ijmultiphaseflow.2006.06.006.

Shahi, Shivam, and Ergun Kuru. 2015. “An Experimental Investigation of Settling Velocity of Natural Sands in Water Using Particle Image Shadowgraph.” Powder Technology 281: 184–92. https://doi.org/10.1016/j.powtec.2015.04.065.

Shahi, S., & Kuru, E. (2016). Experimental investigation of the settling velocity of spherical particles in Power-law fluids using particle image shadowgraph technique. International Journal of Mineral Processing, 153, 60–65. https://doi.org/10.1016/J.MINPRO.2016.06.002.

Shale Tech Solutions Drilling Manual, Model 35 Viscometer, www.shaletechsolutions.com

The Centre for Industrial Rheology (2022). Die Swell Effect. Hampshire. www.rheologylab.com

Turton.R, O. Levenspiel, A short note on the drag correlation for spheres, Powder Technology, Volume 47, Issue 1, 1986, Pages 83-86, ISSN 0032-5910, https://doi.org/10.1016/0032-5910(86)80012-2.

Urbissinova, T. S., Trivedi, J., and Kuru, E. "Effect of Elasticity During Viscoelastic Polymer Flooding: A Possible Mechanism of Increasing the Sweep Efficiency." J Can Pet Technol 49 (2010): 49–56. doi: https://doi.org/10.2118/133471-PA.

Veerabhadrappa, S. K., Doda, A., Trivedi, J. J., & Kuru, E. (2013). On the Effect of Polymer Elasticity on Secondary and Tertiary Oil Recovery. *Industrial and Engineering Chemistry Research*, *52*(51), 18421–18428. https://doi.org/10.1021/IE4026456

Vidhya Enterprises Marsh Funnel, For Industrial, 1, Rs 9500 /unit | ID: 19218478648. (2022). https://www.indiamart.com/proddetail/marsh-funnel-19218478648.html

Werner, B., Myrseth, V., & Saasen, A. (2017). Viscoelastic properties of drilling fluids and their influence on cuttings transport. Journal of Petroleum Science and Engineering, 156, 845-851. https://doi.org/10.1016/j.petrol.2017.06.063.

Wilson, K. C., Horsley, R. R., Kealy, T., Reizes, J. and Horsley, M. (2003) 'Direct prediction of fall velocities in non-Newtonian materials', International Journal of Mineral Processing, 71(1–4), pp. 17–30. DOI: 10.1016/S0301-7516(03)00027-9.

Williamson, D. (2013). Drilling fluid basics. *Oilfield Review*, *25*(1), 63–64. http://www.slb.com/resources/oilfield_review/en/2013/or2013_spr.aspx

Zamir, A., & Ahmad Siddiqui, N. (2017). *Investigating and Enhancing Mud Cake Reduction Using Smart Nano Clay Based WBM*. *8*, 1. https://doi.org/10.4172/2157-7463.1000315

Zamora, M., Broussard, P. N., & Stephens, M. P. (2000). The Top 10 Mud-Related Concerns in Deepwater Drilling Operations. *SPE International Petroleum Conference and Exhibition in Mexico, IPCEM*. https://doi.org/10.2118/59019-MS

Zamora, M., Jefferson, D. T., Powell, J. W. (1993). Hole-Cleaning Study of Polymer-Based Drilling Fluids. Society of Petroleum Engineers. Doi :10.2118/26329-MS.

Zang, Y. H., Muller, R., & Froelich, D. (1987). Influence of molecular weight distribution on viscoelastic constants of polymer melts in the terminal zone. New blending law and comparison with experimental data. Polymer, 28(9), 1577–1582. https://doi.org/10.1016/0032-3861(87)90362-4.

Zhang, G., Li, M., Li, J., Yu, M., Qi, M., & Bai, Z. (2015). Wall Effects on Spheres Settling Through Non-Newtonian Fluid Media in Cylindrical Tubes. http://Dx.Doi.Org/10.1080/01932691.2014.966309, 36(9), 1199–1207. https://doi.org/10.1080/01932691.2014.966309